vol. 4, no. 5

May 1958

THE SOVIET JOURNAL OF

ATOMIC ENERGY

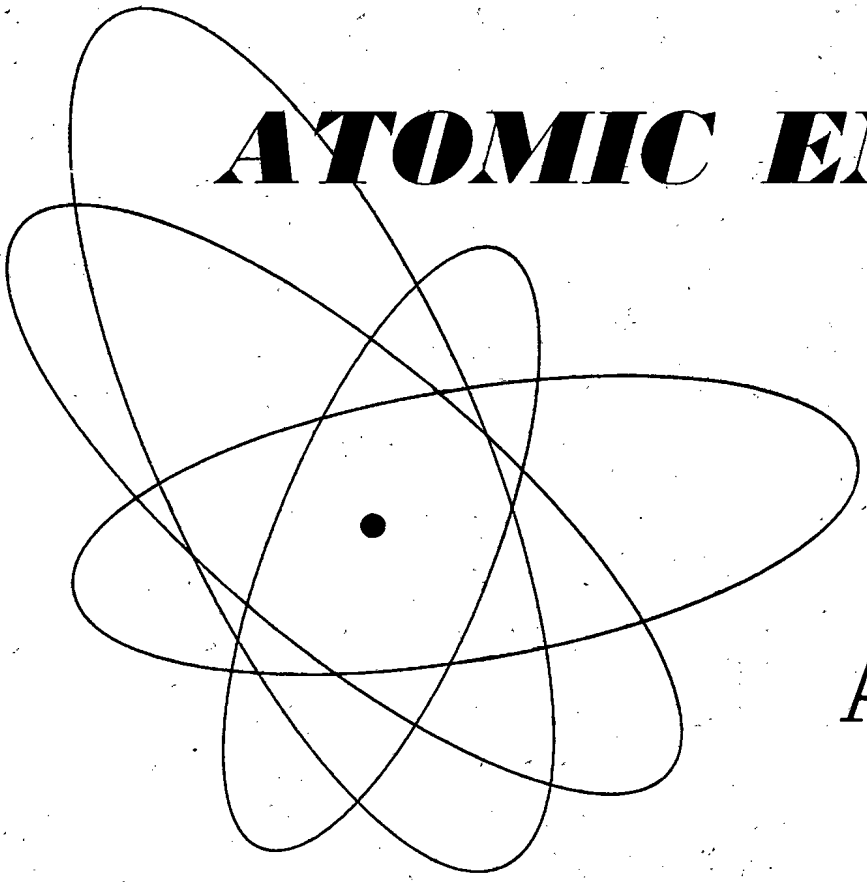

Атомная энергия

TRANSLATED FROM RUSSIAN

CONSULTANTS BUREAU, INC.

recent Russian research
—in complete English translation

A New Method in the Theory of SUPERCONDUCTIVITY

BY N. N. BOGOLIUBOV
V. V. TOLMACHEV
AND D. V. SHIRKOV

IN THIS unprecedented *complete* solution to the perplexing problem of constructing a microscopic theory of superconductivity, the authors explain their new method—*a result of the research of N. N. Bogoliubov and V. V. Tolmachev*—based on a physical and mathematical analogy with superfluidity.

Here they give *calculations for the energy of the superconducting ground state using Fröhlich's Hamiltonian, as well as of the one-fermion and collective elementary excited states;* they provide a detailed analysis of *the role of the Coulomb interaction between the electrons in the theory of superconductivity;* and demonstrate how *a system of fermions is treated with a fourth-order interaction Hamiltonian and establish the criterion for its superconductivity* – all of which is indicated in greater detail in the complete table of contents shown to the right.

cloth bound • 130 pages • $5.75

Complete Table of Contents

CB translations by bilingual scientists include all diagrammatic, photographic and tabular material integral with the text.

CONSULTANTS BUREAU, INC.
227 WEST 17TH STREET, NEW YORK 11, N. Y.

vol. 4, no. 5

May 1958

THE SOVIET JOURNAL OF

ATOMIC ENERGY

ATOMNAIA ENERGIIA

A publication of the Academy of Sciences of the USSR

Annual Subscription $75.00
Single Issue 20.00

Year and issue of first translation:
volume 1, number 1 january 1956

TRANSLATED FROM RUSSIAN

CONSULTANTS BUREAU, INC.
227 W. 17th St., NEW YORK 11, N. Y.

Printed in the United States

SOVIET JOURNAL OF ATOMIC ENERGY

Volume 4, Number 5 May 1958

CONTENTS

CONTENTS (continued)

THE ISOTOPIC CONSTITUTION OF TERRESTRIAL ROCKS AND METEORITES*

A. P. Vinogradov

The lecture cites numerous data on the isotopic constitution of sulfur, oxygen, carbon and light gases in iron, stone iron and stone meteorites. A comparison is made between the isotopic consitution of these elements in meteorites and in different rocks of the earth's crust. An analysis of these data leads the author to a number of important conclusions in the realms of geochemistry and cosmochemistry. Considering that the fractionation of isotopes in the earth's crust is the result of differentiation of terrestrial matter, the author concludes that no such differentiation occurred in the meteoritic material (in which no fractioning of isotopes is observed) and that, therefore, all meteorites must have formed by accretion of particles of primordial cosmic dust.

The overwhelming majority of elements are mechanical mixtures of isotopes. We know that the same elements and the same isotopes exist throughout the cosmos. On the basis of certain theoretical considerations and empirical data on the composition of the earth, meteorites and stars, it was possible to plot a curve which shows with some degree of probability the relation between the abundance of the nuclides in the cosmos and their mass numbers. This curve shows an overwhelming predominance of light elements, light nuclides, in the cosmos. Although our knowledge of the composition of cosmic bodies is far from perfect, we must take into account today the undoubted differences in the distribution of elements even within the boundaries of our solar system. We can speak even more definitely of the differences in the proportions of the isotopes of light elements in the planets and in the stars. The discovery of the so-called carbon-nitrogen and proton-proton cycles not only explained the possibility of variation in the isotopic constitution of hydrogen, carbon, nitrogen, oxygen and other light elements in some stars, but initiated further research in that direction. This research, as you know, has led to the discovery of isotope exchange in hydrogen, carbon, oxygen and other light elements in different types of stars.

Evidently we are not far from the truth when we insist that a continuous evolution is taking place in the nuclide composition of the cosmic bodies of our galaxy.

The variations in the isotope ratios in different stars are the result of thermonuclear processes, of astral nucleogenesis. But, the question arises, are these "hot" processes the only ones responsible for all of the possible variations in the isotope ratios which we observe in the cosmic bodies?

It is to this question that I want to draw your attention now.

The isotopic variations going on in the cold cosmic bodies are extremely small in their productivity and final effect as compared to nucleogenesis in the stars. Perhaps there would be no need to mention them at all if even the smallest variations in the isotopic constitution of igneous rocks or meteorites, for example, did not to some extent point to definite processes which have led to the formation of the earth's crust and its rocks and to the formation of different meteorite types. It is for this reason that I decided to present to you some of the results

* Lecture delivered in September of 1957 in Paris at the International Conference on the Use of Radioactive Isotopes in Scientific Research.

of comparative study of the isotopic constitution of the only cosmic materials which can be studied directly at present, namely, the more deep-seated rocks of the earth, and meteorites.

Before doing this, I must remind you briefly of the nature of the earth's crust and of the different meteorite types.

The earth is composed of a number of concentric shells: atmosphere, hydrosphere, biosphere, lithosphere and mantle.

The earth's crust or lithosphere is the solid outer shell consisting of granitic and basaltic layers. The basaltic layer envelopes the entire earth. The granitic layer covers only about one-half of it. It is absent from the bottom of the Pacific Ocean and, apparently, from the deeper basins of the other oceans. The thickness of the basaltic layer averages 15-25 km, but is much less under the oceans. The granitic layer reaches its maximum thickness of 15 to 20 km on the continents. The earth's crust is distinguishable in the structure of the earth not only by its chemical composition but also by its seismic properties. At a depth of 40 km, it is separated from the underlying materials of the mantle by the so-called Mohorovicic discontinuity. The rocks of the mantle, such as dunite, for example, approach olivine in composition, and sometimes reach the earth's surface by filling the deeper fractures in the crust. On the surface the earth is covered by a veneer of sedimentary rocks.

It is very probable that the igneous rocks of the earth's crust were formed during geologic time as the result of fusion of the materials of the mantle. In order to produce high concentrations of certain elements in the igneous rocks of the crust, for example in granites, a great thickness of the mantle material must have been mobilized. The composition of the mantle, as accepted by most scientists with but a few minor reservations, is identical with that of the stone meteorites known as chondrites. The identity in composition of the iron meteorites and the earth's core, and of chondrites and the ultrabasic rocks of the deeper parts of its mantle was first pointed out by G. A. Daubrée, member of the French Academy of Science and corresponding member of the Russian Academy of Science.

A few words about meteorites.

All meteorites belong to three main classes: a) stones, b) iron-stones and c) irons. The so-called chondrites predominate among the stones. Chemically they are very near the terrestrial ultrabasic rocks. The most interesting characteristic which distinguishes them from terrestrial rocks is their structure. They are composed of the so-called chondrules – solidified droplets of silicate material (Figs. 1 and 2).

The chondrules are cemented together by fragments or powder of broken chondrules. Sponge-like masses of nickel-iron alloy (constituting on average about 12% of the meteorite by weight) and inclusions of troilite are found in the matrix of the chondrites.

The iron-stones, including the so-called pallasites, consist of spongy masses of iron with included chondrules of silicates (mainly olivine and enstatite).

TABLE 1

Falls and Finds of Different Types of Meteorites

Type of meteorite	Finds	Falls
	number	
Iron	409	29
Iron-stone	46	6
Stone	165	547
Total	620	582

The irons contain on the average about 8% of nickel. The most common inclusions in them are troilite-FeS, Schreibersite $(Fe, Ni)_3P$, etc.

The main mass of iron in meteorites exists in two phases – kamacite and taenite, and this determines the structure and composition of iron meteorites (Fig. 3).

The following brief statistics compiled some time ago by Watson show the relative proportion of different meteorites and give an idea of their durability under terrestrial conditions (Table 1).

We shall turn now to the isotopic constitution of a number of elements in terrestrial igneous rocks and in meteorites.

Three processes which lead to the variation in the isotope ratios in igneous rocks and meteorites may be mentioned:

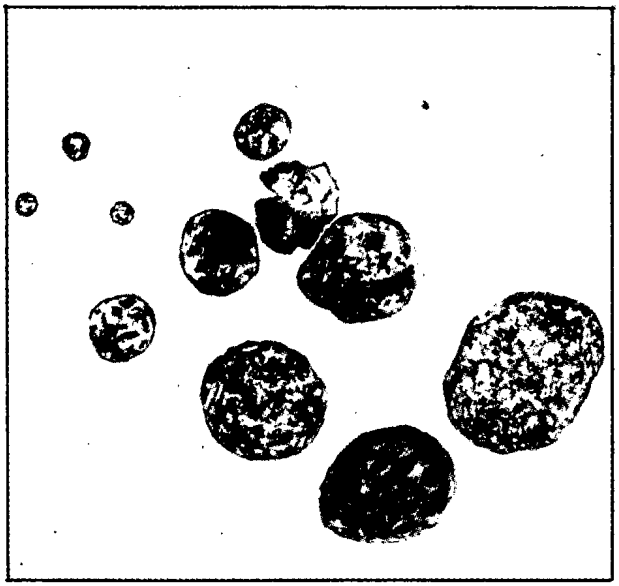

Fig. 1. Chondrules from a meteorite (Nikol'skoe) (×4.5).

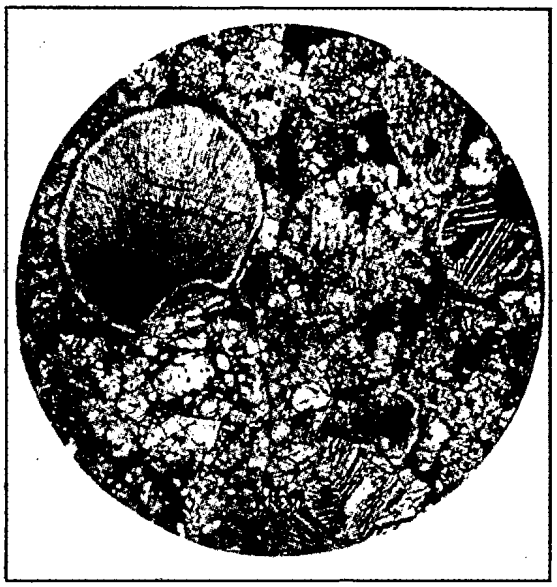

Fig. 2. Chondrules. Under the microscope in transmitted light (× 20).

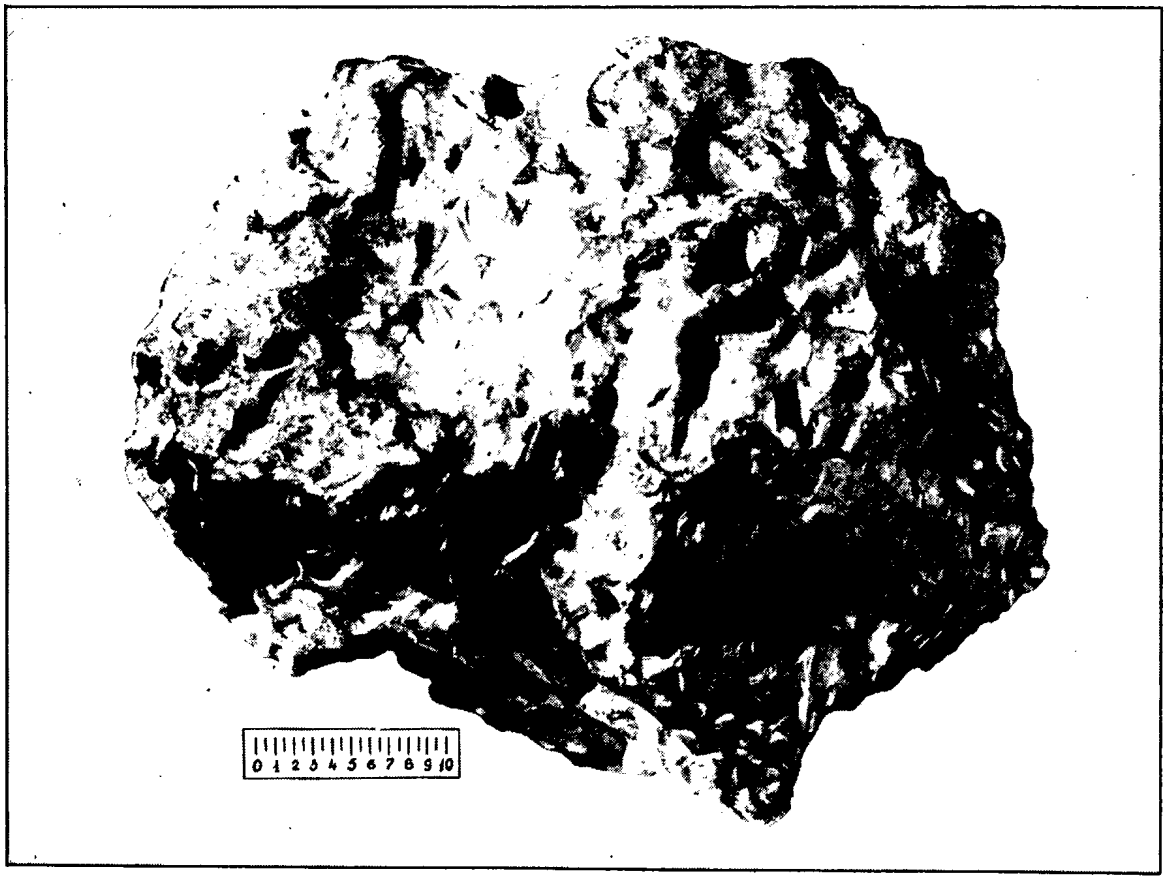

Fig. 3. A fragment of iron meteorite (Sikhote-Alin'). View of the surface.

1. Radioactive decay of uranium, thorium, K^{40}, etc.

2. Spontaneous fission of uranium and throium, and nuclear transformations caused by α-, β- and γ-radiations of uranium, thorium, etc. Nuclear reactions induced by cosmic radiation.

3. Change in the isotope ratio due to isotope exchange or to other similar processes of separation, or to admixture of stable isotopes of radiogenic or other origin.

With very few exceptions, all elements have either radioactive isotopes or some proportion of stable isotopes which are the end products of radioactive decay of the neighboring radioactive isotopes.

A substantial role in the variation of the isotope ratio is played first of all by lead and helium and the end products of radioactive decay of the uranium, actinium, thorium and possibly neptunium series, as well as by the products of some twenty transformations of the type: $K^{40} \rightarrow E \rightarrow A^{40}$, $Rb^{87} \rightarrow Sr^{87}$, $Sm \rightarrow Nd^{143}$, $Bi^{209} \rightarrow Tl^{205}$, etc. It is realized now that these primary processes of radioactive decay do not exhaust the influence of radioactive elements on the composition of rocks and meteorites. Under the influence of α-, β-, and γ-radiations from radioactive elements in rocks and meteorites, secondary nuclear reactions such as (α, n) and $(\alpha, 2n)$ are initiated under favorable geochemical conditions, which affect the light nuclei of beryllium, lithium, boron, etc. It was observed by V. G. Khlopin in the Soviet Union that there is a relatively high content of helium in pegmatites rich in these light elements. In the rare earth pegmatites containing uraninite or thorium minerals, the possibility of formation of a natural source of neutrons similar to $Be \rightarrow Ra$ or $Be \rightarrow Po$, etc., is not excluded. The production of neutrons in rocks and minerals, in its turn, leads to the neutron capture reactions (n, α), (n, p), (n, γ), etc., which cause fission in uranium, and are known for a series of elements, for example for U^{235+n}. As we shall see later, fission of U^{235+n} in nature rivals spontaneous fission of uranium and thorium. Under natural conditions these reactions produce an extensive series of fission fragments. Later I shall return to the production of the inert gases in rocks and minerals as the result of fission of U^{238} and U^{235+n}. Secondary reactions such as (γ, n), $(\gamma, 2n)$ or (γ, n, p) with beryllium and other nuclides are initiated in exactly the same way.

Among these numerous transformations, some have found practical application in geology in the determination of the absolute age of minerals, rocks and the earth's crust, and of the age of the earth and meteorites. Many other reactions require further detailed study.

Pursuing my main topic, I shall consider in some detail only one or two examples of distribution of certain isotopes formed as the result of natural nuclear processes in igneous rocks and meteorites.

The first example is the variation in isotopic constitution of lead and the inert gases in rocks and meteorites. Lead has four stable isotopes: cosmic-Pb^{204}, whose amount does not increase in rocks, radiogenic Pb^{206} and Pb^{207}, and Pb^{208}, which is evidently partly radiogenic. A study of the isotopic constitution of lead in iron meteorites permitted the determination of their age with great accuracy, since lead is not lost from meteorites and the processes which could change its isotopic constitution are virtually absent. Furthermore, on the basis of several hundred determinations of the isotopic constitution of lead from ores of different geologic ages, it was possible to make the first experimental determination of the age of the earth. But the most substantial achievement of the isotopic analysis of lead ores and minerals is the proof of the absence from the earth's crust or mantle of an ore layer, of a permanent storage of lead with uniform isotope ratio (and likewise of a storage of other ore minerals). The lead of the ores separated from magma or the rocks of the earth in some geological period and its isotopic composition marks its age. Moreover, lead always occurs in traces in the ores of iron, copper, etc., also, and its isotopic consitution records the time of separation of these ores from the rocks or magma. It is interesting that the abundant data on the isotopic constitution of lead in ores of different geologic ages and from different localities point to the restriction of the ore-forming processes in time to a limited number of tectonic-magmatic cycles in the earth's crust, not ; however, without a considerable transgression of their boundaries. We immediately recall here the early ideas of metallogenetic epochs of the earth. The use of the isotope ratios in the study of the ore-forming processes in the earth's crust is only beginning. I believe that the study of distribution of radioactive elements and their products in basalts and granites with application of the laws of radioactive transformations must logically lead to the solution of the problem of relation between basalts and granites, a complex and always vital problem.

In this connection I should like to draw your attention to one curious detail of the behavior of lead in stone meteorites, basalts and granites (Fig. 4).

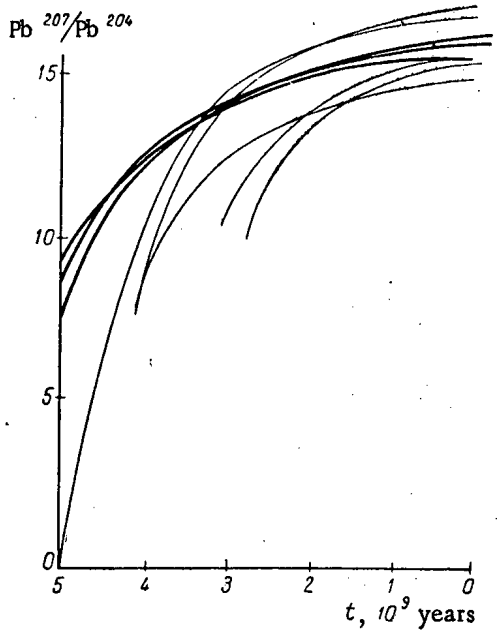

Fig. 4. Change in Pb^{207}/Pb^{204} ratio with time. Heavy lines – in ultrabasic and basic rocks and in meteorites; fine lines – in acid rocks, granites.

If, starting with the present isotopic constitution of lead from stone meteorites, basalts and granites of any geologic age, we extrapolate the possible isotopic ratios for any pair of lead isotopes, for example, Pb^{207}/Pb^{204}, in the past, we shall obtain curves shown in Fig. 4. The curves for stone meteorites and basalts are parallel to each other (and to the "age of the earth" curve). The curves for granites break off very quickly. Further extrapolation of granite curves leads to absurdity. These curves, it seems to me, indicate that, compared with granites, the material of ultrabasic and basic terrestrial rocks and of stone meteorites is more "ancient," more "primordial," has undergone fewer changes and contains lead with less disturbed isotopic ratio. The granitic material has undergone relatively greater changes and the isotope ratio of its lead shows a greater departure from the "primary," normal ratio. This is a detail, but it throws light on the relation between basaltic and granitic materials.

Another example is the isotopic consitution of the inert gases: helium, neon, argon, krypton and xenon in rocks and minerals (Table 2). They form not only as the result of radioactive decay of uranium, thorium, K^{40} and the fission of uranium and thorium, but also, at least so far as meteorites are concerned, as the result of profound nuclear disintegration under the impact of cosmic radiation. I shall consider all these processes of formation of the inert gases in rocks and meteorites together. Under the impact of cosmic particles, protons and others, and under the influence of the secondarily formed neutrons and mesons, new radioactive and nonradioactive nuclides are formed in the meteorites and on the earth's surface (mainly in the atmosphere). The chemical composition of the atmosphere and particularly the isotopic consitution of its inert gases, as we shall see, reflect the composition of the gases in the igneous rocks. Moreover, it is believed that many of the atmospheric gases are the result of degassing of the earth during the entire geologic time. Therefore, knowing the amount of the inert gases added to the atmosphere as the result of the activity of cosmic radiation, we can form an idea of the composition of these gases in the deep-seated rocks of the earth. As for the action of cosmic radiation on the isotopic composition of the inert gases in meteorites, this depends, first of all, on the size of the latter – the smaller the meteorite, the more readily it is pierced, as it were by the cosmic particles. Thus the accumulation of inert gases and other products of reaction between the nuclides and the cosmic particles takes place either on the surface of the meteorite or deep within it, depending on the thickness of the meteorite. It depends also on the duration and intensity of radiation, the age of the meteorite and its chemical composition.

TABLE 2

Isotopic Constitution of Some of the Inert Gases in the Atmosphere, Rocks and Meteorites

Material	A^{40}/A^{36}	A^{38}/A^{36}	Ne^{21}/Ne^{20}	Ne^{22}/Ne^{20}	He^3/He^4
Earth's atmosphere	296	0,187	0,00283	0,097	$\sim 1 \cdot 10^{-6}$
Igneous rocks	—	0,5	—	—	$\sim 1 \cdot 10^{-7}$
Stone meteorites	—	0,6	0,6	0,6	0,02
Iron meteorites	—	1,6	0,89	0,98	0,3

Helium, the most abundant of the inert gases, is produced by radioactive decay or by the action of cosmic particles on matter. It has two isotopes, He^3 and He^4. In the earth's atmosphere, in gases and in rocks, where He^4 is radiogenic, it is 10^6 times more abundant than He^3. The isotope He^3 forms in the atmosphere according to the reaction $N^{14}+n^0 \rightarrow 3He^4 + T^3(He^3)$ (or according to some similar reaction) and is not noticeably absorbed by the rocks. In stone meteorites, He^4 is produced as the result of decay of uranium and thorium and, together with He^3, as the result of the bombardment of meteoritic matter by cosmic particles. The He^3/He^4 ratio in stone

meteorites varies considerably, but is near 0.02. In iron meteorites the nuclei of iron are vaporized under the impact of cosmic particles, and both He^3 and He^4 are produced. The content of uranium and thorium in iron meteorites is negligible and, as was shown by Paneth and others, the He^3/He^4 ratio is 0.3. The amount of helium and the He^3/He^4 ratio change with depth in the meteorite. Thus, terrestrial rocks and stone and iron meteorites differ in the He^3/He^4 ratio both qualitatively and quantitatively (Table 2).

The isotopes of neon and argon behave in a somewhat different way.

The origin of the isotopic consitution of atmospheric neon, and therefore the neon in rocks, has not been sufficiently studied. Not all of the reactions responsible for the isotopic constitution of the atmosphere are clear as yet. Ne^{20} predominates sharply in the atmosphere (90.9% of the total Ne).

It has been shown by many investigators that the Ne/A ratio is of the same order of magnitude in the atmosphere ($3.8 \cdot 10^{-3}$), igneous rocks ($1.7 \cdot 10^{-3}$) and natural gases ($2.5 \cdot 10^{-3}$) as in stone meteorites, and it may be concluded, therefore, that the isotopic composition of terrestrial neon is partly the result of the fission of uranium and partly, of neutron reactions with oxygen and fluorine. We found, however, that the isotope ratio of neon from the Sikhote-Alin' iron is quite different from that of the terrestrial neon. In the meteorite some of the neon isotopes are relicts resulting from vaporization of iron nuclei under the impact of cosmic particles. The ratio of the three neon isotopes is near unity. In the Sikhote-Alin' iron, the amount of neon diminishes somewhat with depth but without noticeable change in the isotope ratio. Approximately the same isotope ratio was found in the neon from stone meteorites. In the latter, it is mainly the nuclides lighter than iron that react with the cosmic particles, and it is possible, therefore, that this is responsible for the slight difference in the isotopic composition of neon (as well as of argon).

In rocks (and hence in the atmosphere) A^{40} predominates, its main source being the decay of K^{40}. The A^{38}/A^{36} ratio in radioactive minerals (the result of neutron reactions) and in rocks is about 0.5. These are the main sources of atmospheric argon. Gerling believes that the isomer K^{38} may also be a source of A^{38}. In stone meteorites A^{40} accumulates as the result of decay of K^{40}, and its amount depends on the age of the meteorite. A^{36} and A^{38} form from vaporization of the nuclei or iron and lighter elements of the stone meteorites. Hence, the A^{38}/A^{36} ratio in rion and stone meteorites must be nearly the same. The content of A^{36}, A^{38} (and also of A^{40}) in iron decreases toward the interior of the meteorite.

A few words about the heavy inert gases. It has been shown by Thode and others that two processes are responsible for the existence of a number of isotopes of krypton and xenon in the earth — the spontaneous fission of U^{238} and the neutron-induced fission of U^{235}. The isotopic constitution of xenon and krypton in radioactive minerals is the result of both of these processes. Under natural conditions the heavier isotopes of these gases predominate. Thus, The Xe/Kr ratio in uranium-bearing and other minerals is 5.0. Although the gases of the igneous rocks and of the atmosphere have practically the same Xe + Kr/A ratio ($1.9 \cdot 10^{-4}$ and $1.2 \cdot 10^{-4}$), the isotopic constitution of the atmospheric xenon and krypton is quite different and so is the Xe/Kr ratio, which is 0.08.

The isotope ratios of the stable isotopes in igneous rocks and in meteorites must be mentioned. As should be expected from thermodynamic considerations, the greatest effect of fractionation of isotopes in nature is observed among the lighter elements. In the rocks of the lithosphere, significant variations of the isotope ratio are observed in sulfur, oxygen, carbon, hydrogen, nitrogen, boron, etc. It is easy to guess that the variations in the isotope ratios in nature are caused by different physicochemical processes occurring in the earth's crust (which are easily reproduced in the laboratory), such as evaporation, diffusion, etc. Both observation and experiment show that isotope exchange is the usual cause of variation in the ratio of the stable isotopes. It takes place in vapors, liquids and melts. It is well known that the equilibrium constant during this exchange approaches unity as temperature rises; i. e., isotope fractionation becomes less and less probable with rising temperature. Geologic periods of time are long enough for isotope exchange to reach equilibrium, as for example during the cooling of magma. Thus, the isotope ratio for different stable isotopes in rocks is in effect a local geologic thermometer of the process, provided there has been no subsequent isotope exchange between the frozen magma and the surrounding rocks.

We have found that the sulfur of the iron meteorites is identical in isotopic constitution with that of stone meteorites. There is, however, a considerable difference in the isotopic constitution of sulfur from igneous rocks, high-temperature sulfide ores and meteorites. This difference is observed in the high-temperature sulfides separated

TABLE 3

Average Isotopic Constitution of Sulfur From Igneous Rocks, Ores and Meteorites

Material	No. of cases	S^{32}/S^{34}
Stone meteorites	13	22.20
Iron meteorites	10	22.20
Volcanic sulfur	15	22.21
Ultrabasic rocks (dunites)	4	22.20
Basalts	2	22.178
Granites	2	21.780
Magmatic sulfides	7	22.138
Hydrothermal sulfides	32	22.148
High-temperature sulfates	–	21.885
Marine sulfates	13	21.75

TABLE 4

Average Isotopic Constitution of Oxygen in Igneous Rocks and Stone Meteorites

Material	Number of measurements	O^{18}/O^{16} in %
Granites	11	4.5
Basic and ultrabasic rocks	8	7.0
Stone meteorites	3	7.0

from the magma at an early stage. It is greater in hydrothermal sulfides. The isotopic constitution of sulfur in basalts and granites is different from that in the meteorites. Only the sulfur from ultrabasic rocks, especially dunites, which are chemically to stone meteorites, has isotopic constitution identical with that of the meteorites. Let us consider now the sulfur of volcanic origin. Its isotopic constitution is very similar, if not identical to that of the meteoritic sulfur. Thus, the isotopic consitution of sulfur of iron, stone-iron and stone meteorites, of the rocks of the earth's mantle and of volcanic sulfur is very much the same and has a definite constant composition. The rocks of the lithosphere and ores contain sulfur with a considerably changed isotopic consitution. Still greater difference in the isotopic constitution of sulfur is observed in the biosphere.

The equilibria which arise in the system $Fe-S-O_2$ at the moment of separation of ore from the magma can be partially computed. It is during this process that the fractionation of the isotopes of sulfur begins.

Evidently this does not occur during the formation of different meteorites, for in all of them sulfur has exactly the same composition. The material of meteorites did not undergo the processes of liquation or fractional differentiation which were responsible for the formation of terrestrial rocks.

Exactly the same tendency of increasing effect of fractionation of isotopes in the rocks of the earth's crust with decrease in depth is observed for the isotopes of oxygen. The isotopic composition of oxygen in stone meteorites is very near that of the oxygen of ultrabasic rocks. The great variation in isotopic constitution of O_2 in granites as compared to other igneous rocks has been noted by many investigators besides ourselves. In granites this variation is from 7.7 to 12.2%, in basic rocks (basalts), it is only from 6.7 to 7%. The greatest variation in isotopic constitution of O_2 is found in granites and stone meteorites (Table 4). The high content of O^{18} in acid rocks– granites – is due to the fact that the quartz molecule SiO_2^{18} accumulates it just as does the CO_2 molecule. The effect of O^{18} of quartz on the isotopic constitution of oxygen is especially noticeable in sedimentary rocks enriched in colloidal SiO_2.

It is clear that even greater variation in the isotopic constitution of O_2 as well as of other light nuclides must occur in the biosphere.

TABLE 5

Average Isotopic Constitution of Carbon in Limestones, Meteorites and Igneous Rocks

Material	No. of cases	Variation of C^{12}/C^{13}	Average C^{12}/C^{13}
Limestones	92	88.1-89.5	89.0
Iron meteorites	13	89.6-91.8	90.6
Stone meteorites	26	89.6-91.2	90.6
Igneous rocks	13	90.3-91.2	90.8

In spite of the vast amount of data on the isotopic ratio of C^{12}/C^{13}, it is very difficult to correlate them. For this reason I shall use largely the data obtained in my own laboratory. On the average, the isotopic constitution of carbon in iron and other meteorites is the same. However, the variation in the isotopic constitution of carbon is much greater in iron than in stone meteorites. Besides the dispersed carbon in irons there are also sparse inclusions of the carbide Fe_3C, cohenite. According to Craig, the C^{12}/C^{13} ratio in the iron of the Canyon Diablo meteorite is 89.45, while in cohenite it it 90.51. It is possible that the observed variations are due to the different ratios of cohenite to the dispersed carbon in different meteorites (Table 5).

The C^{12}/C^{13} ratio in igneous rocks is very close to that in meteorites, but in the former, so far as can be judged from limited data, there is a tendency toward a decrease in the content of C^{13}. This is logical, since greater fractionation of C^{12} and C^{13} takes place in rocks partly because of deposition of great masses of $CaCO_3$, which is strongly enriched in C^{13}.

During this brief period, I have barely had time to touch upon what I consider the most basic point – the variety of processes taking place in the materials of the earth's crust and meteorites under the influence of radioactive elements and cosmic radiation which continually change their isotopic constitution.

I think you understand correctly that each of these processes disturbs the isotopic constitution of matter to a different degree. In terrestrial rocks, radioactive decay has the greatest effect. Reactions induced by α-particles and neutrons resulting from radioactive decay produce a considerably smaller effect. In meteorites the effect of cosmic radiation is of great importance.

The variations in the isotope ratios, mainly in the lighter nuclides in igneous rocks and meteorites, are systematic, as we have seen, but their magnitude is seldom large.

However, today we can no longer speak of the constancy of isotopic consitution. The slight changes in the isotope ratios in lead, inert gases and in a number of light elements are of great importance in geochemistry and cosmochemistry, since they provide clues to the origin of rocks and meteorites. We are convinced that the isotope ratios are different in different igneous rocks and that the isotopic constitution of igneous rocks is different from that of meteorites. We are convinced also that the isotopic constitution of stable light elements varies in a definite way from the deeper parts of the earth toward its surface. This variation is not observed in meteorites. The isotopic constitution of the light elements in different meteorite types has a considerably smaller range of variation than that of the same elements in igneous rocks. The processes of accumulation of the inert gases and their isotopic constitution in igneous rocks (and hence the isotopic constitution of the atmospheric gases) and in meteorites differ, for in the first case they are due mainly to natural radioactivity while in the second case they are largely the result of cosmic radiation.

The difference in the isotopic constitution of rocks and meteorites leads, it seems to me, to the conclusion that the processes of formation of the igneous rocks and meteorites must have been different. The isotopic constitution of lead and of other stable isotopes of the mantle and the crust does not contradict the hypothesis of the origin of igneous rocks from the material of the mantle and of formation of the atmosphere by degassing of the mantle.

The isotopic constitution of meteorites, namely, the identity of stable isotope ratios in light elements of all meteorites, the presence of inert gases with isotopic constitution different from that on earth, etc., points, it seems to me, to the absence during the formation of meteorites, of fusion, liquation, hydrothermal phenomena and other analogous processes of differentation of matter such as occur in the earth's crust.

I believe, for example, that iron and stone meteorites were not formed from the primary meteorite iron-silicate melt, as is usually thought (if this were so, by the way, the stone meteorites would have lost their chondrules) but are the result of accretion of cooled drops of iron-silicate matter (in case of stone-iron meteorites). In this process, at a relatively high temperature (2000°K) the isotopes of sulfur, iron and other elements would be distributed uniformly in the iron-silicate material. Only the appearance at these high temperature of new phases, for example, the formation of carbides, would cause a certain fractionation of the isotopes. This apparently is not contradicted by facts. In brief, the study of variations in isotopic constitution of natural objects and the search for the causes of these variations give geochemists hope of more profound insight into the grandiose processes of formation of cosmic bodies. If this dry account has infused even one of you with enthusiasm, then you must admit that the use of isotopes in geochemistry is a magnificent method.

I thank you very much for your attention.

Received January 30, 1958

ADDRESS GIVEN IN PARIS, SEPTEMBER 12, 1957*

THE FUTURE OF ATOMIC ENERGY

Sir John Cockcroft

At an evening meeting of the 1955 Geneva Conference on the Peaceful Uses of Atomic Energy I was bold enough to deliver an address on the future of atomic energy. Tonight I have been asked to appear once again in the role of a prophet and I will try to describe how these visions of the future have changed during the last two years.

At Geneva our economists and statisticians predicted that the world's total energy requirements would increase by about one and a half times by 1975 and by three times by the year 2000. To meet this enormous increase in the demand for energy rising to the equivalent of seven milliard tons of coal a year it will be necessary to make the fullest use of potential hydroelectric resources, which are capable of doing the work of one milliard tons of coal a year, and also to call on nuclear energy to provide most of the rest of electricity supplies, doing the work of two to three milliard tons of coal a year, leaving coal and oil to provide the rest.

In the middle distance of 1975 electricity production was predicted to increase about four times over the 1955 level — from 1500 milliard kilowatt hours to 6000 milliard kilowatt hours — requiring the equivalent of 3 milliard tons of coal.

During the last two years the countries of Western Europe have taken stock of their energy requirements and have realised that, since their coal production is increasing very little, their increased energy requirements would require very large increases in imports of coal and oil. Thus, if nuclear energy were not developed, the six Euratom countries foresaw their bill for fuel imports rising from 2 billion dollars a year in 1957 to 6 billion dollars in 1975.

Without the development of nuclear energy in the United Kingdom fuel imports for electricity production might increase by up to about £ 350 million.

The Euratom countries have therefore prepared a target plan to install 15,000 megawatts of nuclear power stations by 1967. The United Kingdom Government has decided to build nuclear power stations having a capacity of 5,000-6,000 megawatts by 1965, these stations to do the work of 18 million tons of coal a year and will reduce our fuel imports correspondingly.

By 1975 the Euratom plan would save 100 million tons of coal equivalent a year and the United Kingdom nuclear power development may well save 40-50 million tons of coal equivalent.

The situation in other Western European countries is rather similar, though the time at which nuclear power will become important depends on the date at which hydroelectric supplies are fully utilised. Thus Sweden now obtains three quarters of its energy from imported fuel at a cost of 17% of its total import bill. On the other hand, Swedish hydroelectric resources will not be fully exploited until 1968-70 so nuclear power development is not so urgent. A similar situation prevails in the Soviet Union and the United States.

In the U.S. and USSR abundant supply of conventional fuels and unexploited hydroelectric capacity will delay very large scale exploitation of nuclear power. The latest forecast predicted 3-4,000 megawatts for the U.S. by 1965 and 1,500 megawatts for USSR by about 1961.

In Asian countries, Japan is in a similar situation to Western Europe; India has great resources of hydroelectric power and will only require nuclear energy in regions remote from hydro-supplies, (some Middle East

*This is a reprint of the full original text, supplied by courtesy of Sir John Cockcroft. The Russian translation that appeared in Atomnaia Energiia was a slightly abbreviated version.

countries like Iraq have immense indigenous oil supplies and are hardly likely to be interested in nuclear power this century.

In Africa the great hydroelectric schemes at Owen Falls and Kariba Gorge, and the Volta Scheme of the Gold Coast, together with abundant coal in the other areas, mean that nuclear power applications will be limited in scope during the next two decades.

In Oceania, hydroelectricity is abundant in the South Island of New Zealand and coal is abundant in many parts of Australia, though nuclear power may be important in mining areas and in South Australia by 1965.

By 1965 then, nuclear power will be developing rapidly in Western Europe and more slowly elsewhere.

In Great Britain the nuclear power plan is already being translated into concrete and steel and three nuclear power stations of about 300 megawatts output each are being built for completion in 1960/61. A Somerset station of 500 megawatts output will follow by 1962 and at least 8 further great stations by 1965.

In these plans, and those announced in other countries, two types of nuclear reactors seem likely to play the major role. Britain is basing the first stage of its programme on the gas cooled graphite moderated reactor; the United States and USSR are building their first full scale nuclear power stations with pressurised water reactors.

The first United Kingdom nuclear power stations are characterised by rather high capital costs but low fuel costs resulting from the use of natural uranium. The United States pressurised water reactors have lower capital costs but higher fuel costs due to their use of the more expensive enriched uranium fuel. The relative economies of the two types of power units vary in different countries, depending on the cost of labour, the interest charges and method of financing. Thus the gas-cooled graphite moderated reactor will produce electricity more cheaply in the U.K. than it would in the U.S.

Capital costs of the gas-cooled graphite moderated reactor in particular are, however, likely to fall rapidly with foreseeable increases of ratings and fuel temperatures of reactors, and Sir Christopher Hinton has predicted that nuclear power costs will fall 30% in the decade from 1960-1970, whilst on previous trends the cost of power from coal fired stations may rise up to 10% in this period.

If we turn from predictions to actual experience, we in Britain have by now had fifteen months of experience of operating the Calder Hall nuclear power station, which produced 70 megawatts of electricity using two nuclear reactors as a source of heat. Our experience in operating this power station has so far been very good, better indeed than most conventional power stations. There is in fact little to go wrong in the nuclear parts of a power station except the uranium fuel elements. Any maintenance trouble usually comes from conventional components such as pumps or from mechanical gadgets.

The fuel costs of nuclear power stations depend on the amount of heat which can be extracted from each ton of uranium before the chain reaction runs down. We base our cost forecasts on the assumption that from each ton of uranium we will be able to extract the heat equivalent of 10,000 tons of coal in the 1960 stations. This depends on fuel elements retaining their integrity throughout a life of four to five years. Each Calder Hall reactor contains 10,000 fuel elements – so far only three fuel elements have developed faults – usually tiny cracks in the walls of the sheathing metal. These cracks lead to a small escape of radioactivity into the gas stream which is detected quickly, so that the fuel elements can be changed when convenient. So far as it goes then, Calder Hall experience is favorable for the future of nuclear power development and translates dreams into realities.

We can also foresee the possibility of steadily improving this type of nuclear power station. Conventional engineering improvements will play their part in increasing output and lowering capital costs between 1960 and 1965. The increase in output from the 70 megawatts of Calder Hall to the 500 megawatts of the 1962 Somerset station is an example of this process. We can also foresee a further major improvement in performance by changing from metallic fuels to ceramic fuels such as uranium oxide by the mid 1960's. These have the great advantage of withstanding higher temperatures and they also resist radiation damage better than metal. These two factors should enable heat ratings and efficiency and burn-up to be increased, leading to lower capital costs and lower fuel costs.

We can also foresee that by 1965-70 recycling of plutonium fuel will be well established and that plutonium may be recycled with thorium as a fertile material to lead us into the thorium fuel cycle, which is likely to have better nuclear characteristics than the uranium fuel cycle for thermal reactors. Our experience of radiation damage of plutonium enriched fuels in some carriers has been very favourable.

We can predict then that thorium resources will, from 1970 onward, powerfully reinforce the energy available from uranium resources.

At the Geneva Conference Mr. Jesse Johnson said that in seven countries alone there was available a million tons of uranium, and that the price of uranium oxide would fall towards 10 dollars a pound by 1965. Since then, many more important uranium deposits have been found, especially in Canada, and supplies of well over 30,000 tons a year of uranium oxide are assured, whilst prices seem likely to fall even lower than Mr. Jesse Johnson's 10 dollars a pound.

If the Euratom plan is fully implemented the annual burn-up of European and United Kingdom nuclear power stations in 1975 might require about 5000 tons of uranium a year if plutonium recycling is by then in full swing. Another 5,000 tons of uranium a year would provide for the initial fuel charges of about 5,000 megawatts of new installations a year.

These requirements would be reduced by improvements in the neutron economy of reactors or by the successful introduction of breeder reactors. Britain is now building in the North of Scotland at Dounreay a 60-megawatt (thermal) fast reactor experiment designed to solve the technological problems of highly enriched fuel breeder reactors. We expect this to be commissioned in 1958 and we will accumulate experience in the formidable technological problem of the fast reactor during the course of the following two or three years. If we can solve these problems economically, we would expect that plutonium from our thermal reactor power stations would begin to be used as fuel for breeder power stations by the 1970's, and that the installation rate of breeders would then be adjusted to the output of the thermal stations.

I have so far spoken of the development of nuclear power in large blocks.

The application of nuclear power to ship propulsion and to smaller land stations is also making progress. The United States nuclear submarine, Nautilus, has a remarkable record of trouble-free performance in steaming over 60,000 miles, and already the United States is embarking on the construction of a 20,000 tons combined passenger-cargo ship powered by a 20,000 shaft horse power nuclear propulsion unit of the Nautilus type. The USSR is constructing a nuclear propelled icebreaker.

In Britain, with only modest supplies of enriched fuel, we are studying the application of reactors using natural uranium fuel or fuel of only low enrichment, since these reactors seem more likely to be economic than reactors using highly-enriched fuel. A tanker of the 40,000-60,000 tons class is the most likely candidate for quasi-economic nuclear propulsion since it has a high load factor.

In addition then to the large nuclear propelled navy of the U. S. we can foresee demonstration or prototype commercial ships sailing the ocean by the mid 1960's, but no great turnover to commercial nuclear propulsion till the 1970's.

These comparatively small power units will have application to land stations in the 20/30 megawatt output range. A large part of Britain's exports of conventional power units at present lie in this range. If 20 mw nuclear power stations can be developed to produce power at about 1 d. per unit, with a typical load factor of 50%, they would find a ready use. I think the prospects for these are good by the mid 1960's.

This type of power station will find application in the so-called under-developed countries and for remote mining areas where power costs are abnormally high at present – as much as 3 d. per unit in places like Broken Hill.

If we look still further ahead we see the glittering prospects of releasing energy from controlled thermonuclear reactions properly known as fusion reactors. The principles of a thermonuclear reactor are well known. If deuterium or a mixture of deuterium and tritium is heated up to a temperature of two or three million degrees, nuclear fusion reactions will occur, helium will be formed and neutrons will be emitted. The gas can be heated up and made highly conducting by a powerful electrical discharge either in a torus or in a straight cylindrical tube. The technical problem is to so insulate the hot plasma from the walls of the container vessel that conduction losses become unimportant. The experimenter is helped by the constructive action of the magnetic field produced by the current carried by the plasma. This pinches the plasma into a filament. The filament, however,

is unstable – it tries to turn itself into a helix and wriggles so the experimenter has to overcome this by using additional magnetic fields as the stabilising mechanism. To produce a practical thermonuclear reactor, however, the energy output must exceed the energy input. Radiation losses increase slowly with temperature, whilst the release of fusion energy increases very rapidly. For energy output to exceed energy input, temperatures of about 50 million degrees are required. This is likely to take much longer. Neutrons have already been observed by several groups of experimenters working with straight tubes in the USSR, U.S., and this country, but these have been shown to be due to conventional accelerating processes by strong electric fields and not from high temperature plasmas. It is sometimes difficult to be sure of the origins of neutrons in this work; nevertheless it is likely that temperatures of a few million degrees will be achieved shortly and with these fusion reactions will be produced by high temperature plasmas.

In Britain we have recently put into operation a torus known as ZETA with the objective of reaching temperatures of several million degrees. Promising results have already been obtained but we require time for their interpretation.

The large scale development of nuclear power in the world presents us with new safety problems, and problems of the radiological control. These are now receiving a good deal of attention in Britain and the United States. Designers and operators of nuclear reactors are very conscious of the fact that millions of curies of fission products are locked up in the fuel elements and that over-heating and melting of the fuel elements would release these fission products into the reactor circuit. The reactor design and codes of operation must ensure that temperatures cannot rise sufficiently to melt fuel elements; secondly, that even if melting takes place, the products are contained within the reactor circuit or a containing shell. Research on safety problems is important and is being carried out intensively in the U. S. and U. K. We also have the problem of concentration and storage of the radioactive waste products from the chemical separation plant where fuel elements are processed. In Britain we now evaporate our waste products to small volume and store these in stainless steel tanks. By 1960 we hope to be extracting the long-lived radio-cesium to produce radioactive sources on the megacurie scale for use in industrial processes. This will help the problem of storage of the remainder.

Other fission products such as the radioactive gases are beginning to be extracted and stored and used for industrial purposes, helping thereby to reduce the contamination of the atmosphere.

The use of these large sources of radioisotopes is now being studied actively in many countries. In Britain we have founded the Wantage Radiation Laboratory as a close satellite of Harwell, to carry out such studies. The Laboratory is now equipped with sources of radio-cobalt of up to 10,000 curies, and hopes in due course to equip itself with radio-cobalt sources of half a million curies and later on with still more powerful radio-cesium sources. These sources will be available for research by industry, Government departments and Atomic Energy Authority staff, into application of radiation to chemical processes, to food preservation, to sterilisation and other problems.

At the Wantage laboratory we are investigating many possible uses of radiation to industry. The majority of this type of work has been done in the USA where millions of dollars have been spent on investigations on food preservation or the extension of storage life of food. They have found that the storage life of bacon, ham and sausages can be increased by a factor of 4 or 5. To increase the storage life further would necessitate such big radiation doses that unwanted side effects such as unpleasant taste and flavor would be noticeable.

Scientists working on food preservation are now more and more adopting combined methods of preservation using radiation plus light cooking of the food, or an addition of antibiotics. These combined operations look very promising.

Radiation may also contribute to insect control. We heard at the Geneva Conference of the spectacular work on the elimination of the screw worm by the irradiation of the male flies. We are working now on grain disinfestation, a serious problem in some of the grain producing countries. Although doses of 50,000 R are necessary to kill insects much smaller doses suffice to make their eggs infertile.

Radiation is already playing a new role in sterilisation. Bone and tissue used for transplant are being sterilised in that way in at least one country (USA) and the use of radiation to sterilise hospital blankets, sutures and bandages is being actively investigated at Wantage.

Radiation may be of great importance to the treatment of antibiotics. The dose to reduce bacteria by 10^8 is of the order of $2 \cdot 10^6$ R. This dose produces a temperature rise of only 1-2°C and is therefore an ideal method

for the treatment of heat sensitive drugs like pencillin which at present have to be filtered from bacteria. After that the material has to be aseptically treated. Radiation might be used in the final packaging and give safer drugs. Experiments have shown that the amounts of radiation necessary do not influence the potency of antibiotics like pencillin, streptomycin and others. The importance of radiation to plant breeding is emphasised in a recent report of the Economic and Social Council.

The mutations induced by radiation include both gene changes and chromosomal alterations, and are in general of much the same nature as naturally occuring so-called spontaneous mutations. In both cases the majority are deleterious and only a small proportion – perhaps one in a thousand – are potentially useful. Yet it is on the basis of those relatively rare favorable mutations that all living organisms have evolved through the ages, firstly, through the agency of natural selection and subsequently, in the case of our domesticated crops and livestock, through selection exercised by man himself.

The contribution that radiation makes to plant breeding is that it vastly increases the frequency of appearance of mutations – by fifty or one hundred-fold or more – and so provides a relatively simple means of greatly expanding the variability available to the plant breeder for selection. To this extent it is a most valuable supplement to the normal procedure of collecting and maintaining a representative sample of the natural variability of the crop for use in breeding programmes.

Remembering that this entirely new approach to plant breeding was initiated less than thirty years ago in Europe and only a few years ago in the United States of America, the practical successes that have already been achieved are impressive. In Sweden an improved variety of white mustard of superior yield and oil-content, and a more uniformly-ripening, early, high yielding variety of summer oil rape are already in use, whilst a variety of cooking pea with distinctive fruiting habit and higher yield has recently been released for use in 1957. As an example of the economic return from even one such successful accomplishment, it is of interest that the white mustard variety is the only one grown in Sweden, and the value of the crop may be estimated at about 2 million Swedish crowns, whilst the annual government allocation for all mutation research work in Sweden is less than a quarter of a million crowns.

In addition in that country many promising new types obtained by irradiation in barley, wheat, oats, soya-bean, flax and many other crops are under test. Important characteristics of these new types include short and stiff-strawed types of cereals more resistant to lodging, and so better able to make economic use of fertilizer dressings and better adapted to mechanical harvesting, types with shorter or longer maturity period, and types with changed ecological adaptation in relation to such features as higher or lower rainfall. Other countries reporting promising mutations in a wide range of agricultural and horticultural crop plants include Germany in particular, and such countries as Austria, Belgium, Finland, France, India, Japan, the Netherlands, Norway and the United Kingdom which have so far had smaller irradiation programmes.

Almost all of these European and Asian accomplishments have been achieved through the use of x-rays. It is only from the United States of America that extensive accomplishments with radiation derived from atomic energy programmes sources have so far been reported, but there also x-rays have been extensively used.

The first new strain developed by irradiation to go into production in the United States of America is a bush type of bean derived from a vine type. It was developed from material treated with x-rays in 1941 and was released for the 1957 crop season. Its upright open habit makes it more tolerant of wet weather than the original type and less subject to disease and rotting, and it will also be adaptable to mechanical harvesting.

Most of the characters already mentioned are controlled by only one or a few genes of relatively large effect. Quantitative characters such as yield and quality are determined by a large number of genes of individually small effect. Particularly extensive work with peanuts in the United States of America has already demonstrated the possibility of increasing through irradiation the genetic variability in respect of yield, and by subsequent selection accumulating favourable mutants into a more productive type.

These achievements demonstrate that the induction of useful mutations by radiation is possible with respect to many kinds of characters of diverse genetical types in a wide range of crops.

In addition to the general value of radiation in providing a ready means of furnishing new breeding material, it may on occasion make a unique contribution to crop improvement by raising the frequency of occurrences of certain extremely rare types of mutation of a special nature to a level where they can usefully be employed by

the plant breeder to achieve results that he would have little or no possibility of accomplishing by other procedures. For example, it may provide a means of separating favourable and unfavourable characters that are genetically so closely associated that for all practical purposes they are usually regarded as inseparable. A close association of this nature between resistance to a particular disease and susceptibility to another in oats has already been broken in radiation experiments in the United States of America.

A very interesting new approach is the attempt to achieve cross strains from normally incompatible parents. This is approached by irradiating the pollen of one strain. Some success has been found already and it is likely that this method may yield most interesting new strains.

Some of the physical changes which radiation may produce are well known. Polyethylene can be cross linked by radiation and the resulting polymer can stand up to higher temperatures. Polyethylene melts at 110°C but when irradiated with doses of roughly 107 R, can stand up to 150°C, a very important feature for the electrical cable industry.

At present industry is trying to find new useful radiation induced polymerisation products. Vulcanisation of rubber is generally carried out by using sulphur as the link between different atoms. By using radiation this link may be established without introducing a new element and the resulting product has therefore much better temperature resistant properties. So tires are claimed to last longer.

Radiation energy may be used to make chemicals at present produced by high pressure and temperature or may even be able to give us new compounds.

The use of massive radiation is very new, in fact newer than atomic energy itself. The development is therefore in its infancy, but I believe that the use of radiation may be of very great importance and engineers of future Atomic Power Reactors may be well advised to think about the practical aspects of using some of the immense amount of gamma radiation at present unused, which is locked up in these plants.

I feel somewhat diffident in speaking about the application of radioisotopes to industry in the presence of Dr. Libby who has given us so many excellent lectures on this subject.

However, I cannot miss the opportunity of quoting his estimate that U.S. industry and agriculture is already saving half a billion dollars a year by the use of radioisotopes – at a cost to the U. S. Government of about 3 million dollars. This is a remarkable example of the multiplying and catalysing effect of research. However, still greater advantages are predicted in the future and Dr. Libby predicts the saving will rise to 5 billion dollars a year by 1960.

An interesting example mentioned by him is the use of radioisotopes to facilitate oil well stimulation. This application alone is saving 180 million dollars a year to the oil industry.

Dr. Libby sees also a great extension of process control by labelling with carbon-14 important contributions such as octane going into an oil refinery. This will be done with very low levels of activity since the initial C^{14} content is very nearly zero.

I might also mention the important contribution which radioisotopes, produced in large quantities for us by weapon trials, are making to studies of the circulation of the atmosphere – particularly North-South mixing and also to oceanography.

The potentialities of our newly won access to the inexhaustible energy of the atomic nuclei are enormous. It could be used to destroy our whole civilisation. But if we justify our status of "homo sapiens" and manage by a combined effort of the human race to avoid this, it cannot fail in the long run to provide enormous benefit to mankind.

HEAT TRANSFER IN LIQUID METALS

S. S. Kutateladze, V. M. Borishanskii, and I. I. Novikov

This article is a survey of basic work on heat transfer between solid surfaces and flowing liquefied metal that has been reported by both Soviet and foreign authors. The results of experiments on heat transfer to liquid metals are analyzed for cases where flow took place in both long and short tubes, flat channels, over bundles of rods and over a plate along their longitudinal directions, across cylinders, with free convection and condensation of liquid metal vapors. The effect of additives on the rate of heat transfer is examined. Questions that arise in connection with boiling of liquid metals are discussed, as are problems of wetting effects on fluid friction and on heat transfer rate. Equations for calculation of heat transfer rates are given.

General Discussion

Liquefied metals are high-temperature heat carriers which, due to a high thermal conductivity, provide a high rate of heat transfer.

Concurrently, however, certain unusual properties of liquid metals (a very low ratio of kinematic viscosity to heat conductivity, the high temperature of most liquefied metals, the high corrosive and erosive action of liquid metals on many structural materials, strong oxidizing properties, electrical conductivity, etc.) create difficulties in their study and their practical utilization.

Liquefied metals constitute a distinct class of coolants, characterized by a very low range of Prandtl numbers $Pr=\frac{\nu}{a}=\frac{gc_p\mu}{\lambda}$ (of the order of 10^{-2} to 10^{-3}), which is brought about by their high heat conductivity, since viscosity and specific heat capacity of liquid metals are comparable to those of gases and nonmetallic liquids.

When $\nu \ll a$, molecular transfer of momentum is significantly less intense than the molecular thermal diffusivity. Thus, two important physical phenomena are brought about:

a) the thermal boundary layer thickness is greater than the hydrodynamic boundary layer thickness, and the effect of molecular heat transport is importnt not only in the wall boundary layer but in the turbulent center of the flow channel as well;

b) the rate of heat transport is greater than the rate of motion transport in the motion of a turbulent "eddy" of fluid.

This means that, for liquid metals, in the well-known equation

$$\frac{\lambda_T}{\lambda}=\varepsilon Pr\frac{\mu_T}{\mu} \qquad (1)$$

the coefficient ϵ, which represents the inverse of the turbulent Prandtl number $Pr_T=\frac{gc_p\mu_T}{\lambda_T}$, is less than unity.

It follows that in liquid metals the relative growth of heat conduction due to turbulent transfer, characterized by the quantity λ_T/λ, is less than the relative growth of viscosity by an amount on the order of the Prandtl number, Pr. Thus, in a stream of liquid metal,

$$\frac{\lambda_T}{\lambda} \approx (10^{-2} - 10^{-4}) \frac{\mu_T}{\mu}. \tag{2}$$

Some properties of the quantity ϵ may be illustrated through the following considerations. The following well-known equations may be written for a turbulent current in a plane:

$$-q = (\lambda + \lambda_T) \frac{\partial t}{\partial y} = \lambda \frac{\partial t}{\partial y} + cg\rho\overline{v_y \theta}, \tag{3}$$

$$-\tau = \mu \frac{\partial u}{\partial y} + \rho\overline{v_x v_y}. \tag{4}$$

The mean square value of the pulsating component of velocity is $v^* = \sqrt{\frac{\tau}{\rho}}$.

It follows from these relationships that the coefficient ϵ relating the diffusion of heat content to the diffusion of motion is, in turbulent transfer, a function of at least six quantities:

$$\{v^*,\ y,\ cg\rho,\ \rho,\ \mu,\ \lambda\}, \tag{5}$$

that are made up of four basic dimensions (kg, sec, m, kcal/sec), i. e., must be combined into two dimensionless values

$$\left\{\eta = \frac{v^* y}{\nu};\quad Pr = \frac{cg\mu}{\lambda}\right\}. \tag{6}$$

When the distance from the viscous boundary layer is sufficiently great ($y \gg y_1$), the molecular viscosity may be neglected in Eq. (4) and the quantity μ may therefore be excluded from the group (5). In this case the remaining five quantities, composed of the same four basic dimensions, must be combined into one dimensionless value:

$$Z = \frac{v^* y}{a} = \eta Pr, \tag{7}$$

The preceding is true for the region of the turbulent channel center, where the relative distance from the wall y/δ does not have any noticeable effect (δ in y/δ is the boundary layer thickness or the tube radius).

Thus, in the general case

$$\varepsilon = \varepsilon\left(\eta;\ Pr;\ \frac{y}{\delta}\right), \tag{8}$$

and in the region $y_1 \ll y \ll \delta$

$$\varepsilon = \varepsilon(\eta Pr). \tag{9}$$

Voskresenskii has established that under certain simplifying assumptions regarding the motion of the turbulent "eddy," the function (9) must assume the form

$$\varepsilon = B\eta Pr\left[1 - \exp\left(-\frac{1}{B\eta Pr}\right)\right], \tag{10}$$

where B is a constant that is generally determined experimentally.

From this it follows directly that the coefficient ϵ assumes its lowest value near the boundary of the viscous sublayer and increases in value in the direction of the external boundary of the boundary layer. The few experimental results published to date, give qualitative confirmation to this analysis.

On the basis of many experiments conducted by different authors [1-9], it may be assumed with assurance that the hydraulics of liquid metals is practically identical to that of gases and nonmetallic liquids.

The experiments were conducted in tubes (1.2 to 45 mm in diameter), made of glass, of carbon steel and of chrome nickel steel. The working fluids used were water, mercury, tin, bismuth, an alloy of lead and bismuth, iron and others. The experiments also confirmed that the velocity profile is the same for the flow of metals as for the flow of nonmetallic liquids [2, 10, 11].

Theoretically the heat transfer problem for the flow of liquid metals through tubes, in the laminar regime, is solved in the same manner as for nonmetallic liquids, provided that the relative values of the quantities $\partial t/\partial R$ and $\partial t/\partial x$ are ignored [6, 12, 13]. In the case of turbulent flow there are basic differences connected with the relative values of molecular and turbulent heat conductivities in liquid metals, both in the region of the transition layer and in turbulent channel center.

If the quantity $\partial t/\partial x$, for a fixed tube cross section, is considered equal to the heat balance mean value

$$\frac{\partial t}{\partial x} = \frac{2q}{c\gamma\bar{w}R_0}, \tag{11}$$

then the following convenient integral expression may be derived for Nusselt number:

$$Nu = \left[2\int_0^1 \frac{\left(\int_0^\xi \omega\xi\, d\xi\right)^2}{\left(1+\varepsilon Pr\frac{\mu_T}{\mu}\right)\xi} d\xi \right]^{-1}, \tag{12}$$

where $\omega = w/\bar{w}$ is the relative velocity, and $\xi = R/R_0$ is the relative flow radius.

For laminar flow with a parabolic velocity distribution, it follows from Eq. (12) that Nu = 4.33.

For turbulent flow with velocity distribution in accordance with the $^1/_7$ power law and a limiting value of Prandtl number Pr = 0, it follows from Eq. (12) that Nu = 6.8.

A theoretical analysis indicates that if in the general case, for flow in circular tubes

$$Nu = f\left(Pe;\ Re;\ \frac{L}{D}\right), \tag{13}$$

then for liquid metals, when $Pr \ll 1$, for both laminar and turbulent flow regimes

$$Nu \approx f\left(Pe;\ \frac{L}{D}\right). \tag{14}$$

However, the form of this function depends on the flow regime.

Heat Transfer to a Liquid Metal Flowing in Tubes

Numerous experiments in the study of heat transfer to various liquids have demonstrated some features of the heat exchange mechanism. First of all, at low Peclet numbers the values of Nu found experimentally depart from theoretically predicted values, and this in turn leads to considerable scatter in experimental data. The results of experimental studies conducted by several authors on the heat transfer in mercury, lead-bismuth eutectic, sodium and sodium-potassium alloy, flowing through tubes, are shown in Table 1.

Mercury (Fig. 1). More experiments have been conducted with mercury than with other metals. The regions investigated include the range of Peclet numbers Pe = 20 to 20,000 at mercury temperatures up to 500°C. The results of different authors diverge significantly, reaching disagreements of up to 100%.

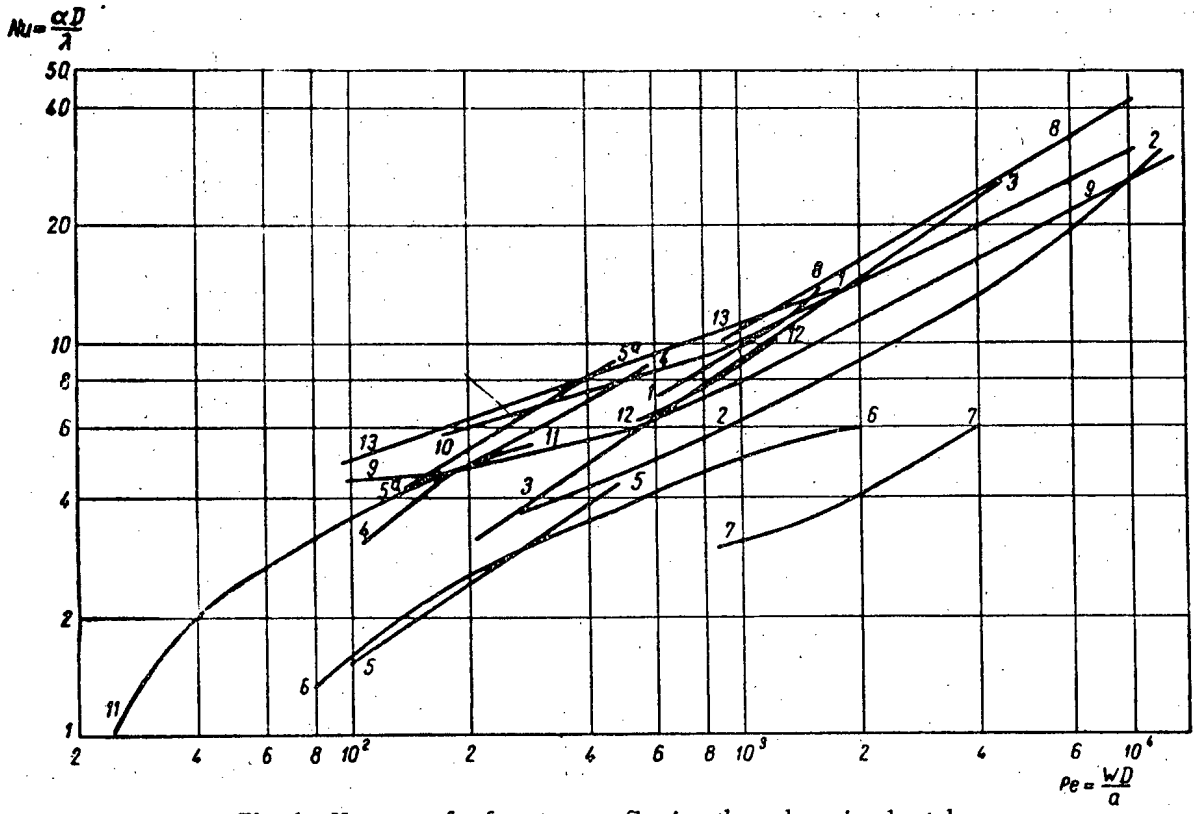

Fig. 1. Heat transfer for mercury flowing through a circular tube. Nu = f(Pe), L/D > 30.

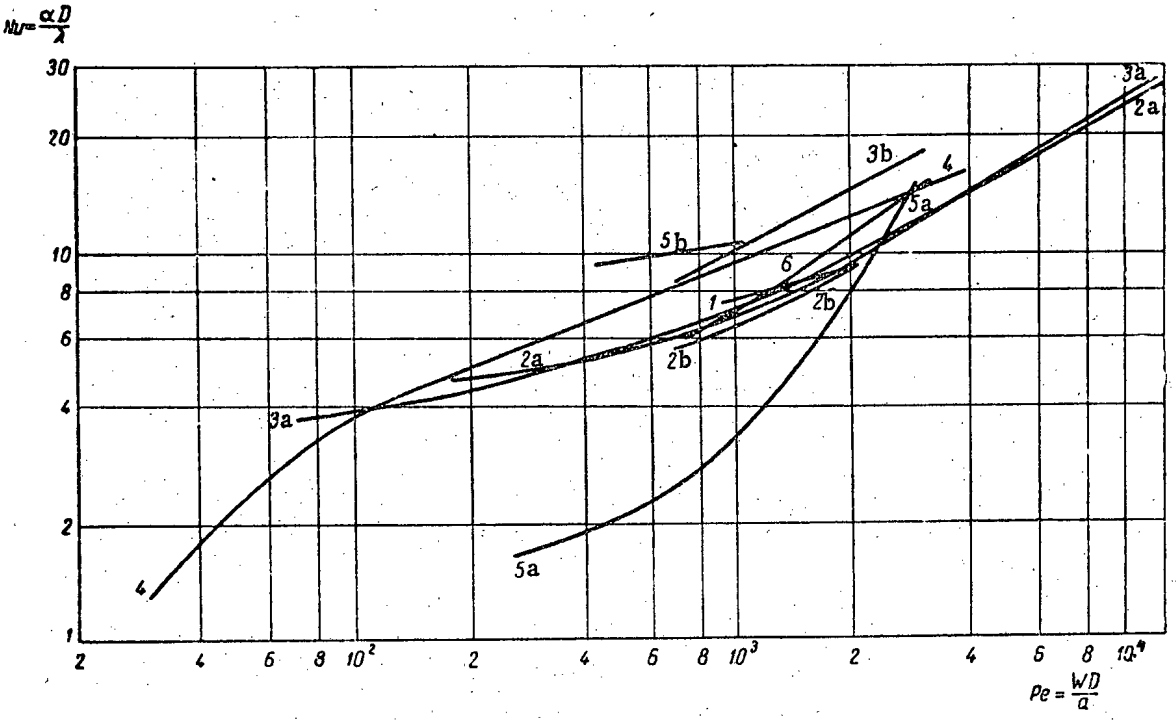

Fig. 2. Heat transfer for eutectic of lead-bismuth flowing in a circular tube. Nu = f(Pe), L/D > 30; a) eutectic, b) eutectic with magnesium.

TABLE 1

Experimental Data from Studies of Heat Transfer to Various Metals

Curve shown in table	Authors	Temperature, °C	Flow channels	Relative lengths, L/D	Peclet no., Pe	Nusselt no., Nu	Remarks
			Mercury (Fig. 1)				
1	Styrikovich, Sorin, Semenovker [1,2]	450—500	Steel and low alloy steel tube 16-40 mm diameter	—	600—1 800	7—14	The work was done in 1939*
2	Mikheev, Voskresenskii, Fedynskii, Kondrat'ev, Kalakutskaia, Petrov and others [7, 8]	20—180	Machined pipe, carbon steel, 4-10 mm diameter	30—81	300—11 000	3.5—30	—
3	Korneev [14]	60—500	Stainless steel tubing, 19, 28 and 40 mm diameter	—	250—4 500	3—25	Tests run with a Hg-Mg amalgam yielded analogous results
4	English and Barret [15]	—	1.3 mm diameter, tube	—	100—700	3—9	Both local and average heat transfer was measured, and showed marked decrease at low Pe numbers.
5	Doody and Jounger [16]	—	12.5 mm diameter	125	100—500	1.5—4.5	Addition of sodium raised heat transfer to Nu = 4-8
6	Bailey, Kop, Batson [17]	—	Steel tube 11 mm diameter	—	70—2 000	1.1—6	—
7	Elzer [17]	—	6-8 mm diameter	40	900—4000	3—6	—
8	Isaacs and Drew [11]	—	38 mm diameter steel tube	140	900—10 000	10—37	—
9	Stromquist [17]	—	9-20 mm steel tube	60—120	100—20 000	4—30	The effect of addition of sodium was not determined
10, 11	Johnson, Glabaugh and Hartnett [18]	—	16 mm diameter steel tube	74	200—10 000	6—30	In the region of Pe = = 20-200 a sharp drop in heat transferred was observed
12	Gilliland, Musser, Page [12]	—	—	—	500—1 500	6—9	The test was made on heat exchangers w/o determination of wall temperature
13	Trefethen [20]	—	—	—	100—2 000	5—14	

* In the years preceding the war, experiments with Hg were conducted also by Dozhkin and Kanaev[3,4].

TABLE 1 (continued)

Curve shown in table	Authors	Temperature in °C	Flow channels	Relative lengths, L/D	Peclet no. Pe	Nusselt no. Nu	Remarks
			Eutectic of lead-bismuth* (Fig. 2)				
1	Seban [17]	—	16.6 mm diameter	72	900—2 000	7—5—9	A drop in heat transfer of 30-40% was observed with time
2	Borishanskii, Kutateladze, Ivashchenko and Shneiderman [5]	—	Of various steels, 9-25 mm tubing	15—100	170—11 000	5—27	Heat fluxes reached $1.3 \cdot 10^6$ kcal/m²·hr Additions of magnesium did not appreciably affect heat transfer
					70—15 000	3.5—30	—
3	Fedynskii, Voskresenskii and Mikheev [7, 9]	—	Common steel tube, 5-10 mm diameter	30—64	1000—10 000	6—20	Experiments with bismuth
4	Johnson, Glabaugh and Hartnett [18]	—	Common steel tube	—	30—4 000	1.5—16	—
5	Untermeyer [17]	—	10 mm diameter tube	—	300—3 000	1.7—16	Addition of magnesium raised heat transfer to Nu = 9-11
6	Lubarsky [17]	—	10 mm diameter tube	100	800—3 500	6—17	The heat transfer was measured in a flat channel heat exchanger
			Sodium (Fig. 3) and alloy of sodium-potassium (Fig. 4)				
1	Deriugin, Mikheev and Fedynskii [7, 8]	—	Copper tube	—	500—3 000	4.5—11	Sodium
			10.3 mm diameter steel tube	45	450—5 000	6—19	Sodium-potassium
2	Novikov and Khabakhpasheva [21]	Up to 350	8.6 mm diameter copper tube	47	100—1 400	5—11	Sodium; part of the experiments were conducted with nickeled surfaces to change degree of wetting the surfaces
3	Borishanskii, Kutateladze, Shneiderman and Savinova [5]	Up to 400	Copper, 34-35 mm diameter	34	90—1 800	3—9	Sodium
4	MacDonald and Quitenton [17]	—	16 mm diameter tubing	~100	60—2 000	2—9	Sodium
2—5	Lyon [17]	—	Nickel tube	76—159	150—1 600	5—15	Heat transfer was measured in 4 heat exchangers of the flat channel type with alloy (48%K + 52% Na) flowing in both passes
6 7	Werner, King and Tidball [17]	—	Steel and nickel tubes	—	100—2 000	5—10 (for steel)	44% Na+56% K
						9—25 (for nickel)	77% Na+23% K

* Best agreement with data for lead-bismuth eutectic is obtained with bismuth [9] and tin.

In the transition and laminar regions, with Pe < 100 there occurs a sharp drop in heat transfer, down to values of Nu ~ 1.

Eutectic of lead-bismuth (Fig. 2). The range of Peclet numbers covered by the experiments was 30 to 15,000. With the exception of the experimental results of Johnson, Hartnett and Glabaugh [18], the results of the other researchers generally agree. At low Pe numbers, Pe < 100 (as in the case of mercury) a sharp drop in heat transfer is observed.

Several reports note [17, 18], that in the case of the eutectic lead-bismuth, a peculiar period of stabilization of heat transfer coefficient, as a function of time, is observed. The stable values of heat transfer coefficients thus noted are lower than initial values by 50-70%. The reason for this effect is not known.

Sodium (Fig. 3). The range of Peclet numbers Pe = 100-3000 has been investigated. The data of [9] and [17] are in mutual agreement and yield Nusselt numbers Nu = 4.5-11. The data of [21] fall at higher values. The mutual spread of experimental data is about 70 to 80% at Pe ~ 100 and 30% at Pe ~ 1000.

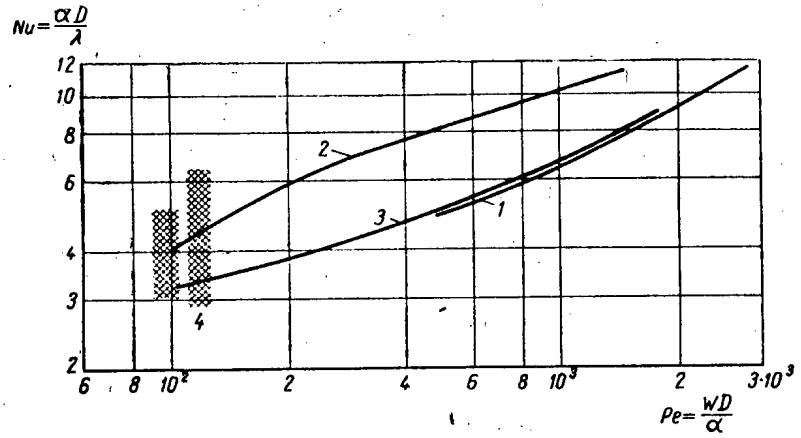

Fig. 3. Heat transfer for sodium flowing in a circular tube. Nu = f(Pe), L/D > 30.

Potassium-sodium (Fig. 4). The interval of Peclet numbers from 100 to 5000 has been studied. The spread of experimental data reaches up to 80%.

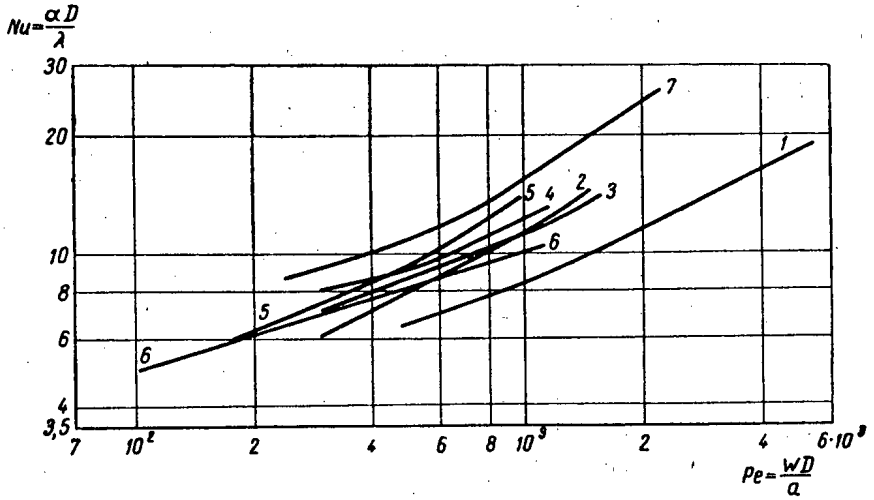

Fig. 4. Heat transfer for an alloy of sodium-potassium flowing in a circular tube. Nu = f(Pe), L/D > 30.

The effect of additives. A comparison of the work reviewed does not lead to any definite conclusion regarding the effect of surface active substances on the heat transfer to liquid metals. The experiments with mercury-magnesium amalgams, conducted by Korneev, and the experiments of Stromquist with mercury including additions of sodium, did not show any effects of the additives on heat transfer. However, the data of Doody and Jounger, conducted at the same Peclet numbers, indicate that the addition of sodium to mercury noticeably improves heat transfer. The experiments of Lubarsky, Borishansky and Kutateladze on the addition of magnesium to a eutectic of lead-bismuth did not lead to any noticeable improvement in heat transfer. The data of Untermeyer indicate a considerable improvement in heat transfer. A comparison of experiments for determination of surface material effects on heat transfer leads to the conclusion that in a qualitative sense heat transfer apparently is higher in those cases where the metal wets the heating surface. However, it is not possible at this time to make a quantitative evaluation of this effect.

The following equations may be recommended for calculation of heat transfer to liquid metals flowing in standard tubes [5, 7]:

$$Nu = 3{,}3 + 0{,}014Pe^{0{,}8}, \tag{15}$$

$$Nu = 5 + 0{,}0021Pe. \tag{16}$$

In these equations $300 < Pe < 15{,}000$, and $Re > 10{,}000$.

In the region of low peclet numbers, Pe = 20 to 300, calculations may be carried out by the approximate equation following, until more detailed data is obtained:

$$Nu = 0{,}7Pe^{1/3}. \tag{17}$$

For sodium (with tube surface wetting and very clean equipment) in the region of Peclet numbers 100 to 1400 the following equation may also be used [21]:

$$Nu = 5{,}9 + 0{,}015Pe^{0{,}8}. \tag{18}$$

The above discussion applies to average heat transfer with fluid flowing in long tubes. A number of investigations have been concerned with heat transfer in fluids flowing through short tubes. A comparison of the results of many investigations with the results of theoretical calculations has been made by Lubarsky and Kaufman [17]. It has been established that heat transfer in the entrance region is higher than it is after flow has been stabilized. As a first approximation it may be assumed that at L/D > 30 the effect of the entrance region on average heat transfer is low. For short tubes a correction factor according to Kondrat'ev and Mikheev [8] may be used as follows

$$\varepsilon_l = 1{,}72\left(\frac{D}{L}\right)^{0{,}16}. \tag{19}$$

Heat Transfer to Liquid Metal Flowing in Flat Channels

Annular ducts. Experiments with mercury and a eutectic of lead-bismuth included the interval of Peclet numbers Pe = 45 to 1700. In experiments with sodium and an alloy of sodium-potassium this interval was Pe = = 10 to 1000. A comparison of all this data, shown in Figs. 5 and 6 allows as a first approximation, the use of the equations for circular tubes given above with equivalent hydraulic diameter used in place of tube diameter, $D_e = D_2 - D_1 = 2\delta$ where δ is the width of the channel.

Flat ducts. Heat transfer in flat channels, using mercury, was measured by Sinich [17] and using an alloy of sodium-potassium it was measured by Tidball [22]. The experiments were conducted in the range of Peclet numbers Pe = 300 to 1000 and yielded values of Nu = 4-5 (Figs. 5 and 6). When the wall temperature was constant the value of the constant term in the expression for Nu was somewhat lower than when q = const.

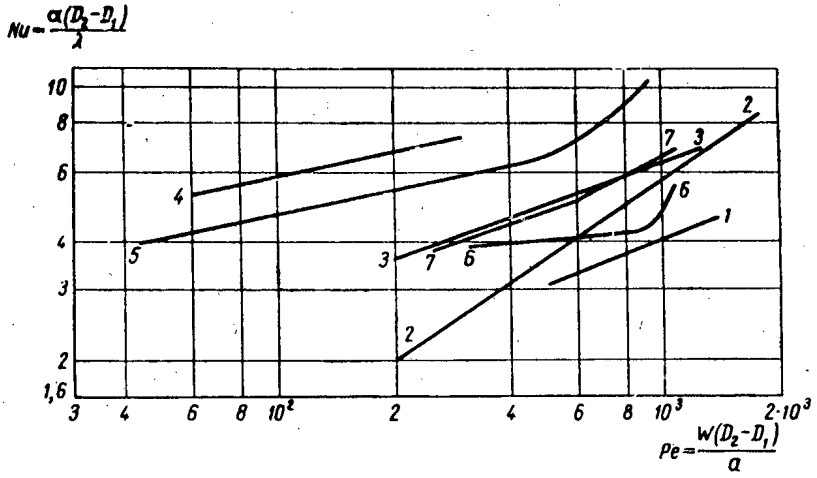

Fig. 5. Heat transfer for heavy metals (mercury, lead-bismuth) flowing through channels. $L/D_e > 30$. Results of experiments with mercury: 1) Stirikovich, Sorin and Semenovker; 2) Korneev ($D_2/D_1 = 1.35$); 3) Mikheev, Fedinskii ($D_2/D_1 = 1.55$); 4) Trefethen ($D_2/D_1 = 1.4$); 5) Trefethen ($D_2/D_1 = 1.75$-2.31); 6) Sinich (flat channel, $\delta = 6.3$ mm). Results of experiments with eutectic of lead-bismuth: 7) Lubarsky ($D_2/D_1 = 1.25$).

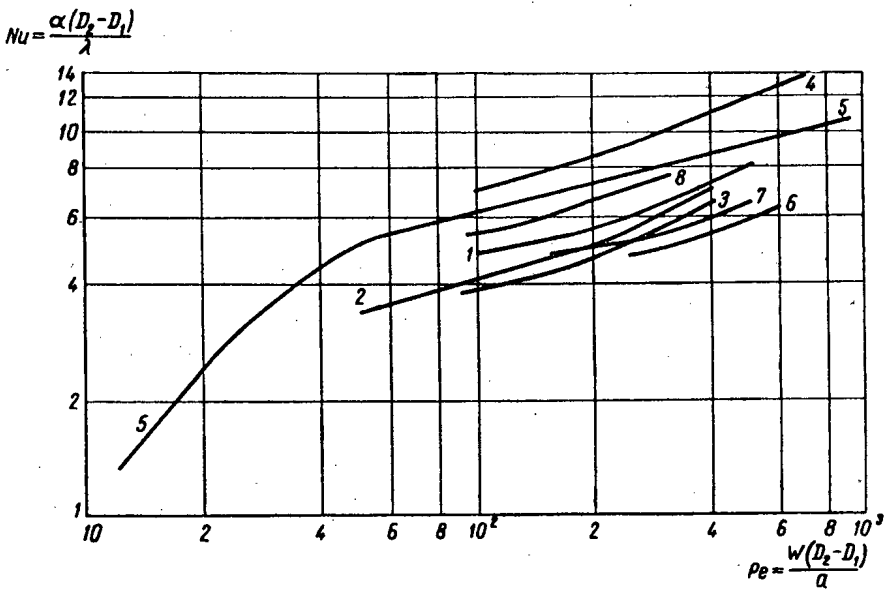

Fig. 6. Heat transfer for light metals (sodium, sodium-potassium) flowing in channels. $L/D_e > 30$. Results of experiments using an alloy of sodium-potassium: 1) Lyon ($D_2/D_1 =$ $= 1.37, 1.43$); 2) Lyon ($D_2/D_1 = 1.23$); 3) Werner, Kling, Tidball ($D_2/D_1 = 1.83$ — steel); 4) same, nickel; 5) Hall, Kraft and Jenkins; 6) Tidball (flat channel) initial results; 7) same, final results. Results of experiments with sodium: 8) Hall, Kraft, Jenkins ($D_2/D_1 =$ $= 1.25$).

Heat Transfer in Flow of Liquid Metal Coolant Along the Length of a Bundle of Rods

The order of magnitude of the numbers that characterize heat transfer when liquid metal coolant flows along the length of a bundle of rods may be derived from data on the heat transfer coefficients cited by Tidball [22], Schwenk and Shannon [23], Rosenblatt and Brooks [24]. The empirical equation proposed by Brooks and

Rosenblatt should be used only with great caution, since it is accurate only for conditions that are close to the experimental conditions under which it was obtained.

The authors (Brooks and Rosenblatt) recommend the equation

$$\frac{\alpha D_{st}}{\lambda} = 612\left(\frac{wD_{st}}{a}\right)^{0,6}\left(\frac{S}{F}\right)^{1,2}, \tag{20}$$

where D_t is the external tube diameter; S is the cross sectional area of flow between the tubes in the bundle; F is the heat transfer surface area; α is the heat transfer coefficient.

The heat transfer obtained when liquid flows over a plate surface, with channel width infinite, is determined through the integral equations for boundary layer.

In liquid metals the Prandtl number is much less than unity ($Pr \ll 1$) and $\delta_T > \delta$, where δ_T and δ are the thermal and hydrodynamic boundary layer thicknesses, respectively. In the region where $D < y < \delta$ the velocity component w_x varies in accordance with usually accepted laws for the hydrodynamic boundary layer of an incompressible liquid.

In the region $y > \delta$

$$w_x = w_0 = \text{const}.$$

A solution for a laminar boundary layer may be obtained by introducing the usual approximate profiles of velocity and temperature represented by fourth-power polynomials.

For $\overline{Nu} = \frac{\bar{\alpha}L}{\lambda}$ where L is the length of plate, the following equation may be used with satisfactory accuracy

$$\overline{Nu} = 1,1\sqrt{(1 - Pr^{1/3})\,Pe}, \tag{21}$$

where $Pe = \frac{w_0 L}{a}$.

For a turbulent boundary layer Kutateladze and Fedorovich have developed two limiting methods.

In the first method a linear distribution of tangential pressures and thermal currents was assumed through the boundary layer thickness, while the $^1/_7$ power law was used for velocity distribution. The turbulence in the region $\delta < y < \delta_T$ was assumed equal to zero.

Over the range $10^3 < Pe < 2 \cdot 10^5$ a third approximation is expressed by the equation

$$\overline{Nu} = 0,38Pe^{0,65}. \tag{22}$$

In the second calculation a linear distribution was assumed in the range $0 < y < \delta$ and λ_T constant when $\delta < y < \delta_T$ under the conditions $\tau = \tau_{st} = \text{const}$. This should lead to the largest value of α.

In the interval $10^3 < Pe < 10^5$ it was found that

$$\overline{Nu} = 0,46Pe^{0,65}. \tag{23}$$

The difference in results obtained from these two methods is about 20%.

Heat transfer when the flow is across a bundle of cylinders differs in the case of liquid metals from the case of nonmetallic liquids as a function of the equation $Nu = f(Pe)$ as well as in the nature of the heat transfer coefficient distribution around the circumference of the cylinder. The latter is clearly evident in the data of Andreevski, Borishanski and Kutateladze, that are shown in Fig. 7.

Heat transfer under conditions of free convection in liquid metals is also very closely related to the condition that $Pr \ll 1$. The regime of thermal perturbations, in which the deciding role is played by molecular heat conductivity under conditions of free convection, arises in the flow zone with negligibly small molecular friction. In connection with this, a theoretical analysis shows that with $Pr \ll 1$ the relationship

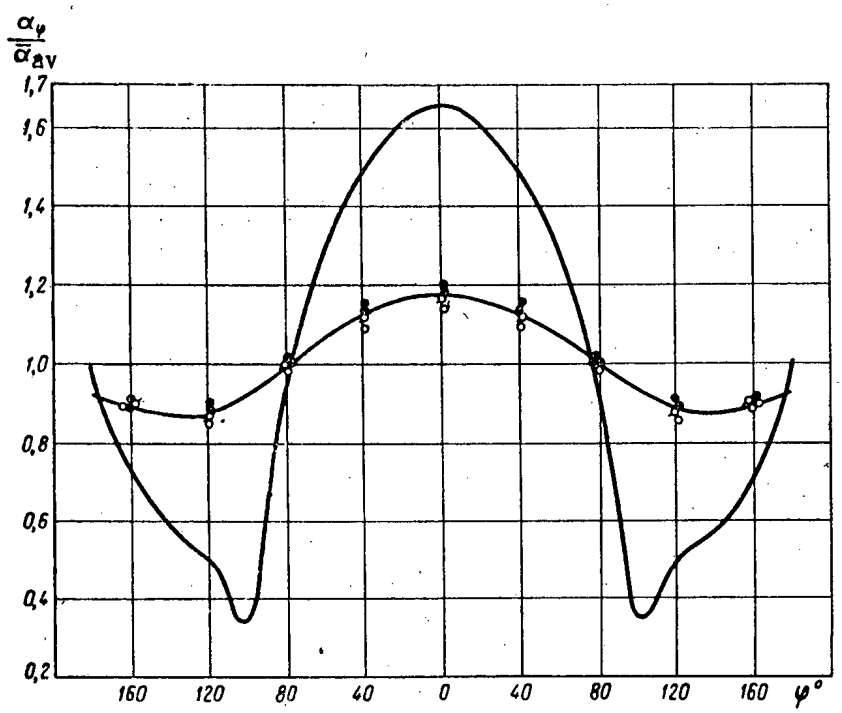

Fig. 7. Heat transfer with flow across a single tube. Gradually varying curve — metal (experiments of Andreevski, Borishanski, Kutateladze); sharply varying curve — air. ○) Pe = 450; ϕ) Pe = 600; ●) Pe = 800; ⊗) Pe = 1000.

$$Nu = f(GrPr) \tag{24}$$

should be replaced by the relationship

$$Nu = f(GrPr^2). \tag{25}$$

The approximate equation for heat transfer was obtained by Squire:

$$\overline{Nu}Gr^{-1/4} = 0{,}679\left(\frac{Pr^2}{Pr+\frac{20}{21}}\right)^{1/4}. \tag{26}$$

An analogous equation was obtained by Eckert.

When Pr → 0 Eq. (26) takes on the form corresponding to Eq. (25).

Fedinskii studied [9] heat transfer under free convection to mercury, tin, an alloy of lead-bismuth and sodium. The experiments were conducted with horizontal cylinders of 25.6 and 85 mm diameters, and with a vertical plate. After study of the results of these experiments as well as the experiments of Saunders for mercury, Kirpichev, Mikheev, Eigenson and others, the following empirical relationship was obtained for nonmetallic liquids:

$$\overline{Nu}Gr^{-1/4} = 0{,}54\,Pr^{0{,}3+0{,}02\,Pr^{-1/3}} \tag{27}$$

Hymen, Bonilla and Ehrlich studied [25] heat transfer under free convection near horizontal cylinders of 6.3 mm and 38.1 mm diameters. The experiments were conducted with mercury, lead, bismuth, an alloy of lead-bismuth, sodium, an alloy of sodium-potassium, water, toluol and five different silicates.

After generalization of the experimental data, the authors obtained this equation:

$$\overline{Nu}Gr^{-1/4} = 0{,}54\left(\frac{Pr^2}{0{,}952+Pr}\right)^{1/4}. \tag{28}$$

At sufficiently large Gr numbers the heat transfer relationships for free convection undergo a change. Physically this is explained by the fact that the laminar character of the flow near the heat transfer surface is completely upset and instead there arises a so-called thermal turbulence. The character of the fluid motion becomes on the average (statistical average) the same at all sections of the heat transfer surface. In this case the rate of heat transfer may be described by the equation

$$Nu = \varphi(Pr)\, Gr^{1/3}. \tag{29}$$

For media that have Pr > 0.5 it is common to consider that the transition from $Nu \sim Gr^{1/4}$ to $Nu \sim Gr^{1/3}$ occurs at $GrPr > 2 \cdot 10^7$.

In the experiments of Hymen, Bonilla and Ehrlich the tube diameter had an effect on this transition.

The analysis of the experiments, that was run by Fedinskii, indicated that in Eq. (29) the quantity (Pr) φ practically coincides with the right side of Eq. (27). Therefore it may be considered with sufficient accuracy for practical purposes that for all media the following equation applies:

$$Nu = \Phi\left(\frac{Pr^2 Gr}{1+Pr}\right). \tag{30}$$

When the vapors of liquid metals are condensed the condensate deposits out either in the form of droplets or in the form of a continuous film. For metals as contrasted to other substances the droplet type of condensation is the more characteristic. In addition the thermal resistance of the condensate film, when it forms, is extremely small.

This is explained by the fact that the high heat conductivity of the metal vapors leads to a basic redistribution of thermal resistances of the condensate itself and of the diffusion area near the surface of the condensate. Because of this the supposition, common in the theory of film condensation, that the temperature at the surface of the film is practically exactly equal to the saturation temperature at the center of flow channel, is not justified in the case of metal vapor condensation.

TABLE 2

Heat Transfer During Condensation of Sodium Vapors

Saturation temperature t, °C	631	725	866
Heat flux q, kcal/m²·hr	$1.5 \cdot 10^5$	$1.92 \cdot 10^5$	$2.66 \cdot 10^5$
Coefficient of heat transfer α, kcal/m²·hr:			
experimental results	$5.55 \cdot 10^4$	$5.85 \cdot 10^4$	$6.50 \cdot 10^4$
results from film condensation equation on the assumption that $t_f = t^*$	$84.5 \cdot 10^4$	$74.0 \cdot 10^4$	$61.2 \cdot 10^4$

Calculations indicate that when Pr → 0 turbulence leads to a certain increase in thermal resistance of the condensate film, and not to a decrease, as is the case for nonmetallic liquids.

In Table 2 are shown some data from Bonilla and Meysner on heat transfer under conditions of sodium vapor condensation.

Thus, experiment confirms that the thermal resistance of the condensate film proper is extremely small. It follows that the type of condensation has little effect on the heat transfer in the case of liquid metal vapors.

The diffusion theory of heat transfter under conditions of droplet condensation leads to the conclusion, that for this case

$$\alpha \sim \frac{1}{(t'' - t_{st})^n}, \tag{31}$$

where n ≈ 0.5.

According to the experiments of Gel'man, when mercury vapors condense an even more sensitive dependence applies:

$$\alpha = \frac{1{,}2 \cdot 10^5 \sqrt{p}}{\Delta t} + \sqrt[3]{\gamma'' w''}, \tag{32}$$

where p is the pressure in atmospheres absolute; γ'', w'' are the weight flow velocities in $kg/m^2 \cdot sec$.

The boiling of metals, in general, conforms to the same laws as the boiling of nonmetallic liquids.

In Fig. 8 are shown the relationships of heat transfer coefficient on the temperature potential for the boiling of water and for the boiling of an amalgam of magnesium and mercury over a horizontal tube under conditions of free convection (surface boiling, with the surface immersed in a large liquid volume). For both metallic and nonmetallic liquids the nature of the relationship under investigation is identical.

Poor wetting by the coolant of the heating surface leads to an earlier initiation of film boiling. When the liquid does not wet the heating surface then film boiling for all practical purposes exists steadily at any heat flux densities.

Addition to the liquid of surface-active substances may change the degree of wetting of the surface. For example, the addition of an insignificant quantity of magnesium to mercury or of an insignificant quantity of sodium, significantly improves the contact between the liquid and steel. This is particularly noticeable in boiling heat transfer because of the basic effect of the degree of wetting on the character of the flow of a vapor-liquid mixture.

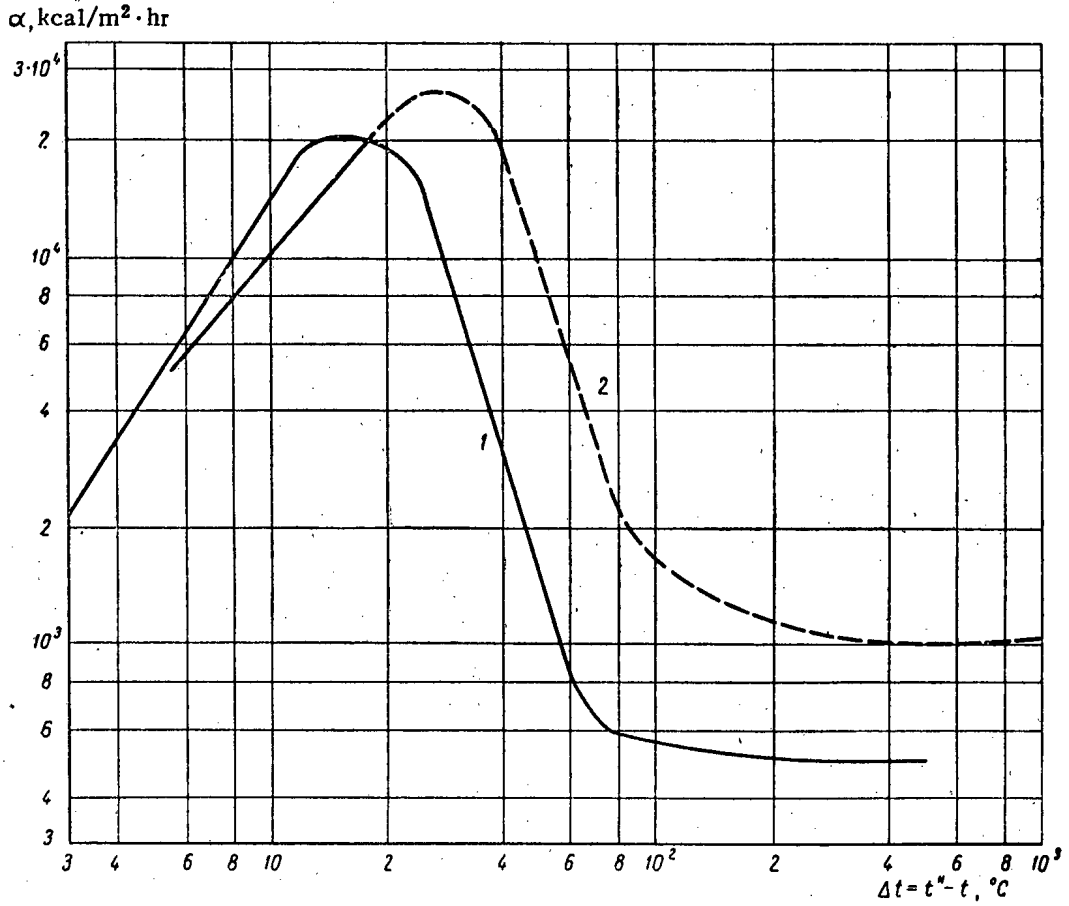

Fig. 8. Heat transfer for boiling of an amalgam of mercury and for boiling of water in a large liquid volume. 1) Magnesium-mercury amalgam; 2) water.

The effect of wetting on the hydraulic resistance to the flow of a vapor-liquid mixture was studied for flow of boiling mercury. In vertical tubes the motion of two-phase current averaged over a sufficiently long period of time, always possesses axial symmetry. In inclined and horizontal tubes this occurs only at high flow velocities. When the velocities are not high the flow separates into layers (the lower portion of the tube perimeter is immersed in liquid while the upper portion is in contact with vapor), and this decreases cooling of this surface. When the flow has not separated into layers or when the separation is not well developed the distribution of the liquid and vapor phases depends basically on the degree of wetting of the tube surfaces by the liquid. A liquid that adheres to the walls forms a continuous film on the surface thus ensuring a high cooling rate with nucleate boiling regime. The vapor thus formed flows away into the center of the flow channel.

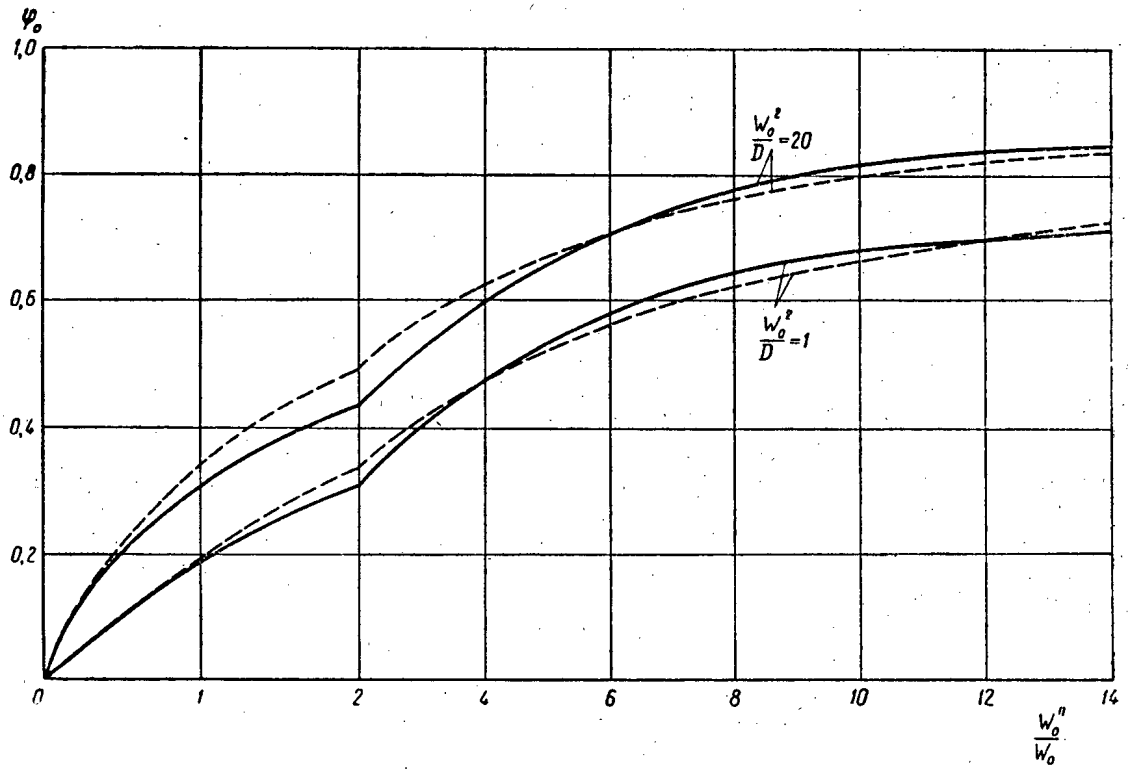

Fig. 9. Cross section portion filled with mercury vapors in a vertical tube. —) Mercury at a pressure of 5-15 atmos; ---) water at a pressure of 5 atmos.

When the liquid does not wet the tube surface (for instance, in the case of mercury flowing through glass or steel tubing) the vapor bubble motion is reversed: vapor bubbles separate out between the tube wall and the liquid steam. At the center of the flow channel there is essentially only liquid moving in a pulsating stream [26].

The change in the composition and distribution of a two-phase stream, as a function of wetting of the walls by the liquid, does not significantly affect the hydraulic flow resistance, although it basically affects heat transfer. This is because the integral hydrodynamic characteristics of a two-phase flow depend on the volumetric concentrations of the phases and are affected but little by the detailed stream composition. In connection with this it may be noted that the flow characteristics of a vapor—liquid mercury mixture are near the water-steam mixture characteristics.

In Fig. 9, the basic hydrodynamic characteristic is given from the data of Gremilov [27] in terms of one coordinate φ (the volumetric vapor concentration) and the other coordinate w_0''/w_0 (the ratio of the vapor velocity to liquid velocity). The parameter used was the Froude number w_0^2/D stated to an accuracy corresponding to $g = 9.81$ m/sec^2, where D is the internal tube diameter. The number was constructed from steam-water data and from mercury-mercury vapor data flowing in vertical tubes.

When a liquid that does not wet the tube surface boils, heat transfer may be improved by increasing the frequency of flushing the tube.

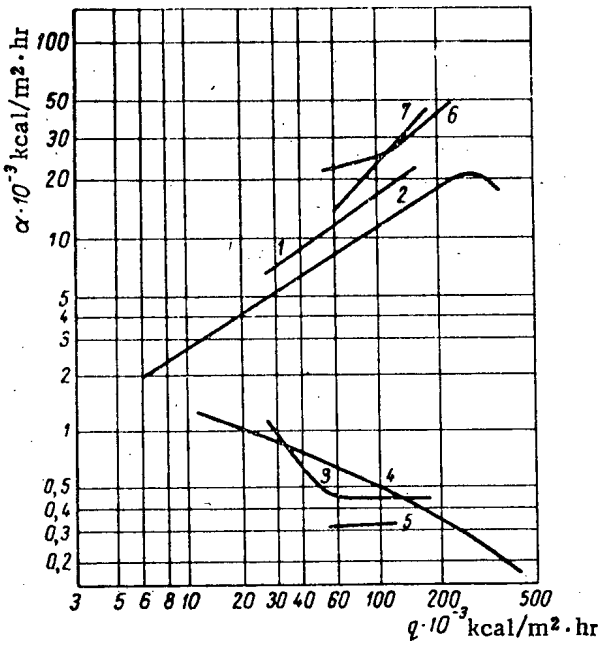

Fig. 10. Heat transfer with boiling of various liquid metals in large volumes. 1) Magnesium-mercury amalgam in vertical tubes; 2) magnesium amalgam of mercury flowing over the exterior of a tube; 3) film boiling of an amalgam of mercury; 4) boiling of pure mercury; 5) boiling of cadmium; 6) boiling of an alloy of sodium-potassium; 7) boiling of sodium.

According to the data of Lozhkin and Kanaev [3], when mercury boils in a tube that has a spiral insert of strip iron, the percentage of flushing of tube surfaces by liquid reached ~ 70% as compared with ~ 12-20% in the absence of this turbulence generator.

Figure 10 shows the dependence of α on q when liquid boiling in certain metals occurs over a large volume [6, 28, 29]. For metallic liquids that wet the heating surface (sodium, potassium-sodium alloy, magnesium amalgam of mercury), in the region of heat fluxes $q < q_{cr}$ the usual relationship between coefficient of heat transfer and heat flux density holds true, $\alpha = Aq^n$, where $n \approx 0.7$.

For liquids that do not wet the heating surface (mercury, cadmium) the values of α that apply are characteristic for film boiling regime.

Figure 11, which shows the results of the experiments of Korneev [14] with a mercury-magnesium amalgam, indicates that the rate of heat transfer in nucleate boiling is practically independent of the concentration of magnesium. However, the transition to film boiling occurs at various heat fluxes $q_{cr\,1}$ as a function of magnesium concentration.

It is well known that with fully developed nucleate boiling the coefficient of heat transfer depends very little on the liquid flow velocity [30]. Data on boiling heat transfer

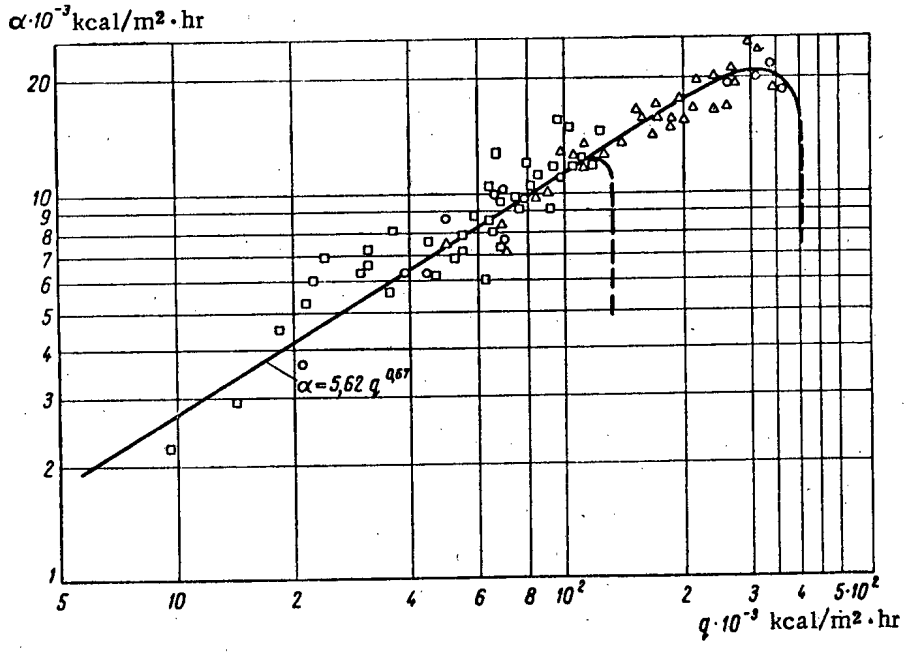

Fig. 11. Heat transfer with nucleate boiling of magnesium-mercury amalgam. Percentage of magnesium: □) 0.01%; △) 0.03%; ○) 0.04%.

of magnesium amalgam in free convection within a large volume and in natural convection in a tube are close to each other and confirm this assertion for liquid metals.

When the liquid does not wet the tube surface this statement no longer is true. There is evidenced a basic influence by the flow velocity w_0 and by the tube diameter D. A certain decrease of the value of α as $\underline{q}$ increases is noted [1, 2, 12].

When a mercury amalgam boils in horizontal tubes the coefficient of heat transfer is not uniform around the tube circumference. A decrease in heat transfer at the upper part of the tube depends on the heat flux density, which creates an increase of steam content in the upper part of the unsymmetric, two-phase fluid stream. The velocity $w_{0,1}$ after which heat transfer in the upper part of the tube remains at a constant high level, may be determined through the empirical equation [14]:

$$w_0' \approx 22 \cdot 10^{-5} q^{0,42} D^{0,76} \text{ m/sec.} \quad (33)$$

Here $\underline{q}$ is measured in kcal/m^2·hr, D in mm.

When $w_0' > w_{0,1}''$ the heat transfer coefficient is determined by the empirical equation

$$\alpha = 12 q^{0,67} w_0^{0,3} D^{-0,45}. \quad (34)$$

These equations have been checked at $5000 < q \leq 70{,}000$ kcal/m^2·hr, $13 < D < 40$ mm, $1 < p < 120$ atmos and $1 \leq w_0'' < 19$ m/sec.

LITERATURE CITED

[1] M. A. Styrikovich, I. E. Semenovker and A. R. Sorin, Sovetskoe Kolotyrbostroenie 9, 316 (1940).

[2] M. A. Styrikovich and I. E. Semenovker, J. Tech. Phys. (USSR) 10, 16, 1324 (1940).

[3] A. N. Lozhkin and A. A. Kanaev, Binary Installations [in Russian] (MAShGIZ, 1946).

[4] A. A. Kanaev, Sovetskoe Kolotyrbostroenie 2, 18 (1953).

[5] V. M. Borishanskii and S. S. Kutateladze, Energomashinostroenie 6, 5 (1957); 4 (1958).

[6] S. S. Kutateladze, Basic Heat Transfer Theory [in Russian] (MAShGIZ, 1957).

[7] M. A. Mikheev, V. A. Baum, K. D. Voskresenskii and O. S. Fedinskii, Coll: Reactor Building and Reactor Theory [in Russian] (Izv. AN SSSR, 1955), p. 139.

[8] M. A. Mikheev, Heat Transfer Principles [in Russian] (Gosenergoizdat, 1956).

[9] L. I. Gel'man, Teploenergetika 3, 47 (1958).

[10] H. E. Brown, B. H. Amftead, and B. E. Short, Trans. ASME 79, 2, 279 (1957).

[11] S. E. Isakoff and T. B. Drew, General Discussion of Heat Transfer, Inst. Mech. Eng. and ASME (1951), p. 405.

[12] R. C. Martinelli, Trans. ASME 69, 8, 947 (1947).

[13] R. E. Lyon, Chem. Eng. Progr. 47, 275 (1951).

[14] M. I. Kornev, Teploenergetika 4, 44 (1955); 7, 30 (1955).

[15] D. English and T. Barret, General Discussion of Heat Transfer, Inst. Mech. Eng. and ASME (1951), p. 458.

[16] T. C. Doody and A. H. Jounger, Chem. Eng. Prog. Symposium Ser. 5, 33 (1953).

[17] B. Lubarsky and S. J. Kaufman, "Review of experimental investigation of liquid metal heat transfer," Report NACA No. 1270 (1956).

[18] H. A. Johnson, W. J. Glabaugh and J. P. Hartnett, Trans. ASME 75, 6, 1191 (1953); 76, 4, 505 (1954).

[19] E. R. Gilliland, R. J. Musser and W. R. Page, Coll: General Discussion of Heat Transfer (1951), p. 402.

[20] L. M. Trefethen, Coll: General Discussion of Heat Transfer (1951), p. 436.

[21] I. I. Novikov, A. N. Solov'ev, E. M. Khabakhpasheva, V. A. Gruzdev, A. I. Pridantsev and M. Ia. Vasenina, Atomnaia Energiia No. 4, 92 (1956).

[22] R. Tidball, Chem. Eng. Progr. Symposium Ser. 5, 233 (1953).

[23] H. C. Schwenk and R. H. Shannon, Power 99, 11, 92 (1955).

[24] R. D. Brooks and A. L. Rosenblatt, Mech. Eng. 75, 5, 363 (1953).

[25] S. C. Hymen, C. T. Bonilla and S. W. Ehrlich, Chem. Eng. Progr. Symposium Ser. 49, 5, 21 (1953).

[26] A. N. Lozhkin, Krol', J. Tech. Phys. (USSR) 8, 21 (1938).

[27] D. I. Gremilov, Coll: "Combined power stations and power cycles," Trudy TsKTI 23, 86 (1952).

[28] R. E. Lyon, A. S. Foust and A. L. Katz, Chem. Eng. Progr. Symposium Ser. 49, 5, 21 (1953).

[29] Liquid Metals Handbook, Sodium (NaK) Supplement (Washington, 1955).

[30] Coll: Heat Transfer Problems with State Changes [in Russian] (Gosenergoizdat, 1953).

Received November 4, 1957

EVALUATING THE ECONOMIC FEASIBILITY OF USING SPECIAL HEAVY CONCRETES FOR RADIATION SHIELDING

A. N. Komarovskii

The first part of this article is a survey of the work of foreign authors dealing with the economics of using various concretes for biological radiation shielding at nuclear reactors and at charged particle accelerators. Several of these authors affirm that it is economically justifiable to use heavy concretes for these purposes. However, others advocate the use of common concretes with mineral aggregates. The second part of the article gives the results of corresponding economic analyses conducted in the USSR. These analyses lead to the conclusion that the use of special heavy concretes is justifiable only in exceptional cases.

The authors of a number of works dealing with biological radiation shielding note the advantages of special heavy (including iron ores and iron scrap) concretes, as well as the advantages of barites concretes over common concretes with mineral aggregates. Greutz and Downes [1] conclude that it is economically justifiable to use more expensive magnetite concrete for particle accelerators, because in view of its high density (3.9 tons/m^3) there is less floor area required for the same amount of shielding. Beck and Horner [2] reach the same conclusion.

Callan in [3], a paper devoted to concrete shields for nuclear reactors, notes that in many cases (for example, small reactors) heavy concrete including special aggregates is better than common concrete despite the high cost, since the heavy concrete shield can be made thinner.

Lane [4] recommends the use of concrete shielding weighing 3.5 to 4 tons/m^3 for high power reactors, while Stephenson [5] states that the best heavy concrete for reactor or isotope storage shielding is barites concrete.

On the other hand, there are convincing arguments for the use of common concrete using local aggregates, but this does not exclude the use of special concretes in details of the shield or when over-all dimensions must be kept low.

Thus, the American firms "Pacific Gas and Electric Co." and "Bechtel Corp." that are designing large dual-purpose reactors of 500 mw thermal power, note in their report to the Atomic Energy Commission of the USA [6] that there are no economic advantages in favor of high density concretes. The same is stated in analogous reports by other companies (Monsanto Chemical Co. and Union Electric Co.) that participated in the design of large power reactors. These companies decided to use common concrete in their reactor installations.

Glen [7], summarizing the shielding design experience at the Oak Ridge National Laboratory (USA) notes that the thickness of shielding around a stationary reactor in contrast to the shielding around a small reactor, is not a significant factor, since decreasing the cost of shielding around a stationary reactor is far more important.

Price, Horton and Spinney [8] in their summary of shield design experience state that special heavy concretes using metallic or ore aggregates cost ten times as much as common concretes. This high cost of heavy concretes necessitates very careful treatment in selection of its constituents and handling methods, while the high density makes it impossible to use common building fixtures and complicates pouring and setting the concrete. These factors are significant for the total cost of the reactor shield. The authors also note that the use of steel

scrap and in particular steel shot in concrete is feasible only in those cases when design requirements call for very compact shielding. For example, the use of special heavy concrete in the upper shield of the English research reactor DIDO reduced the length of fuel element assemblies and made possible the use of convenient handling tools for their removal (the cost advantages thus realized were greater than the additional costs of the special concrete). The authors make the general conclusion that common concrete is one of the cheapest shielding materials while costly heavy concretes can yield economic advantages only in shielding of small sized reactor cores.

TABLE 1

Economic Characteristics of Some Concretes (Data from Institute of Atomic Energy of the Academy of Sciences, USSR)

Type of concrete	Density, tons/m³	Shielding effectiveness, %	Cost rubles/m³	Cost normalized to unit effectiveness, rubles/m³	Economy, rubles/m³	Cost increase, rubles/m³
Common concrete	2,2	100	350	350	—	—
Sand concrete without coarse aggregates	2,0	90	180	200	150	—
Concrete with iron ore	2,2	150	700	470	—	120
Concrete with metal scrap	5,5	250	2000	800	—	450

In the work mentioned above, [5], it is also noted that since the cost of steel is high in comparison to other materials used in concrete (in addition, stratification may occur in such concrete) the use of metal aggregates in concrete shields is usually not justifiable.

The results of studies conducted in the USSR point to the use of common concretes. Thus both design and analysis work conducted at the Institute of Atomic Energy of the Academy of Sciences, USSR indicates that the exterior walls of accelerators as well as of some reactors should be made of concrete using locally available aggregates, and that no attempt should be made to make wide use of special heavy concretes. Some results of this study are shown in Table 1.

TABLE 2

Costs of Metallic Rubble, Shot and Ores in Various Parts of the USSR (with transportation costs included)

Material	Unit of measurement	Cost in rubles				
		Central region	Central Urals	Southern Urals	Western Siberia	Eastern Siberia
Metal rubble	ton	760,08	757,80	758,22	761,46	793,19
Metallic shot, 6 mm diameter	ton	714,96	763,25	756,17	812,97	850,63
Iron ore (magnetite or hematite)	ton	128,85	71,75	72,90	100,72	146,95
Rubble made of this ore	ton	134,45	76,68	78,13	106,32	152,55
Sand extracted from this ore	ton	158,45	104,84	106,29	130,32	176,55
Iron ore (limonite)	ton	100,11	101,13	102,89	178,52	234,37
Rubble extracted from iron (limonite) ore	ton	105,71	106,73	108,49	184,49	239,97
Sand extracted from iron (limonite) ore	ton	129,71	130,73	132,49	208,12	263,97
Barite ore	ton	464,30	389,41	383,61	339,18	398,68
Rubble from barite ore	ton	469,90	395,01	389,21	344,78	404,28
Sand from barite ore	m³	493,90	419,01	413,21	368,78	428,28
Mineral sand	m³	29,30	41,40	33,90	33,90	35,50
Common rubble	m³	53,80	59,40	65,00	53,90	62,90

TABLE 3

Comparative Data on Concrete Shielding for Large Reactors in Various Regions of the USSR

Concrete aggregates	Concrete density, tons/m³	Average cost of 1 m³ of concrete, rubles					Cost of concrete shielding, %					Total reactor building volume, %	Total cost of building and shielding, %				
		Central regional	Central Ural	Urals West-ern Siberia	East-ern Siberia		Central regional	Central Ural	Urals West-ern Siberia	East-ern Siberia			Central regional	Central Ural	Urals West-ern Siberia	East-ern Siberia	
Mineral sand and rubble (98%), iron ore and iron scrap (2%)	2,3 / 4,4	249	238	304	260		100	100	100	100		100	100	100	100	100	
Mineral sand and iron ore (magnetite or hematite)	3,0	571	476	1 409	775		120	101	243	153		98	105	101	142	112	
Iron ore (magnetite or hematite)	3,6	786	—	1 609	—		138	—	241	—		96,5	108	—	140	—	
Fine iron ore (hematite or magnetite) and metal scrap (64%) mineral sand and rubble (36%)	4,2 / 2,3	2 316	2 295	2 713	2 500		222	237	220	241		95	130	128	133	129	
Mineral sand and iron scrap	4,2	2 316	2 345	2 712	2 650		348	373	348	398		95	164	161	170	171	

In 1956 a study was made of the economics of using various concretes in various parts of the USSR for shielding of large reactors. Various shield designs were examined for various concrete compositions. This made possible the calculation of total concrete volume required with different types of concrete, the calculation of the extent of the work required to erect the buildings and the assembly of cost figures for comparison of each of the design alternatives, with all costs incident to a reactor installation considered and not only its shielding costs (as was done in all work published previously).

The following types of reactor installation shields were considered:

– shielding, 98% common concrete by volume (γ = 2.3 tons/m³) and 2% special heavy concrete (γ = = 4.4 tons/m³);

– shielding made of special heavy concrete (γ = = 3.0 tons/m³) using common sand and coarse iron ore aggregates;

– shielding made of special heavy concrete (γ = = 3.6 tons/m³) using both coarse and fine iron ore aggregates;

– shielding part of whose volume (the reactor shield proper) is made of special heavy concrete (γ = = 4.2 tons/m³) using fine iron ore aggregate and coarse iron scrap aggregate, while the rest of the volume (the walls of the central reactor chamber, etc.) is made of common concrete (γ = 2.3 tons/m³);

– shielding made of special heavy concrete (γ = = 4.2 tons/m³) using mineral sand and both coarse and fine metal scrap aggregates.

In assembling the cost data for special high density concrete the following material availability data was used: iron ore for the central region was obtained from Krivoi Rog, iron ore for the central Ural region was obtained from Goroblagod, and for Siberian regions was obtained from Kuznetsk; metal rubble for the central region was obtained from a factory in Yaroslavl, for the central Ural regions was obtained locally, and for the Siberian regions from a factory in Novosibirsk.

The costs of these materials (Table 2) were obtained through realistic estimates and FOB prices obtained from purchasing agents; the costs of transportation were obtained from actual conditions as they existed throughout 1957.

The basic data from the estimates are given in Table 3. On the basis of these estimates the following conclusions may be made:

1. The use of special heavy concretes using iron ore aggregates, and also the use of concretes with coarse

aggregates of iron ore and fine aggregates of mineral sand, in the biological shielding of reactors, results in relatively low (1-12%) construction cost increases as compared to the costs of a building in which common concrete only is used.

2. The use of metal scrap for the coarse aggregate increases the cost by 28-33% when the heavy concrete is used for the shielding of the reactor proper only, and increases the cost by 60-72% when the heavy concrete is used for the central chamber shield.

TABLE 4

Comparative Figures on the Concrete Shielding of the Circular Accelerator of 7 Bev (for the central region of the USSR)

Concrete aggregates		Concrete density, tons/m³	Volume of concrete in the shield		Reduction in building size when special heavy concretes are used		Cost of building and shield	
coarse	fine		m³	%	area m²	volume m³	millions of rubles	%
Mineral rubble	Mineral sand	2,3	13 024	100	—	—	43	100
Iron (hematite) ore	Mineral sand	3,0	10 024	76,5	545	3 790	43,18	100
Iron (limonite) ore	Iron (limonite) ore	3,0	10 024	76,5	545	3 790	43,22	100
Barite ore	Barite ore	3,1	9 775	—	540	3 874	48,16	112
Iron (hematite) ore	Iron (hematite) ore	3,5	8 138	62,5	547	5 000	43,13	100
Iron scrap	Iron (hematite) ore	4,4	6 837	52,2	666	6 222	48,16	112

TABLE 5

Comparative Figures on the Concrete Shielding of the Linear 35 Mev Accelerator (for the central region of the USSR)

Concrete aggregates		Concrete density, tons/m³	Volume of concrete in shield		Reduction in building size when special heavy concretes are used		Cost of building and shield	
coarse	fine		m³	%	area m²	volume m³	millions of rubles	%
Mineral rubble	Mineral sand	2,3	15 100	100	—	—	18 678	100
Iron (hematite) ore	Mineral sand	3,0	11 500	76	315	4 493	19 419	115
Iron (limonite) ore	Iron (limonite) ore	3,0	11 500	76	315	4 493	20 024	119
Barite ore	Barite ore	3,1	11 053	73	337	5 040	26 863	160
Iron (hematite) ore	Iron (hematite) ore	3,5	8 400	56	370	5 095	21 027	125,5
Iron scrap	Iron (hematite) ore	4,4	7 876	52	457	5 754	28 476	172

Thus in any case, it is better to use common concrete for the biological shielding of reactors. A possible exception is when the reactor is built near a source of inexpensive heavy ores, as well as in the construction of extremely complicated and expensive foundations and reactor bases, when a reduction of the shield dimensions by use of special heavy concretes may change somewhat the cost figures in favor of the heavy concretes.

The economics of using heavy concretes for shielding of reactors that are enclosed in gas tight steel shells whose cost and volume decrease with increasing concrete density (as a result of decreasing shield size) require additional investigation. However, preliminary estimates indicate that in these cases as well, the total cost of erection of a stationary reactor with common concrete shielding is lower than the cost of a reactor with special heavy concrete.

Analogous study was made on the economics of using special heavy concretes for the biological shielding around a 7 Bev synchrophasotron and a 35 Mev linear accelerator. The erection costs were estimated for the conditions of the Central region, and designs and cost figures were assembled for different types of heavy concretes.

This work was conducted in accordance with the methods outlined above. A comparison was made of total building costs for the entire accelerator facility under the following versions of shielding:

– shield of common concrete (γ = 2.3 tons/m^3);

– shield of concrete with coarse (Krivoi Rog hematite) and fine (mineral sand) aggregates (γ = 3 tons/m^3);

– shielding of concrete with coarse and fine aggregates of Lipets limonite ore (γ = 3 tons/m^3);

– shielding of concrete with coarse and fine aggregates of Salair barites ore (γ = 3.1 tons/m^3);

– shielding of concrete with coarse and fine aggregates of Krivoi Rog hematite iron ore (γ = 3.5 tons/m^3);

– shielding of concrete with fine aggregate made of Krivoi Rog hematite iron ore and coarse aggregate of metal scrap (γ = 4.4 tons/m^3).

The basic figures of these estimates are given in Tables 4 and 5.

This work has made possible the following conclusions:

1. The use of special heavy concretes in the biological shielding around large circular accelerators does not yield any economic advantages by comparison with common concrete, but does not produce any noticeable cost increases either; concretes including barites ores and metallic scrap, whose use increases shielding costs by approximately 12%, are an exception.

2. The use of special heavy concretes for shielding of large linear accelerators increases building costs by 15-20%, and the use of concretes with barites ores, up to 60%, while metallic scrap concretes increase costs by up to 72%.

If all that has been presented above is taken into account together with the difficulties in obtaining and transporting special aggregates for heavy concretes, as well as the complexity of preparing the concretes, then the general conclusion may be reached that the use of special heavy concretes for shielding nuclear reactors and accelerators is not justifiable either technically or economically.

An exception may be the case where the reactor building is situated near a source of iron ores. The use of heavy concrete may prove to be justified for over-all shielding or for shield details around nuclear reactors and accelerators in the following circumstances:

– when the reactor or accelerator are housed in a small building and it is essential to reduce shielding dimensions to fit the equipment into the available space;

– when it is essential to reduce the lengths of experimental openings (for example, collimating openings in accelerators);

– if the shield thickness required with common concrete reduces the angle of vision of the operator or the experimenter (through viewing windows);

– when it is essential to maintain a constant shielding worth over the entire shield area, even with local thickness reductions (experimental openings, gas and water ducts, etc.);

– when it is necessary to erect very complicated and expensive bases and foundations for the installation, when a reduction of over-all shield size through the use of special heavy concretes will change the cost relationships so as to favor the heavy concretes.

LITERATURE CITED

[1] E. Greutz and K. Downes, Appl. Phys. 20, 12 (1949).

[2] C. Beck and C. R. Horner, Concrete 63, 2, 11 (1955).

[3] E. Callan, Concrete Inst. 25, 1 (1953).

[4] J. A. Lane, Nucleonics 13, 6, 57 (1955).

[5] R. Stephenson, Introduction to Nuclear Engineering (Gostekhizdat, Moscow, 1956).*

[6] "Industry teams report on A-power," I-II, Chem. Eng. 60, 7, 8 (1953).

[7] H. M. Glen, Oak Ridge National Laboratory, "Material of biological shielding," 2nd Nuclear Engineering and Science Conference, March 11-14, 1957, Philadelphia.

[8] B. Price, C. Horton and K. Spinney, "Radiation shielding," Atomic Energy Research Establishment, Harwell, 1957.

Received December 14, 1957

* Russian translation.

DEFORMATION SYSTEMS OF α-ZIRCONIUM

Iu. N. Sokurskii and L. N. Protsenko

The deformation systems of α-zirconium iodide have been studied in coarse-grained polycrystalline specimens deformed by upsetting. The orientation of the grains was determined from Laue patterns obtained in a special back-reflection camera using a small-diameter beam. The indices of the deformation systems were determined by the two-surface method and by the pole locus method.

It was found that α-zirconium is deformed by slip along the $(10\bar{1}0)$ plane in the $[\bar{1}2\bar{1}0]$ direction and along the $(10\bar{1}1)$ plane. A number of twinning systems have been discovered in α-zirconium: a) K_1 $(10\bar{1}2)$, η_1 $[\bar{1}011]$, K_2 $(10\bar{1}\bar{2})$, η_2 $[10\bar{1}1]$ and s = 0.173; b) K_1 $(11\bar{2}1)$, η_1 [1126], K_2 (0001), η_2 [1120] and s = 0.629; c) K_1 (1122), η_1 [1123] and in one case, d) K_1 $(11\bar{2}3)$, η_1 $[\bar{1}\bar{1}22]$.

It is known that β-zirconium is very plastic, much more plastic than other metals with a hexagonal lattice. The plasticity of a material is determined by a number of factors, in particular by the type and number of the deformation systems. The literature contains no exact data on the deformation systems of zirconium, with the exception of a few brief statements in the book by Lustman and Kerze [1].

In the case of titanium, which is analogous to zirconium in physical and mechanical properties, a number of new deformation systems have been found [2, 4], which have not been observed in metals with a hexagonal lattice. The occurrence of these deformation systems was also to be expected in zirconium.

Since attempts to obtain single crystal specimens by the strain-annealing method and by phase recrystallization were unsuccessful, all the investigations were made on polycrystalline zirconium iodide.

The specimens 5 × 5 × 7 mm in size with a rather coarse grain (average diameter 0.5-1.5 mm) were obtained by long annealing (~ 10 hrs) at 830°C. Two specimens were studied. Two mutually perpendicular faces on each of these specimens were ground and polished, and were etched in a 20% alcoholic solution of hydrofluoric acid to reveal the grain boundaries. The coarsest grains were selected for investigation, these being situated near the edge formed by the two polished surfaces and visible in both surfaces.

The orientation of the grains was determined by means of a special back-reflection camera using a primary beam of a diameter not exceeding 0.2 mm. The camera was fitted with a microscope to enable the specimen to be arranged so that the Laue pattern was obtained only from the grain, the orientation of which was to be determined. The distance from specimen to film was reduced to 16 mm in order to cut down the exposure time.

After the orientation of a number of grains had been determined, the specimens were deformed by upsetting, at room temperature, in a direction parallel to the edge formed by the two surfaces investigated.

The deformation lines on the surfaces of grains of known orientation were studied with the aid of an optical microscope and were photographed. The angle between these lines and the edge formed by the two surfaces investigated was measured on the photomicrographs. The results were plotted on a Wulff-Bragg net and evaluated in accordance with current technique [5].

Determination of Twinning Systems

(10$\bar{1}$2) twins. The (10$\bar{1}$2) plane of twins of this type was identified by the two-surface method [5].

The results of the determination of the indices of this twinning plane and also of the other deformation systems are shown on the standard crystallographic projection of the α-zirconium crystal (Fig. 1). The trace of the same twin ($\bar{1}$102) (Fig. 2) was discovered on both the grain surfaces investigated. The pole of the twinning plane was determined in a well-defined manner as the position of intersection of the arcs of great circles perpendicular to the corresponding traces of the twinning plane.

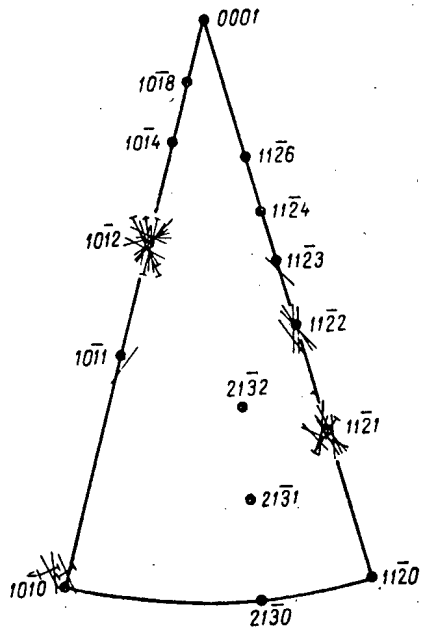

Fig. 1. Standardard polar diagram of α-zirconium on which are marked portions of the great circle arcs used for the determination of the indices of the K_1 planes, twinning systems and the indices of slip planes. ✓) results of the determination of the indices by the two-surface method.

Deformation Systems of Zirconium

Twinning

Twinning plane		Twinning direction		Magnitude of shear	
K_1	K_2	η_1	η_2	s theor	s exp
(10$\bar{1}$2)	(10$\bar{1}\bar{2}$)	[$\bar{1}$011]	[10$\bar{1}$1]	$\frac{1}{\sqrt{3}}\frac{a}{c}\left(3-\frac{c^2}{a^2}\right)$	0,173
(11$\bar{2}$1)	(0001)	[$\bar{1}\bar{1}$26]	[11$\bar{2}$0]	$\frac{a}{c}$	0,629
(11$\bar{2}$2)	—	[11$\bar{2}\bar{3}$]	—	—	—
(11$\bar{2}$3)	—	[$\bar{1}\bar{1}$22]	—	—	—

Slip*

Slip plane	Slip direction
(10$\bar{1}$0)	[1$\bar{2}$10]
(10$\bar{1}$1)	—

* Slip along the base plane was not observed.

Figure 1 also shows that in the region of the (10$\bar{1}$2) pole, a large number of arcs of great circles intersect which are perpendicular to the traces of these (10$\bar{1}$2) twins, found on only one of the surfaces investigated, i. e., they were identified by the pole locus method [6]. (10$\bar{1}$2) twins are found in the majority of hexagonal metals and have been well studied. The shear direction in twinning η_1 [$\bar{1}$011] in the given case, is determined as the position of intersection of the twinning plane and the plane of symmetry perpendicular to it. The twins often have a lenticular shape and become thinner when they approach a grain boundary or another twin of this type (Fig. 3).

The magnitude of the shear s was calculated from the measured values of the angles between the normals to the polished surfaces and the normals to the surfaces of the twin lamellas (see for example [5]). The measurement of these angles was made by means of an optical goniometer. The measured value of the angle $2\varphi = 86.5 \pm 1.5°$ corresponds to K_2 (10$\bar{1}\bar{2}$) and η_2 [10$\bar{1}$1]. The calculated value of the angle for this plane is $2\varphi = 85°04'$.

Twinning shear is comparatively slight ($s_{exp} = 0.173$), and therefore no exceptionally high stresses occur in the matrix and the twins may be fairly wide.

The table shows the data characteristic of the (10$\bar{1}$2) twins, as well as the formula for calculating the magnitude of the shear, showing that the sign of the deformation (shear) depends to a considerable extent on the value of the ratio c/a. If $c/a < \sqrt{3}$ (in the case of zirconium, c/a = 1.589), shear is in the [$\bar{1}$011] direction, if $c/a > \sqrt{3}$ (in the case of zinc, c/a = 1.856), the direction of shear is reversed.

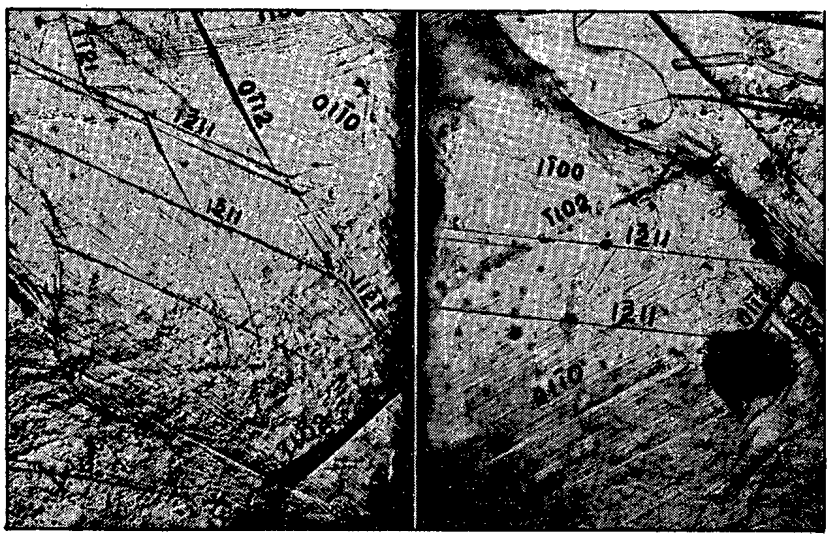

Fig. 2. Mutually perpendicular surfaces of α-zirconium after deformation (× 100).

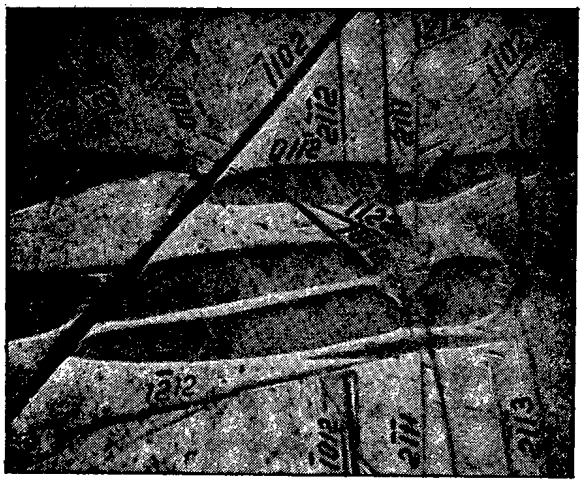

Fig. 3. Twins in α-zirconium (× 500).

(11$\bar{2}$1) twins. Twins of the (11$\bar{2}$1) type were likewise identified by the pole locus method and the two-surface method (Figs. 1 and 2).

The direction of shear η_1 [1$\bar{1}$26] in the present case is also determined by the plane of symmetry of the zirconium lattice. The magnitude of the shear was determined in the same way as in the preceding case. The measured value of the angle $2\varphi = 73 \pm 1.5°$, which corresponds to K_2 (0001) and η_2 = [11$\bar{2}$0]. The calculated value of the angle $2\varphi = 72°22'$, which is in good agreement with the experimental value. The shear in (11$\bar{2}$1) twinning is quite large (see table), and therefore, considerable stresses are set up in the matrix surrounding the twin. These stresses obviously also limit the width of the twins.

(11$\bar{2}$2) twins. (11$\bar{2}$2) twins could not be identified by the two-surface method, since they are usually very short and thin (Fig. 3). As will be seen from Fig. 1, however, their presence is quite reliably confirmed by the pole locus method. The direction of shear η_1 [11$\bar{2}$3] is determined in a well-defined manner as the line of intersection of the plane of symmetry with the twinning plane. It was not possible in this case to determine the magnitude of the shear, K_2 and η_2.

(11$\bar{2}$3) twins. Since only one system of (11$\bar{2}$3) twins was found (Figs. 1 and 2), the cited indices of the twinning plane cannot be said to have been determined with sufficient reliability. There is no doubt, however, that the indices of none of the twinning systems determined in the foregoing can be ascribed to these twins.

Determination of Slip Systems

Zirconium is very easily deformed by slip. Systems of slip lines can be seen in most of the grains of the deformed metal; they are even observed in specimens deformed at the temperature of liquid nitrogen.

The slip lines are usually situated at more or less the same distance apart (0.5-1 μ), which is well shown in Figs. 4 and 5. The height of the steps formed during slip is 0.1 μ. In a number of instances, the occurrence of 2 or 3 systems of slip in one grain was observed (Fig. 2). This fact indicates either that slip does not occur

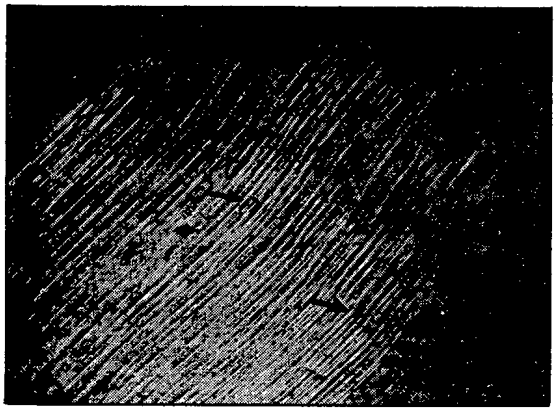

Fig. 4. Surface of deformed zirconium. Slip lines and fracture bands (× 500).

Fig. 5. Electron micrograph of the surface of deformed zirconium. Slip lines (× 5000).

along the base plane, but along a plane having a high factor of recurrence, or that slip along such a plane occurs at the same time as slip along the base plane.

The indices of the slip planes were determined by the two-surface method and the pole locus method. It was found that in most cases the slip plane in zirconium is the $(10\bar{1}0)$ plane. In one case, the slip plane $(10\bar{1}1)$ was found by the pole locus method (Fig. 1). No instance of slip along the base plane was found, even when the grain orientation with respect to the applied force was most favorable for the action of this system of deformation. The direction of slip in the $(10\bar{1}0)$ plane was determined from the Laue pattern of the deformed grain as the direction perpendicular to the axis of rotation of the grain under the action of the applied load.

The direction of slip in the $(10\bar{1}1)$ plane was not determined.

In a number of instances, a pronounced inflection of the slip lines was observed indicating extreme lack of uniformity in the deformation. Fracture bands were also observed (see the arrows in Fig. 4).

As a result of the investigations made, it has been found that in zirconium deformed at room temperature, a large number of deformation systems occur, substantially similar to the deformation systems of titanium. The slip planes in zirconium have a high factor of recurrence and slip occurs readily even at low temperatures (−196°C). This circumstance is undoubtedly one of the causes of the ihgh plasticity of zirconium. It was not possible, however, to find instances in zirconium of slip along the base plane or K_1 $(11\bar{2}4)$ twins, observed in titanium by a number of investigators. It is not unlikely that by deforming single crystals, favorably oriented with respect to slip along the base plane, it will also be possible to obtain slip along the base plane in zirconium.

LITERATURE CITED

[1] B. Lustman and F. Kerze, Metallurgy of Zirconium (N. Y., Toronto, London, 1955), p. 348.

[2] F. D. Rosi, C. A. Dube and B. H. Alexander, J. Metals 5, 257 (1953).

[3] T. S. Liu and M. A. Steinberg, J. Metals 4, 1043 (1952).

[4] F. D. Rosi, F. C. Perkins, and L. L. Seigle, J. Metals, 8, 115 (1956).

[5] E. O. Hall, Twinning and Diffusionless Transformation in Metals (London, 1954).

[6] R. W. Cahn, Acta Metallurgica 1, 5 (1953).

Received December 14, 1957

CHOICE OF BASIC PARAMETERS FOR HIGH-ENERGY LINEAR ELECTRON ACCELERATORS*

G. A. Zeitlenok, V. V. Rumiantsev, V. L. Smirnov, L. P. Fumin, V. K. Khokhlov, I. A. Grishaev and P. M. Zeidlits

The choice of basic operating parameters for high-energy linear electron accelerators is analyzed. The length of the accelerator, the number of sections, the required power supply, and the cost of construction and operation are considered as functions of the electric field strength along the axis of the waveguide, the sections of which are supplied independently by radio-frequency sources. The minimum costs of accelerator construction and operation are independent of the final electron energy. It is shown that it is most desirable to use radio-frequency sources of highest possible power (greater than 20 megawatts) for supplying the accelerator section. Consideration is given to the problem of increasing the length of the useful part of the radio-frequency pulse.

A comparative analysis shows that the most effective accelerating system for a linear travelling-wave electron accelerator is a disc-loaded waveguide operating in the $\pi/2$ travelling-wave mode (Fig. 1).

The method of applying power to a high-energy linear accelerator is a consideration of prime importance.

It is obvious that a high-energy accelerator must be divided into sections which are supplied by separate sources. There are several ways in which radio-frequency power (rf) can be supplied to an accelerator.

1) The rf power in any one section does not flow into following sections (independent section supply);

2) several sections may be coupled by common power flow;

3) rf power is recovered in each section or group of sections.

It can be shown that the best system for high-energy linear electron accelerators is the one in which the sections are supplied independently (Fig. 2).

One of the most important parameters in an accelerator of this type is the electric field strength E along the axis of the accelerator system. This quantity determines the basic parameters, the cost of accelerator construction and the power consumed in operation; hence the greatest care must be exercised in choosing it.

For a given electron energy an increase in the electric field strength along the axis of the accelerating system implies a reduction in the length of the accelerator. A short accelerator has certain advantages: the ease with which the earth's magnetic field can be compensated, increased useful length of the rf pulse (because of the reduction in the time required to establish steady-state conditions in the feed waveguide), and the reduction in the radial divergence of the beam. These considerations indicate the desirability of increasing the electric field strength.

When the quantity E is increased the cost of construction and the cost of required shielding against harmful radiation are both reduced because of the shorter length. However, the cost of an accelerator is not determined solely by its length; the number of required rf generators increases as E increases, assuming a given power for the individual generators. We consider this problem in greater detail.

* Reported at the All-Union Conference on High-Energy Particle Physics, 1956.

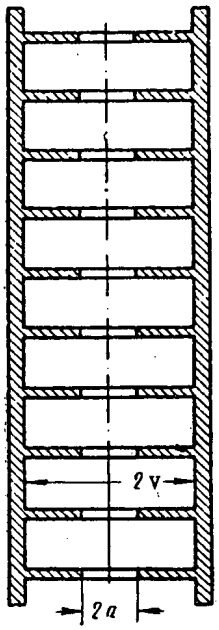

Fig. 1. Diagram of a disc-loaded waveguide. 2v is the diameter of the waveguide; 2a is the diameter of the coupling aperture in the disc .

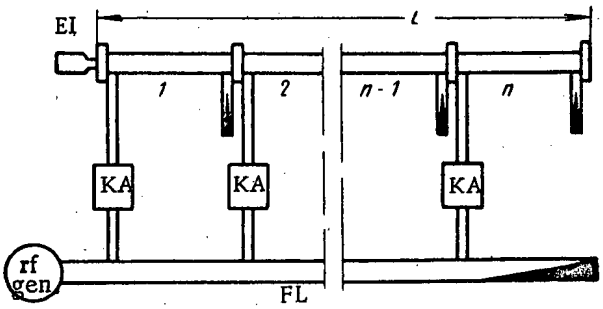

Fig. 2. Diagram of a linear accelerator with independently supplied sections. EI) electron injector, rf gen.) rf generator, FL) feed line, KA) klystron amplifier.

For a given electron energy at the output of the accelerator W_{out} the accelerator length L is determined by the mean electric field along the axis of the accelerating system E_m:

$$L = \frac{W_{out}}{eE_m}, \qquad (1)$$

where e is the charge of the electron.

In an accelerator in which independent supplies are used E_m is determined by the mean field strength in a section. In each section the field strength falls off exponentially as a function of length since rf power is dissipated because of absorption in the walls of the waveguide. As is well known, the mean electric field in a section is

$$E_m = \frac{1}{l}\int_0^l E_0 e^{-\frac{z}{l_{0E}}}\,dz = \frac{E_0 l_{0E}}{l}(1-\alpha), \qquad (2)$$

where E_0 is the strength of the electric field at the beginning of the section, l is the length of a section, l_{0E} is the decay length of the field and $\alpha = e^{-\frac{l}{l_{0E}}} = \frac{E_{z=l}}{E_0}$ is the field decay factor.

In sections which are not coupled by power flow the factor α may reasonably be taken as 0.5. Then l is determined uniquely by l_{0E} while the mean field strength in a section is determined by the rf power at the input to the section. Thus, for a given energy, having determined E_m and l, it is possible to compute the total length of the accelerator and the number of required sections, i. e., the number of rf generators.

For a given wavelength the geometric dimensions of the waveguide are determined by the rf power and the electric field in the initial section of the accelerator.

The radius of the coupling aperture in a disc-loaded accelerating system (Fig. 1) is found from the well-known expression [1] for the power at the input to the section:

$$S = \frac{k^2 a^4}{960} E_0^2, \qquad (3)$$

where S is the rf power in watts at the beginning of the section, a is the radius of the coupling aperture in cm, $k = \frac{2\pi}{\lambda}$ (λ is the wavelength in cm), E_0 is in v/cm. With given values of S and λ the quantity a depends only on E_0. The curves in Fig. 3 show the dependence of ka on E_0 for various values of S. The radius of the coupling aperture and radius of the waveguide v are related uniquely by the dispersion equation [2]. In Fig. 4 is shown this relation for the case $\beta = 1$.

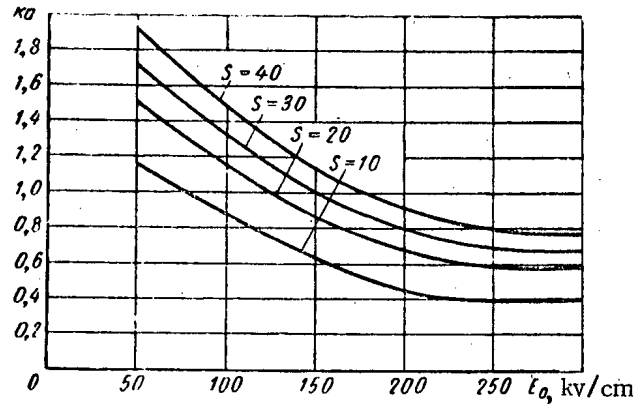

Fig. 3. The quantity ka ($k = \frac{2\pi}{\lambda}$, a is the radius of the aperture in disc) as the function of field strength E_0 for various values of the rf power S (megawatts) at the beginning of the section.

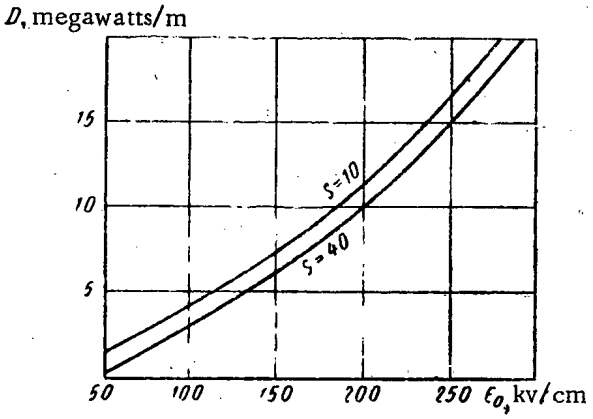

Fig. 5. The dependence of the rf power loss in the walls of the waveguide D on field strength for various values of rf power S (megawatts).

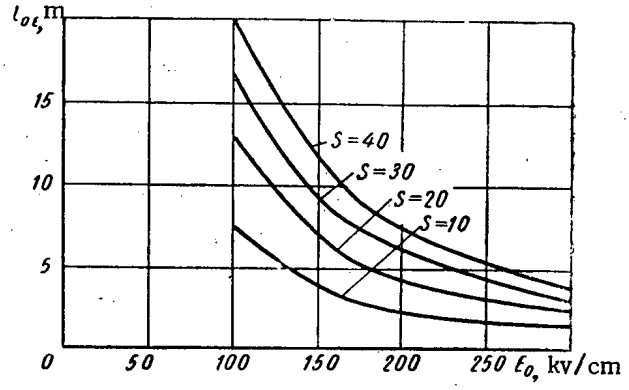

Fig. 6. The field decay length l_{0E} as a function of field strength E_0 for various values of rf power S (megawatts).

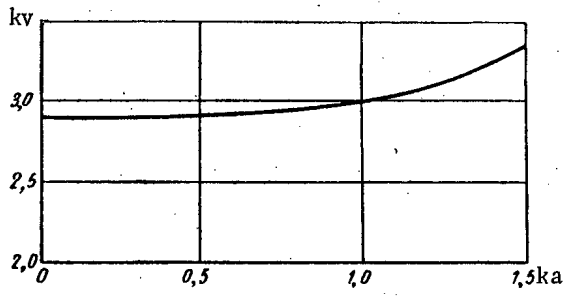

Fig. 4. The relation between kv and ka (v is the radius of the waveguide, a is the radius of the aperture in the disc, $k = \frac{2\pi}{\lambda}$).

The field decay length $l_{0E} = \frac{2S}{D}$, where D is the rf power loss in the waveguide walls. In Fig. 5 is shown the dependence of D on E_0 for S equal to 10 and 40 megawatts. The relations between l_{0E} and E is determined from these curves (Fig. 6).

The curves in Figs. 3, 4 and 6 make it possible to determine the dependence of accelerator length, number of sections and total required power on electric field. In Figs. 7, 8 and 9 these relations are given for various values of the power at the input of the section with α = = 0.5 (in order to make the results more useful the quantities are normalized to the energy of the accelerated electrons W_{out}).

The curve showing the dependence of normalized accelerator length on electric field (Fig. 7) is an equilateral hyperbola. It follows from Eqs. (1) and (2) that

$$\frac{L}{W_{out}} = \frac{r}{E_0}, \qquad (4)$$

where

$$r = \frac{1}{e\frac{l_{0E}}{l}(1-\alpha)}. \qquad (4a)$$

When α = 0.5, r = 1.39/e.

The relation between normalized number of sections and electric field is given by straight lines with different slopes [8]. We can approximate the relation by the equation

$$\frac{n}{W_{out}} = pE_0 + q, \qquad (5)$$

where p and q are the coefficients in the function for the power at the section input. The values of these coefficients, determined from Fig. 8, are presented in the table.

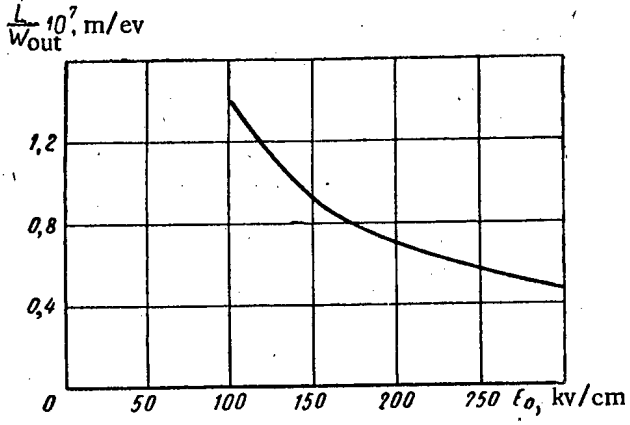

Fig. 7. Normalized accelerator length L/W_{out} as a function of field strength E_0.

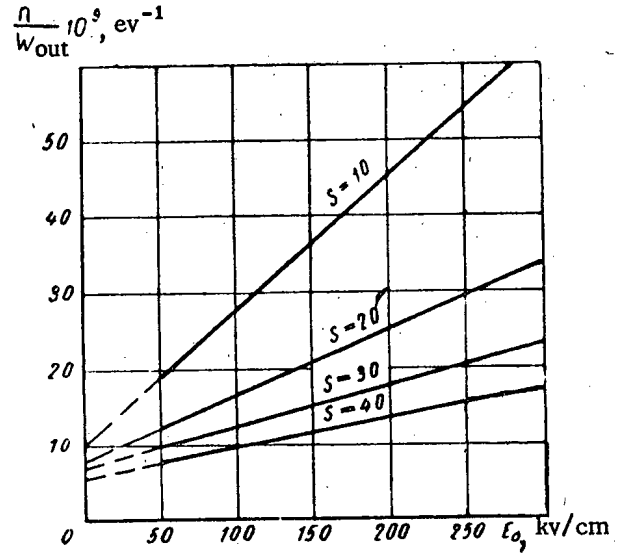

Fig. 8. Normalized number of sections n/W_{out} as a function of field strength E_0 for various values of the rf power S (megawatts).

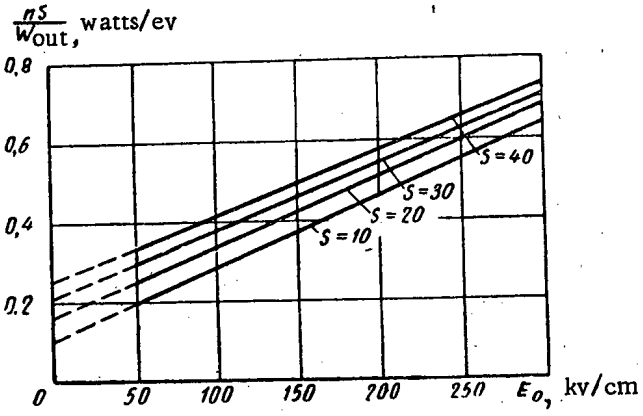

Fig. 9. Normalized total rf power nS/W_{out} as a function of field strength for various values of the rf power S (megawatts).

Values of p and q

S, megawatts	10	20	30	40
$p \cdot 10^9$, cm/v · ev	0,178	0,0875	0,055	0,042
$q \cdot 10^9$, ev^{-1}	10	7,8	6,95	5,95

Using the dependence of L/W_{out} and n/W_{out} on E_0, we find the value of E_0 for which the accelerator cost is a minimum.

We consider the accelerator elements whose cost of construction is proportional to length. These include the following:

1. The frame which supports the accelerating system (the width and height of this frame remain unchanged for any accelerator length).

2. The foundation for the accelerator system.

3. The accelerating system (disc-loaded waveguide).

4. The concrete shielding required to protect personnel against dangerous radiation.

The accelerator elements whose construction cost is proportional to the number of sections include:

1. The rf generators. In the first approximation the total space for these installations is proportional to the number of generators, that is, the number of sections.

2. The vacuum system. The cost of construction of the vacuum system is determined basically by the number of vacuum sections.

Calculations indicate that for a given value of the decay factor, for example, $\alpha = 0.5$, the admittance of a vacuum section is only slightly dependent on geometric dimensions since an increase in the length of a section implies an increase in the diameter of the coupling aperture in the loading disc and a corresponding increase in waveguide diameter. Hence, as a first approximation it may be assumed that the power required for the vacuum installation for a section remains fixed. In order to simplify the calculation it may be assumed that the number of vacuum sections is directly proportional to the number of rf sections.

3. The rf generators for driving the accelerator sections.

4. The waveguide system for supplying rf power and the phasing system.

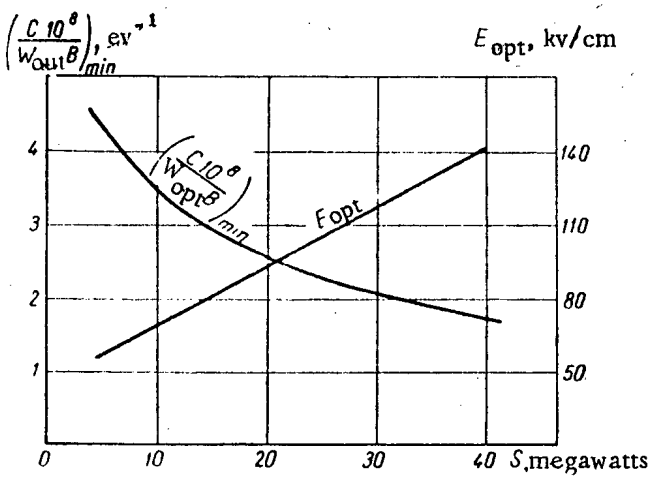

Fig. 10. The quantity E_{opt} and the normalized minimum construction cost of an accelerator $(C/W_{out})_{min}$ as a function of rf power S (megawatts).

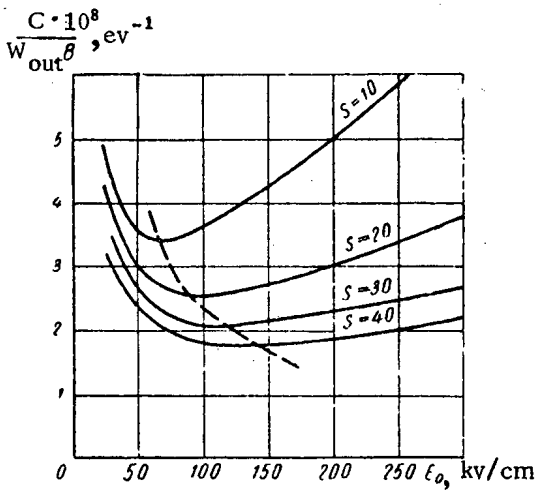

Fig. 11. Normalized accelerator construction cost as a function of field strength E_0 for various values of the rf power S (megawatts) (the dashed curve passes through points of minimum cost).

The items which consume most of the electrical power in the accelerator are the klystron power amplifiers. Hence, the required electrical power is proportional to the total rf power nS (Fig. 9). Since the cost of the electrical power installation increases much less rapidly than the power itself, in making rough calculations it may be assumed that the electrical power cost remains constant and independent of E_0.

Other items whose cost remains independent of accelerator length and number of sections are the electron extraction system, the target installations and the laboratory and various associated installations.

We are interested here only in costs which are proportional to accelerator length L and number of sections n. The sum of these two items C is given by the expression

$$C = AL + Bn, \qquad (6)$$

where A refers to costs involved in the construction of a linear meter of accelerator (elements whose cost is proportional to the length of the accelerator) and B refers to costs involved for a single section of the accelerator (those elements whose cost is proportional to the number of sections).

Substituting Eqs. (4) and (5) in Eq. (6), we have

$$\frac{C}{W_{out}} = \left[A\frac{r}{E_0} + B(pE_0 + q) \right], \qquad (7)$$

For a given rf power at the input of a section the cost depends only on E_0. The optimum electric field strength E_{opt} corresponding to minimum cost is determined from the equation $\frac{d}{dE_0}\left(\frac{C}{W_{out}}\right) = 0$:

$$E_{opt} = \sqrt{\frac{Ar}{Bp}} \leqslant E_{lim}. \qquad (8)$$

where E_{lim} is determined by the electrical breakdown properties of the accelerating system. The coefficient p is determined by S (cf. table). If α = const, then r = const, and from Eq. (8) it follows that E_{opt} depends only on S and is independent of the terminal energy of the accelerated electrons.

In Fig. 10 is shown the dependence of E_{opt} and the normalized cost $(C/W_{out})_{min}$ on rf power S. In plotting these curves it is assumed that the ratio $\frac{A}{B} = 6 \cdot 10^{-2}\ m^{-1}$.

The cost of accelerator construction starts to increase sharply when the input power becomes smaller than 20 megawatts.

In Fig. 11 is shown the normalized construction cost as a function of electric field strength E_0. The curves exhibit wide minima and the widths of these minima increase with increasing input power S. The cost increases very rapidly when $E_0 < E_{opt}$; for $E_0 > E_{opt}$ the cost increase becomes slower for larger values of S.

It is also possible, in this way, to plot curves for operating power. In Fig. 12 is shown the dependence of normalized operating power C/W_{out} on the electric field strength. These curves are similar to those shown in Fig. 11. The minima of the power consumption curves lie in the region of small E_0 and the consumption increases sharply to the left of the minimum point.

The optimum values of the electric field corresponding to minimum operating costs are smaller than the values of E_{opt} which determine the lowest constructional costs.

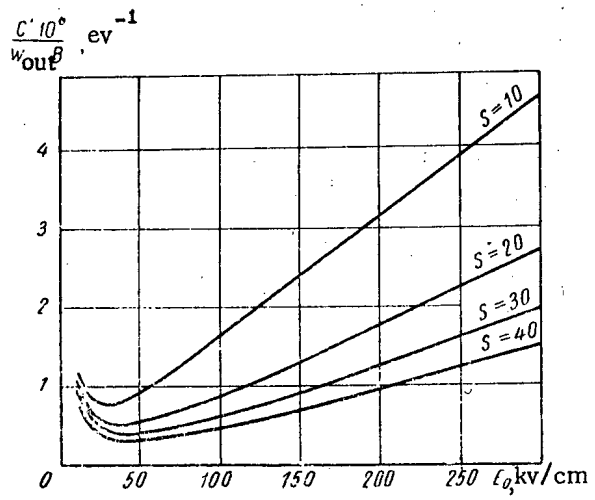

Fig. 12. Normalized accelerator operation cost as a function of field strength E_0 for various values of the rf power S (megawatts).

The curves in Figs. 11 and 12 indicate that the power output of the rf generators used to supply power to the accelerator section should be as high as possible.

Thus, the cost of construction and operation of a high-energy accelerator is characterized by minima which correspond to definite values of the electric field strength. These minima in the cost are independent of electron energy at the accelerator output.

It follows that the optimum values of the basic parameters for a high-energy linear electron accelerator (field E_0, rf power source, geometric dimensions of the accelerating system and section length) are also independent of the electron energy at the accelerator output.

In high energy accelerators the problems involved in obtaining the highest possible current are of special importance.

All other conditions remaining the same, the average current in a linear accelerator is determined by the length of the rf pulse. However, the pulses which can be obtained from presently available high-power rf generators are of extremely short duration so that it becomes fruitful to investigate means by which these pulses can be used more effectively in accelerating particles.

The electron acceleration actually takes place only during part of the rf pulse from the generator. This useful part of the pulse is limited by the transient processes involved in establishing steady-state rf oscillations in the accelerating system itself and in the feeder waveguides.

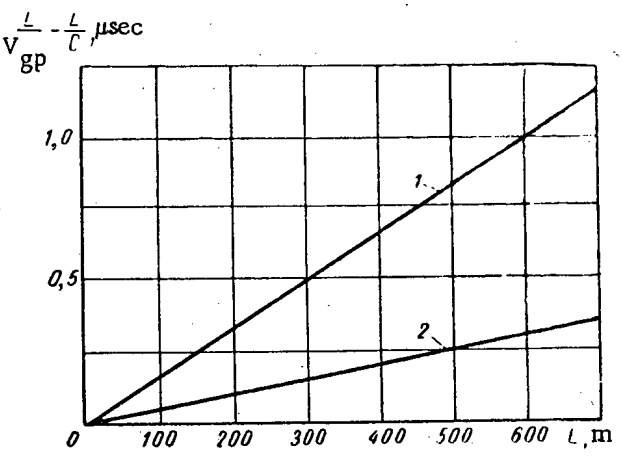

Fig. 13. Reduction in the useful part of the rf pulse due to the feeder line (rectangular waveguides) as a function of accelerator length L. 1) Waveguide cross section 72 × 34 mm^2; 2) waveguide cross section 110 × 54 mm^2.

In systems in which the sections are supplied independently this transient period is smaller than in other types of systems.

The electron traversal time in a high-energy linear accelerator is comparable with the duration of the rf pulse obtained from the klystron generator in each section. Thus, in order to obtain the most complete utilization of these pulses for electron acceleration it is necessary that the generators be switched on in a time sequence rather than simultaneously. This situation can be achieved if the signal which controls the application of the high voltage to the klystron and the rf power from a given generator are forced to propagate with the velocity of the electron being accelerated, that is to say, with the velocity of light. This condition can be satisfield without great difficulty in the first case; in the second case, however, it poses a difficult problem. There are two means by which this problem can be solved: increasing the velocity of the electromagnetic waves in the feeder waveguide and increasing the duration of the pulse which excites the rf power.

The velocity of propagation of the rf power in the waveguide is nothing more than the velocity of propagation of the pulse front, i. e., the signal group velocity v_{gp}. It is determined by the type of waveguide which is used. After the pulse front reaches a given point in the waveguide a transient process occurs and it is only after a certain time interval Δt that the rf oscillations at a given point may be assumed to have reached steady-state conditions. Calculations carried out by G. Ia. Liubarskii indicate that this time interval is small as compared with the propagation time. Hence Δt will not be taken into account in the following.

We now estimate the time required to achieve steady-state conditions in a system in which the accelerator sections are supplied independently (cf. Fig. 2), assuming for simplicity that the time required to reach steady-state conditions is equal to the propagation time. Using this procedure it is possible to determine the duration of the useful part of the rf pulse; it is assumed that the electrons reach an accelerator section when steady-state conditions have already been achieved. The duration of the useful part of the pulse τ_0 is given by the expression

$$\tau_0 = \tau - \left[\left(t - \frac{L}{c}\right) + t_к + t_y + t_d\right], \tag{9}$$

where τ is the length of the rf pulse from the klystron, $t = L/v_{gp}$ is the propagation time for a pulse in a smooth waveguide of length L, c is the velocity of light, t_k is the time required for steady-state conditions to obtain in the klystron, t_y is the propagation time for the rf oscillations in an accelerator section and t_d is the time spread due to variations in the firing time of the trigger discharge gap.

The propagation for the rf pulse in the waveguide section τ_y is determined by the decay factor α for the accelerating field in the section. When $\alpha = 0.5$, $t_y + t_k \approx 0.7$ μsec.

The reduction in the length of the useful part of the rf pulse due to the feeder line is $L/v_{gp} - L/c$. The magnitude of this difference is determined by the value of v_{gp} in the feeder waveguide and is shown in Fig. 13 for standard rectangular waveguides.

A radical solution to the problem is the use of a coaxial waveguide ($v_{gp} = c$) as the feeder line. In this case the feeder line does not introduce any reduction in the length of the useful part of the rf pulse.

When a rectangular waveguide is used it is necessary to increase the duration of the rf pulse at the input to the feeder line by an amount $L/v_{gp} - L/c$. In this case, the high-voltage pulse at the accelerator klystron for the first section must be delayed by an amount $L/v_{gp} - L/c$ with respect to the triggering voltage pulse. A special synchronization circuit must also provide appropriate time displacement in the application of the high-voltage to the other klystrons.

When above-indicated methods are used the useful part of the rf pulse is determined only by the time required to establish steady-state conditions in the accelerating section and the klystron, and the instability in the firing time of the trigger discharge. The ratio of the useful part of the pulse to the total pulse is independent of the final energy of the accelerated electrons.

LITERATURE CITED

[1] L. Levine, Contemporary Waveguide Theory [Russian translation] (IL, 1954).

[2] W. Walkinshaw, J. Appl. Phys. 20, 634 (1949).

Received May 14, 1957

SECONDARY NUCLEAR REACTIONS IN THE BOMBARDMENT OF TIN BY FAST PROTONS

M. Ia. Kuzuetsova, V. N. Mekhedov, and V. A. Khalkin

A radiochemical method has been used to study the capture of products arising in disintegration of target nuclei.

Using the measurements of yields of radioactive isotopes of tellurium (Z = 52) and iodine (Z = 53) obtained from tin (Z = 50) irradiated by protons with energy from 170 to 660 Mev excitation curves are plotted for the secondary reactions which lead to the formation of products with charges 2 and 3 units greater than the charge of the original nucleus. The cross sections for these reactions increases with increasing energy of the incident protons: $\sigma(\alpha, xn)$ and $\sigma(Li, xn)$ are respectively 18.5 ± 5 and 0.17 ± 0.1 mbarns for E_p = 170 Mev and 50 ± 6.5 and 1.6 ± 0.5 mbarns for E_p = 660 Mev. The cross sections for lithium capture by tin in a comparable proton energy interval are in good agreement with the results of investigations of similar reactions in copper, tin and lead but are found to be 50 times smaller than the cross sections obtained by Marquez and Perlman.

The observed cross sections for the secondary lithium capture can be explained only by assuming that these nuclei acquire energies greater than that which can be obtained in evaporation or fission of the target nuclei.

Secondary reactions of the (α, xn) type can be explained satisfactorily on the basis of an evaporation mechanism for the formation of the helium nuclei.

When various elements are bombarded with protons with energies of several hundred million electron volts one observes formation of radioactive nuclides with atomic numbers larger than that of the original nucleus [1-6]. These nuclides are produced chiefly in capture of the disintegration products $_2He^4$, $_3Li$ and $_4Be$ by the target nuclei. The cross section for these secondary reactions is small. At energies of 340-480 Mev $\sigma_{Z+2} \approx \approx 10^{-29}$ cm^2 and $\sigma_{Z+3} \approx 10^{-31}$ cm^2. In both cases the cross section increases noticeably with increasing energy. For example, when copper is bombarded by 2.2 Bev protons the germanium formation cross section increases by a factor of 10 as compared with the cross section obtained with 340 Mev protons.

The data obtained by different authors on the secondary-reaction cross sections are in satisfactory agreement. The single exception is the work reported by Marquez and Perlman [2] in which the capture cross section for lithium by tin is, in order of magnitude, almost equal to the cross section for the capture of α-particles, i. e., a factor of 50-100 greater than for other elements.

The present work has been undertaken for two reasons: firstly, to check the data obtained in [2] on the cross section for the formation of iodine isotopes in the irradiation of tin and, secondly, to obtain additional data required for an understanding of the secondary-reaction mechanism.

EXPERIMENTAL METHOD

Tin samples of high purity (impurity content less than 10^{-4} %) wrapped in aluminum foil were irradiated by protons at different radii in the synchrocyclotron chamber. The target weights were 0.2-0.5 g. The irradiation lasted for 1-2 hrs. The intensity of the proton beam was determined from the Na^{24} accumulation in an aluminum monitor. In the proton energy region which was investigated the cross section for the $Al^{27}(p, 3pn)Na^{24}$ reaction was taken as 10 mbarns.

Iodine extraction. After irradiation the samples were dissolved in fuming concentrated nitric acid, containing calcium persulfate, 30 mg of iodine (KIO_3) and 50 mg of tellurium(nitric acid solution). The solution was diluted to 80-100 ml and the iodate was reduced to the iodide by sodium sulfate. The iodine was distilled successively through two absorbers. The first absorber was filled with a 1 M solution of HNO_3 and the second with a 1 M solution of NaOH. Then the elementary iodine was extracted twice with chloroform.

In the measurements a target of PdI_2 was used. As a rule the chemical yield of the carrier was 60-70%. A special check showed no loss of radioactive iodine due to absorption in tin dioxide formed when the metallic tin was dissolved in the HNO_3.

Tellurium extraction. When the iodine extraction was completed contents of the distillation flask were evaporated and the residue of tin dioxide was dissolved in concentrated hydrochloric acid. After removal of the excess HNO_3 the tellurium was precipitated by tin dichloride. The residue was centrifuged and again dissolved in a mixture of hydrochloric acid and nitric acid. 1-2 mg of the reverse carriers were added to the solution: selenium, antimony, arsenic, copper, etc. and it was evaporated until practically dry. The selenium, antimony, gold, and arsenic were separated by double evaporation of a solution with three ml of HBr. All traces of the HNO_3 were removed simultaneously. The residue was dissolved in a 3 M solution of HCl and the tellurium was precipitated from the boiling solution by sulfur gas. The evaporation of the HBr solution and the precipitation of metallic tellurium by sulfur gas were carried out twice. In order to keep the tellurium pure from contamination by precious metals it was distilled in a hydrogen stream at a temperature of 800-900°C. The condensate was washed in nitric acid and evaporated with HCl and HBr. The metallic tellurium precipitated by the sulfur gas was deposited on the target. The chemical yield was 20-40%.

Radioactivity measurements. The measurements of sample activity were carried out with an end counter with a mica window approximately 3 mg/cm^2 thick. The following iodine isotopes were found: I^{126} (β, K, T = = 13 days); I^{124} (β, K, T = 4.5 days); I^{123} (K, T = 13 hrs); I^{121} (β, K, T = 1.8 hrs); I^{120} (β, T = 30 min). The K-capture fractions in I^{126}, I^{124} and I^{121}, according to our measurements, which will be published, were 50, approximately 60 and approximately 60%, respectively. One half-life of approximately six days was found in tellurium. This activity was assigned to Te^{118} (K, T = 6 days), which was detected by means of the daughter nuclei Sb^{118} (β, T = 3.5 min, E_β = 3.1 Mev). It was impossible to distinguish periods corresponding to Te^{119} (K, T = 4.5 days), on the decay curve because of the proximity of the half-lives for Te^{119} and Te^{118} and the low efficiency for x-rays. A 2.5 hr activity (Te^{117}) was not observed.

EXPERIMENTAL RESULTS

The identification of the reaction products with charges 2 and 3 units greater than that of the original nucleus and the production cross sections for the products at various proton energies are shown in Table 1. In this table are shown the arithmetical averages of the experimental deviations for the cross sections as determined from three papers.

The low radioactivity of the targets and the large number of iodine isotopes complicated the resolution of the decay curve and the determination of the yields for individual products. The formation cross section for I^{121} may be taken as completely reliable. The total cross section may be somewhat high because of internal-conversion electrons in I^{123}. * It would seem that the absolute uncertainty in the total cross section is small since the

* In determining the I^{123} production cross section internal-conversion electrons were taken into account. The efficiency for x-ray detection of the end counter found with a standard I^{125} sample (K, T = 60 days) was 2%. Supplementary measurement with a cylindrical counter with aluminum walls verified the analysis of the decay curves. In this case I^{123} was not detected but the yield of the other isotopes were found in agreement with the data obtained with the end counter.

TABLE 1

Cross Sections for the Production of Isotopes of Tellurium and Iodine in the Bombardment of Tin by Protons of Various Energies (mbarns)

Isotope	Half-life	Data of present work				Data of [6]	
		170 Mev	340 Mev	480 Mev	660 Mev	340 Mev	480 Mev
Te^{118}	6 days	3,6 ±1,0	16,5 ±1,5	14,5 ±7,7	10 ±1,3	5,0	11
I^{120}	30 min	0,02±0,01	0,03±0,01	0,10±0,01	0,27±0,2	0,05	—
I^{121}	1,8 hrs	0,02±0,005	0,067±0,003	0,15±0,03	0,24±0,007	0,17	0,45
I^{123}	13 hrs	0,11±0,08	0,3±0,07	0,56±0,16	0,97±0,2	0,18	0,38
I^{124}	4,5 days	~0,01	0,024	0,035	0,06±0,008	} 0,11	0,41
I^{126}	13 days	~0,01	0,02	0,048±0,006	0,06±0,01		
Total cross section for iodine isotope		0,17±0,1	0,44±0,084	0,9 ±0,2	1,6 ±0,5	0,51	1,24

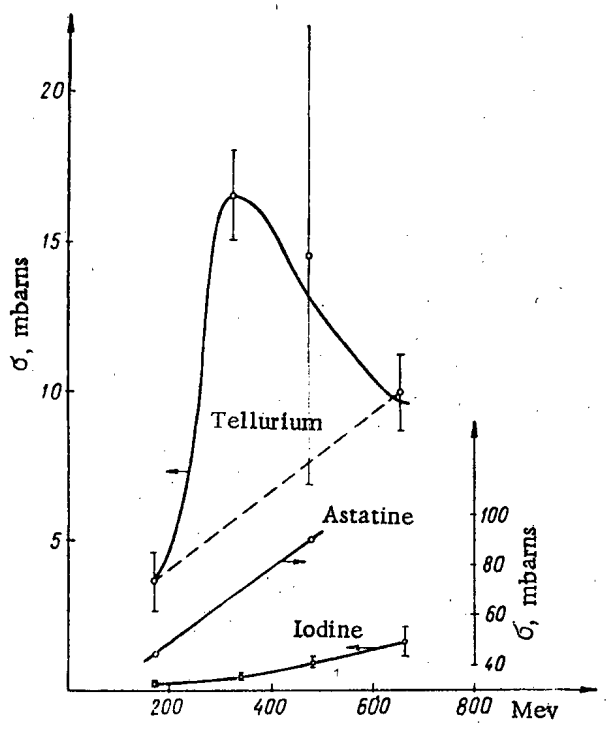

Yields of iodine and tellurium from tin for protons of various energies.

results of [6] (Table 1), obtained by a somewhat different method, are in rather good agreement with the present data. Moreover, the cross sections which have been found are approximately the same as the cross sections for the production of germanium isotopes and At^{211} in bombardment of copper and lead by protons [3] (cf. Table 2). Thus, it follows from the present data that the cross section for the secondary reaction involving lithium capture by tin at proton energies of 340 Mev is 50 times smaller than the values obtained by Marquez and Perlman [2]. In the present work the same iodine isotopes were found but the relative yields were very much different from the data reported in [2].

The possibility that the cross section measured in the present work was too low because of iodine loss in the target due to heating in the vacuum chamber of the synchrocyclotron during the bombardment was excluded by control experiments. In these experiments the bombardment was carried out on tin samples sealed in a thin-walled glass ampule. The cross sections for the production of iodine isotopes obtained in this case were in agreement with the cross sections shown in Table 1. An analysis of possible contaminants indicates that any contribution due to impurities in the formation of active iodine is negligible. Thus, the separation of barium (Z = 56) showed that any contribution to disintegration of impurities could be responsible for only $^1/_{25}$ of the active iodine.

The variation in the iodine production cross section with increasing proton energy is shown on the lower curve in the figure. The steeper increase in the cross section in the proton energy region above 400 Mev is due primarily to the increased yield of light iodine isotopes and can be explained by the formation of these isotopes in capture of fast protons with subsequent emission of two π-mesons and several neutrons. Unfortunately, the scarcity of experimental data makes it impossible to estimate the contribution arising from these reactions and to delineate the energy region in which they occur.

Only the α-production cross section was determined from the cross sections for secondary capture of Te^{118} particles (cf. Table 1). It reaches a maximum value at a proton energy line between 340-500 Mev and then falls off (cf. figure). A similar pattern is observed for the formation of light isotopes of astatine from bismuth

[1] and Ga^{66} from copper [5]. The peculiar dependence may best be explained by the existence of supplementary Te^{118} production reactions due to fast protron capture by target nuclei with the subsequent emission of π^--mesons and several neutrons. It is more difficult to explain the effect on the curve of changes in the spectrum and the probability for α-particle production because there is no explanation for the drop in the curve in the high-energy region.

TABLE 2

Cross Sections for Secondary Capture of α-Particle and Lithium Nuclei for Copper, Tin, Bismuth and Lead

Reaction	Original element	Reaction product	Experimental cross section 10^{-30} cm^2	Extrapolated cross section 10^{-30} cm^2	Literature reference
α-Particle capture	Cu	$Ga^{66}+Ga^{67}+Ga^{68}$	26 (340)	90	[3]
	Sn	Te^{118}	8 (480)	40	Present work
	Bi	$At^{210}+At^{211}$	80 (480)	80	[1]
Lithium capture	Cu	$Ge^{66}+Ge^{68}+Ge^{69}$	0,3 (340)	0,6	[3]
	Sn	$I^{120}+I^{121}+I^{123}+I^{124}+I^{126}$	0,9 (480)	0,9	Present work
	Pb	At^{211}	0,04—0,08	0,16—0,32	[1]

It is possible to estimate the contribution of the (α, xn) reaction in the production of Te^{118} in the region 180-660 Mev if it is assumed that: 1) at proton energies of 180 and 660 Mev the Te^{118} is produced basically through this reaction and 2) in this energy region the Te^{118} production cross section in the (α, xn) reaction changes in linear fashion (dashed line on the figure). The integrated energy dependence for the total cross section for the (α,xn) reaction in tin is found to be approximately the same as the dependence of the astatine production cross section in bismuth bombardment (solid line in the figure). The last fact may be considered verification of the present interpretation. At proton energies of 480 Mev the integrated value of the Te^{118} production cross section in the (α, xn) reaction is 8 mbarns.

DISCUSSION OF RESULTS

In comparing the present data with data reported by other authors [1, 3] it is necessary to estimate the total tellurium production cross section. For this purpose it is sufficient to multiply the Te^{118} production cross section by a factor of approximately 5.* The total tellurium production cross section determined in this way (40 mbarns at E_p = 480 Mev) is found to be approximately the same as the cross section for the formation of gallium isotopes from copper [3] and At^{210} and At^{211} from bismuth [1] in a comparable incident-particle energy range (Table 2).

It is interesting to compare the presently available data on secondary-reaction cross sections. These data are shown in Table 2. In this table are shown the experimental cross sections obtained at various proton energies (the energy values in Mev are shown in brackets). In a number of cases not all the reaction products are observed. Hence, in order to make a comparison it is necessary to extrapolate the cross sections at the same energy of the bombarding particles and to take account of the unobserved reaction products. The extrapolated cross sections for E_p = 480 Mev are shown in the next to the last column in Table 2. In extrapolating the cross sections it has been assumed that the energy dependence of the secondary-reaction product yields in copper is similar to those in tin and bismuth. Correction factors which take account of the increase in cross section as the energy is changed from 340 to 480 Mev were found to be 1.0 for gallium isotopes and 2.0 for germanium. The correction factor for

* In studying the production of astatine from bismuth [1] it was found that the astatine is formed mainly as a result of (α, 2n) and (α, 3n) reactions. Assuming a similar mechanism for Te^{118} production and taking account of the abundances of the tin isotopes Sn^{116} and Sn^{117} (20%) we obtain the factor of 5 indicated above.

the unobserved products of α-particle capture in the copper case was approximately 3 (the isotopes Ga^{66}, Ga^{67} and Ga^{68} obtained mainly from the (α, 2n) and (α, 3n) reactions in the Cu^{65} isotope, characterized by an abundance of 30%. For tin this factor is 5 as indicated above. In determining the total cross section for the production of astatine from lead the At^{211} production cross section was multiplied by a factor of 4. However, the extrapolated cross sections for astatine is too low as a consequency of the incomplete chemical separation of At^{211} in [1].

It is apparent from Table 2 that the α-particle capture reaction is characterized by approximately the same cross section in nuclei with entirely different atomic numbers.

The reaction cross section for lithium capture is approximately two orders of magnitude lower than the cross section for α-particle capture and is also essentially independent of the atomic number of the bombarded elements.

The last finding is somewhat unexpected. In the literature it is reported that the yields of the light nuclei Li^8 and Be^7 are reduced noticeably with increasing Z of the target nucleus [2, 7]. Hence, the cross section for secondary capture of lithium should be reduced by approximately a factor of 10 in going from copper to lead.

If the observed cross section for the capture of α-particles can be explained satisfactorily by assuming that these particles are formed in an evaporation process, the interpretation of the lithium reaction requires other assumptions. In analyzing the yield of iodine from tin, Marquez and Perlman [2] assume that all the lithium nuclei are emitted with energies of 80 Mev. However, their calculations lead to computed production cross sections for Li^8 or Be^7 which are 500 times higher than the experimental cross sections.

A calculation based on the Marquez and Perlman scheme, using the iodine yield obtained in the present experiments with E_p = 340 Mev, gives a value of approximately 0.5 mbarns for the lithium production cross section. This quantity is approximately ten times larger than the Li^8 production cross section in xenon [7] or Be^7 in silver [2] in bombardment by protons of approximately the same energy. However, this discrepancy is not of great importance in view of the qualitative nature of the estimate and the fact that lithium isotopes other than Li^8 can take part in the secondary reactions. The cross section for the production of lithium nuclei with energies higher than Coulomb barrier can be estimated from the result of a study of stars from fragments in photoemulsions. Such fragment observations ($Z \geq 4$) have been carried out at the synchrocyclotron by Lozhkin and Perfilov [8]. An analysis of the results of this work shows that the cross section for the formation of lithium is 0.1 mbarns, a value which is in rather good agreement with the present computed value.

A calculation carried out under the assumption that all the lithium nuclei are formed with energies of 40 Mev yields a value which is approximately 15 times greater than the value of the cross section obtained from a calculation in which it is assumed that the nuclei have energies of 80 Mev.

Using the iodine isotope yield an attempt was made to approximate the energy spectrum $f(E)$ of the emitted lithium nuclei. The estimate was made on the basis of the expression*

$$B = n \int_0^{\infty} f(E)\, dE \int_{E_0}^{E} \frac{\sigma(E)\, dE}{-\frac{dE}{dx}}$$

and indicates that the assumption of a steeply dropping spectrum leads to a value of the lithium production cross section which is much too high. Thus, for a spectrum extending to 80 Mev following a $1/E^2$ relation the value σ_{Li} = 1 mbarn is obtained. For a $1/E^8$ spectrum the quantity σ_{Li} is found to be approximately 20 mbarns, i. e., considerably larger than the experimentally observed cross section for the formation of Li^8 for Be^7. The basic error in these estimates arises as a result of the uncertainty in the excitation function for the (Li, xn) reactions; these are approximated by analogy with the excitation function for (α, xn) reactions.

* In this expression: B is the capture product yield, n is the number of tin nuclei in 1 cm^3; $-\frac{dE}{dx}$ is the energy loss of the lithium nuclei in ionization, E_0 is the initial energy in the excitation function for the capture of lithium by tin $\sigma(E)$.

Because of the qualitative nature of the calculations it is impossible to draw any definite conclusions as to the energy spectrum of the reacting nuclei. However, these estimates do indicate that if one is to explain the the observed cross section for secondary capture of lithium nuclei it is necessary to assume that these nuclei are formed with energies considerably greater than those which would be obtained in evaporation or fission of the original target nuclei. It is reasonable to suppose that the emission of fast fragments, which are responsible for the secondary reactions, occurs in the collision of the incident protons with the substructure of the nucleus which is formed as a result of fluctuations in the density of nuclear matter. Such ideas have already been proposed several times in the literature [8, 9] but no final theory for this effect has as yet been suggested. We propose that, along with other methods of investigation, a successful understanding of the features of this interaction mechanism will be achieved by further study of secondary reactions.

The authors are indebted to B. V. Kurchatov, V. G. Solov'ev, and I. Iu. Levenberg for help in carrying out the present work and to V. P. Dzhelepov, M. G. Meshcheriakov and G. A. Leskin for a number of valuable critical remarks.

LITERATURE CITED

[1] B. V. Kurchatov, V. N. Mekhedov, M. Ia. Kuznetsova, L. I. Kurchatova and N. I. Borisova, Combined Report of the Joint Institute for Nuclear Research No. 633 (1951).

[2] L. Marquez and I. Perlman, Phys. Rev. 81, 953 (1951).

[3] R. E. Batrel, D. K. Miller and L. T. Seaborg, Phys. Rev. 84, 671 (1951).

[4] A. Tarnevich and N. Sugarman, Phys. Rev. 94, 728 (1954).

[5] A. P. Vinogradov, I. L. Alimarin, V. I. Baranov, A. N. Lavrukhina and F. I. Pavoltskaia, Conference of the Academy of Sciences USSR on the Peaceful Use of Atomic Energy (Division of Chemical Sciences) Izv. Akad. Nauk SSSR 1955, p. 97.

[6] B. V. Kurchatov, V. N. Mekhedov, L. I. Kurchatova, M. Ia. Kuznetsova and L. V. Kuznetsova, Combined Report for the Joint Institute of Nuclear Research No. 258 (1953).

[7] S. C. Wright, Phys. Rev. 79, 838 (1950).

[8] O. V. Lozhkin and N. A. Perfilov, J. Exptl. Theoret. Phys. (USSR) 31, 913 (1956).*

[9] D. I. Bloc Blokhintsev, Usp. Fiz. Nauk 61, 137 (1957).

Received June 18, 1957

* See English translation.

DOSE CHARACTERISTICS OF A MIXTURE OF URANIUM FISSION FRAGMENTS

K. K. Aglintsev, A. N. Gorobets, V. P. Kasatkin, and E. S. Kondakova

Results are presented for calculations for the different dose characteristics of fragment elements: the percentage composition of the mixture for a uranium exposure time t_0 = 100 days and a cooling off period τ = 15-540 days, the time variation of the activity of the mixture for t_0, equal to 60, 100 and 150 days. The calculated data are in satisfactory agreement with the results of radiochemical analyses.

The gamma constant of the mixture is essentially independent of t_0 (within the limits 60-150 days) and also remains approximately constant for values of τ ranging from 15-180 days.

The operation of nuclear reactors results in the formations of appreciable numbers of radioactive fragment nuclides. The practical utilization of preparations made from a mixture of fission fragments requires a knowledge of the radiochemical composition and dose characteristics of these mixtures. Obviously, special attention is merited by those nuclides which are characterized by relatively high yields and long half-lives and the two- or three-member chains which contain such nuclides. Data on these nuclides are given in Table 1 [1-4]. In those cases in which the nuclide is not produced directly in uranium fission but results from the decay of the fragment nuclei the table indicates the chain which leads to the formation of this nuclei. No gaseous fission fragments (krypton, iodine, xenon) are shown in Table 1 since these escape from the fragment mixture.

TABLE 1

Yields and Decay Chains for Certain Fission Fragments

Nuclide	Fission yield, %	Chain
Sr^{89}	4,8	—
Sr^{90}	5,8	—
Sr^{91}	5,1	—
Y^{90}	—	$Sr^{90} \rightarrow Y^{90}$
Y^{91}	5,9	—
Zr^{95}	—	$Sr^{91} \rightarrow Y^{91}$
Nb^{95}	6,0	—
Ru^{103}	—	$Zr^{95} \rightarrow Nb^{95}$
Ru^{106}	2,9	—
Rh^{106}	0,4	—
Cs^{137}	—	$Ru^{106} \rightarrow Rh^{106}$
Ba^{140}	5,9	—
Ba^{141}	6,3	—
La^{140}	4,6	—
La^{143}	—	$Ba^{140} \rightarrow La^{140}$
Ce^{141}	3,8	—
Ce^{141}	5,7	—
Ce^{143}	—	$Ba^{141} \rightarrow La^{141} \rightarrow Ce^{141}$
Ce^{144}	5,4	—
Pr^{143}	6,2	—
Pr^{144}	—	$La^{143} \rightarrow Ce^{143} \rightarrow Pr^{143}$
Nd^{147}	—	$Ce^{144} \rightarrow Pr^{144}$
Pm^{147}	2,6	—
Pm^{147}	2,6	—
	—	$Nd^{147} \rightarrow Pm^{147}$

A calculation of the activity of nuclides formed directly in fission or in two-member chains leads to the expressions:

$$(\lambda_1 N_1)_\tau = F p_1 (1 - e^{-\lambda_1 t_0}) e^{-\lambda_1 \tau},$$

$$(\lambda_2 N_2)_\tau = \frac{F p_1 T_1}{T_1 - T_2} (1 - e^{-\lambda_1 t_0}) e^{-\lambda_1 \tau} + \frac{F p_1 T_2}{T_2 - T_1} (1 - e^{-\lambda_2 t_0}) e^{-\lambda_2 \tau},$$

where p_1 is the fission yield, t_0 is the length of time the uranium is exposed in the reactor, τ is the time reckoned from the termination of exposure, λ_1, λ_2, T_1 and T_2 are the decay constants and the half-lives of the nuclides, and F is the number of fission events per kilowatt of reactor power.

In Fig. 1 are shown the results of the calculation of the percentage radiochemical content of uranium

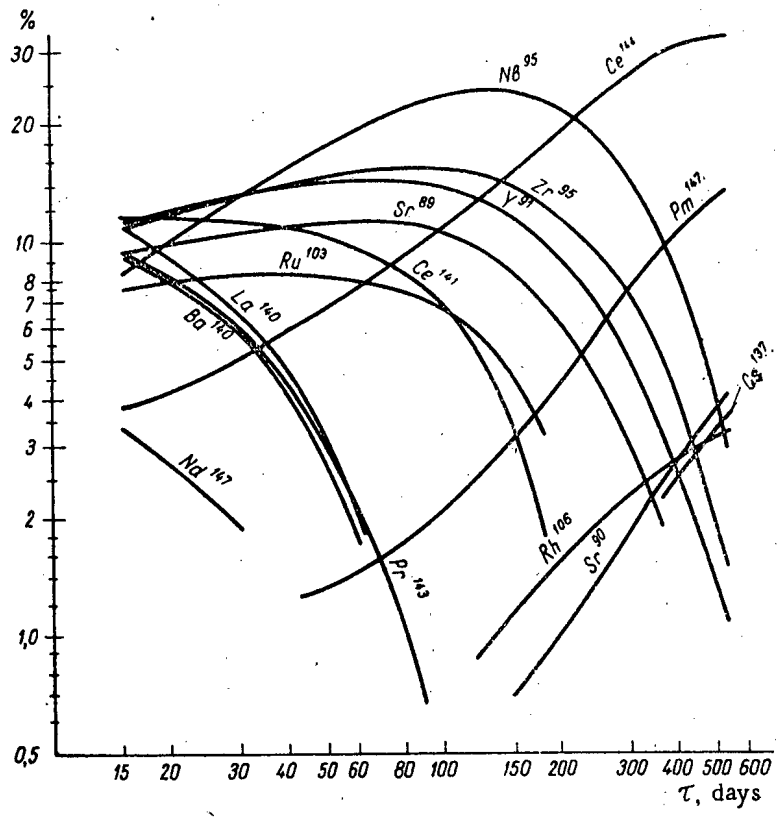

Fig. 1. Radiochemical composition of a mixture of uranium fission fragments of different age (t_0 = 100 days). The Pr^{144} and Y^{90} content are determined from the curve for Ce^{144} and Sr^{90}.

TABLE 2

Percentage Content of Isotopes for Various Cooling-Off Times for Fission Fragments t_0 = 100 days

Nuclides	% content τ=45 days		% content τ=400 days	
	calc.	exptl.	calc.	exptl.
$Sr^{89}+Sr^{90}$	11,2	11,4	4,3	7,2
$Y^{90}+Y^{91}$	14,1	17,7	5,3	5,0
Zr^{95}	14,2	13,6	4,2	3,2
Nb^{95}	15,9	12,8	8,5	4,6
Ru^{103}	8,3	5,1	—	—
Rh^{106}	—	—	2,7	1,0
Cs^{137}	—	—	2,6	2,9
Ba^{140}	3,4	3,9	—	—
La^{140}	4,0	—	—	—
$Ce^{141}+Ce^{14}$	17,0	—	30,2	33,0
Pr^{143}	3,7	—	—	—
Pr^{144}	6,5	—	30,2	33,0
Pm^{147}	1,2	—	10,2	11,5
$La^{140}+Pr^{143}+Pm^{147}$	8,9	9,2	—	—
$Ce^{141}+Ce^{144}+Pr^{144}$	23,5	24,2	60,4	66,0

fission fragments for t_0 = 100 days and τ = 15-540 days. In Fig. 2 is shown the time variation of the total activity, A, of fission fragments for t_0 equal to 60, 100 and 150 days.

Table 2 contains a comparison of the calculated data and the results of radiochemical analyses of a mixture of uranium fission fragments for t_0 equal to 100 days and τ equal to 45 and 400 days.

It is apparent from Table 2 that the experimental and calculated data are in satisfactory agreement.

The dose characteristics of a mixture of fission fragments are determined by the energy distribution of the electron in the β-spectrum of the mixture, the energy of the γ-rays and the number of γ-photons per β-particle. The data on the β-spectrum determine the penetrating power and the surface and depth doses in the field of a radiator for any configuration; the data on the γ-spectrum determines the γ-constant and the penetration power of the γ-radiation.

The β-spectrum of a mixture of fission fragments is extremely complicated: in a mixture of fission fragments one encounters β-spectrum with maximum energies ranging from 0.16 Mev (Nb^{95}) to 3.5 Mev (the partial

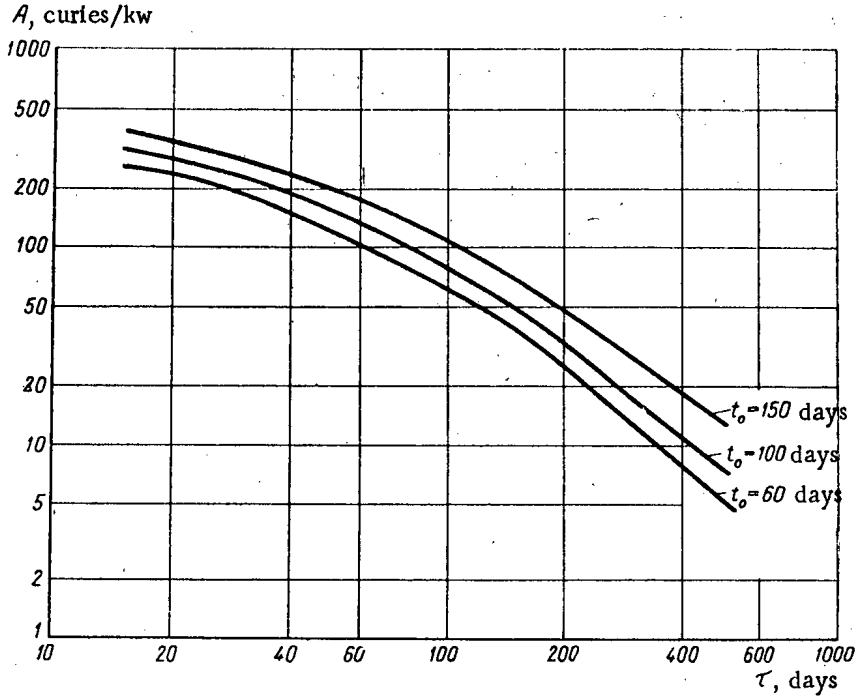

Fig. 2. Time variation of the total activity of a mixture of uranium fission fragments.

β-spectrum of Rh^{106}). The relations between the soft and hard β-spectrum change continuously in accordance with the composition of the mixture of fission fragments.

The main γ-radiators in a mixture of fission fragments are: Zr^{95}, Nb^{95}, Ru^{103}, Rh^{106}, Cs^{137}, Ba^{140}, La^{140}, Pr^{144}, Nd^{147}. The remaining nuclides are either very soft ($h\nu < 200$ kev) or very weak γ-radiators.

In a fresh mixture ($\tau \leq 60$ days) the most important γ-radiators are: Ba^{140}, La^{140}, Zr^{95}, Nb^{95} and Nd^{147}; in a medium age mixture ($60 < \tau < 360$ days) the most important radiators are Zr^{95} and Nb^{95}; in an old mixture ($\tau > 360$ days) the important radiators are Cs^{137}, Rh^{106}, Pr^{144}.

The γ-constant of the mixture, i. e., the dose in r/hr at a distance of 1 m from a preparation of 1 curie strength is obtained by summing the values of the γ-constants of the individual nuclides multiplied by their fractional content in the mixture. The results are shown in Table 3.

As is apparent from Table 3 the γ-constant remains approximately constant within the limits 0.15-0.17 r/hr-curie-meter for a mixture of age τ = 15-180 days, and then falls off rapidly to 0.07-0.08 r/hr-curie-meter for τ = 360 days and finally to 0.02 r/hr-curie-meter for an age of 540 days.

This dependence of the γ-constant on the age of the fission fragments is due to the fact that at ages greater than 180 days the amount of Zr^{95} + Nb^{95} falls off rapidly and is not compensated by the slow increase in the long-lived nuclides Cs^{137} and Rh^{106}.

TABLE 3

Values of the γ-Constant for a Fragment Mixture as a Function of τ and t_0

t_0 \ τ	15	30	45	60	90	120	150	180	360	540
60	0,175	0,160	0,150	0,152	0,155	0,155	0,155	0,155	0,080	0,020
100	0,175	0,170	0,150	0,155	0,155	0,155	0,150	0,140	0,070	0,020
150	0,170	0,160	0,165	0,155	0,155	0,155	0,150	0,140	0,065	0,020

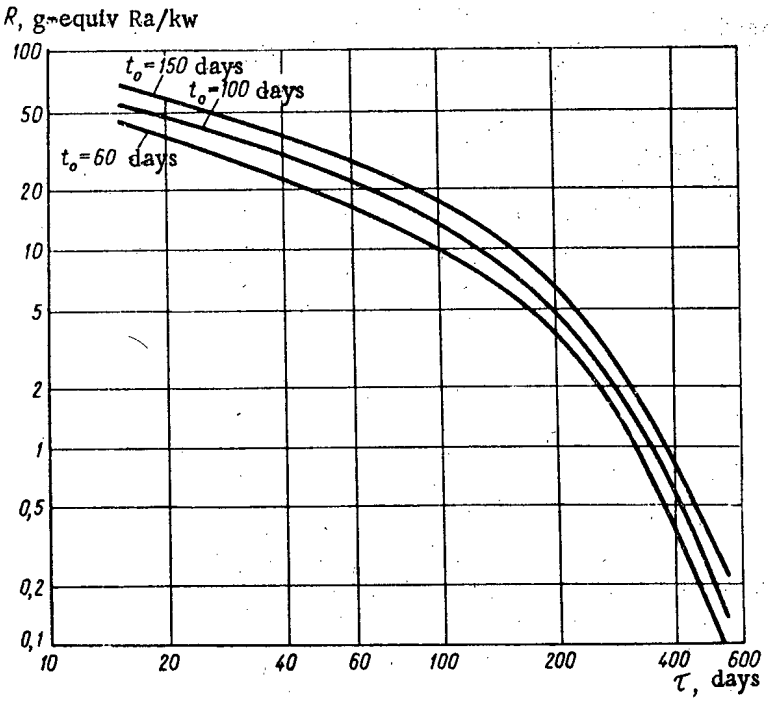

Fig. 3. Time variation of a γ-equivalent of a mixture of uranium fission fragments.

The conversion from the values of the γ-constant in r/hr-curie-meter to the γ-equivalent preparation in g-equivalents of radium is carried out by dividing by the factor 0.84. Values of the γ-constant 0.02, 0.07, and 0.15-0.17 r/hr-curie-meter correspond to values of the γ-equivalent of 0.024, 0.096 and 0.18-0.20 g-equiv. Ra/curie.

An examination of Table 3 indicates that the basic dose characteristics of a mixture of fission fragments – the γ-constant for the number of g-equivalents of radium per curie is essentially independent of t_0 the duration of the uranium exposure in the reactor when t_0 lies between 60 and 150 days. Precisely the same change in the γ-constant with age τ of the mixture is found for different values of t_0. From Fig. 2 it is also apparent that when t_0 is increased the activity of the mixture increases; this situation is especially noticeable at high values of τ. Comparing the data in Fig. 2 and Table 3 it is easy to find the γ-equivalent R of a fragment mixture, expressed in g-equivalents of radium per kilowatt of reactor power. These values are shown in Fig. 3.

LITERATURE CITED

[1] C. Coryell and N. Sugermann, Radiochemical Studies. The Fission Products (McGraw-Hill, N. Y. 1951).

[2] G. Reed and A. Turkevich, Phys. Rev. 92, 1473 (1953).

[3] L. Glendenin et al., Proc. Intern. Conf. Peaceful Uses of Atomic Energy, Geneva, 1955 (N. Y., 1956), vol. 7, p. 3.

[4] W. Hardwick, Phys. Rev. 92, 1072 (1953).

Received September 5, 1957

LETTERS TO THE EDITOR

BREMSSTRAHLUNG IN NUCLEAR FISSION*

A. I. Alekseev

The Coulomb interaction between nuclear fragments leads to electromagnetic radiation in the decay of nuclei. The calculation of this radiation can be simplified considerably if account is taken of the following. The electromagnetic radiation is most intense while the fragments move in a region with dimensions of the order of the Bohr radius of the mother atom; in this region the moving fragments have not yet been "covered" by the electrons and thus the Coulomb interaction is strongest. The probability that the nuclear fragments will attract electrons of the mother atom is very high [1] since in all cases of nuclear decay the fragment velocity is no greater than the mean velocity of the electrons in the atom. If the fragment velocity is much smaller than the mean velocity of electrons in the outer shell of the mother atom the ionic charge of decay products is essentially zero at the beginning of the trajectory [1], i. e., there is almost complete shielding of the fragments by the electrons of the mother atom. In what follows we shall be interested only in the continuous bremsstrahlung of the fragment and shall neglect the radiation associated with individual photons due to changes of the electronic shells in covering the fragments. A consideration of the mass defects of nuclei shows that in heavy nuclei energies ranging from several million electron volts to 200 Mev are liberated in a single fission event [2]. At these energies the de Broglie wavelength of each fragment is much smaller than the dimensions of the region of intense radiation. Thus, in the decay of a nucleus with charge Z into two fragments with mass numbers A_1 and A_2 we find

$$\frac{\lambda_s}{a} = \frac{e^2}{\hbar c} \frac{Z}{\sqrt{2A_s}} \left(\frac{m_e}{m}\right)^{1/2} \left(\frac{m_\oplus c^2}{E_s}\right)^{1/2}, \tag{1}$$

where λ_s is the de Broglie wavelength of the sth fragment (s = 1.2); a is the Bohr radius of the mother atom; m and m_e are the masses of the nucleon and electron, respectively; E_s is the kinetic energy of the sth fragment after fission; $e^2/\hbar c = 1/137$. In decay of heavy nuclei the energy E_s is usually reckoned in the order of millions of electron volts so that in fission the ratio λ_s/a is smaller than 10^{-2}. As is well known, the fact that the de Broglie wavelength is small compared with the characteristic dimensions of a charge means that a classical description can be used in analyzing the motion of the particle . Hence, we can use classical considerations to compute the electromagnetic radiation characteristic of the flight of fragments from the point at which they escape through the potential barrier out to infinity. This analysis, however, is not applicable in the small region close to the point at which the fragments pass through the potential barrier (i. e., the point at which the classical momentum of the fragment is zero); in this region the basic requirement for applying a classical description is not satisfied [3]:

$$\frac{d}{dr}\left(\frac{\hbar}{p(r)}\right) \ll 1, \tag{2}$$

where $p(r) \equiv \sqrt{2\mu(E - U(r))}$ is the classical momentum of a particle of mass μ moving with a total energy E in a potential U(r). Estimates show that the region of values of r in which the requirement in (2) is not satisfied is of the order $\Delta r = 10^{-2} R$ (R is the point at which the fragment escapes from the potential barrier, being determined by the equation $E - U(r) = 0$), so that the fragment radiation in this region is small as compared with the total bremsstrahlung.

* The present report is part of a diplomate thesis carried out by the author in 1952 at MIFI under the direction of A. B. Migdal.

We consider the decay of a nucleus into two fragments with mass numbers A_1 and A_2 and charges Z_1 and Z_2. In moving in a region with dimensions of order a the fragments interact in accordance with Coulomb's law; outside this region the fragments are covered by electrons so that the interaction is described by a more complicated relation. However, an estimate indicates that the bremsstrahlung outside the region of order a is $(R/a)^3$ times smaller than the bremsstrahlung inside this region. We can thus neglect completely the bremsstrahlung outside the region a. It is sufficient to consider the fragment motion inside this region. Because of the Coulomb interaction the fragments are accelerated. In accordance with the laws of classical electrodynamics a charge which moves with accelerated motion must radiate. Under these conditions the time for intense fragment radiation is a/v (v is the mean relative velocity of the fragment), so that the energy is radiated mainly as a wave of frequency ω which is smaller than v/a:

$$\omega < v/a. \tag{3}$$

At these frequencies λ_ω is large compared with the dimensions of the region of intense radiation $a/\lambda_\omega = v/c \ll 1$ so that most of the fragment radiation is dipole radiation which, in the present case, is characterized by the following spectral distribution:

$$d\mathcal{E}(\omega) = \frac{4}{3\pi}\frac{e^2}{\hbar c}\left(\frac{Z_1}{A_1}-\frac{Z_2}{A_2}\right)^2\frac{A_1A_2}{A_1+A_2}\frac{E}{mc^2}|f(\omega)|^2\hbar d\omega, \tag{4}$$

where

$$f(\omega) = \int_0^\infty \frac{\exp\left[-i\frac{\omega}{\omega_0}(\mathrm{sh}\xi+\xi)\right]}{\cosh\xi+1}d\xi,$$
$$\omega_0 = \left(\frac{2(A_1+A_2)E}{A_1A_2m}\right)^{1/2}\frac{2E}{Z_1Z_2e^2}. \tag{5}$$

Here $d\mathcal{E}(\omega)$ is the amount of energy radiated (over the entire trajectory of the fragments) in the form of waves with frequencies lying within the interval $d\omega$; E is the kinetic energy of both fragments at infinity; m is the mass of the nucleon. In the integral given in (5) the finite upper limit of integration, which is determined by the dimensions of the region of intense radiation a, is replaced by ∞. The error which arises in this procedure is of the order R/a.

At low frequencies $\omega \ll \omega_0$ the radiated energy is independent of frequency:

$$d\mathcal{E}(\omega) = \frac{4}{3\pi}\frac{e^2}{\hbar c}\left(\frac{Z_1}{A_1}-\frac{Z_2}{A_2}\right)^2\frac{A_1A_2}{A_1+A_2}\frac{E}{mc^2}\hbar d\omega. \tag{6}$$

At high frequencies $\omega \gg \omega_0$ the energy radiated at a frequency ω is inversely proportional to the square of the frequency:

$$d\mathcal{E}(\omega) = \frac{2}{3\pi Z_1^2Z_2^2}\left(\frac{e^2}{\hbar c}\right)^{-1}\left(\frac{Z_1}{A_1}-\frac{Z_2}{A_2}\right)^2\times \times\left(\frac{E}{mc^2}\right)^2\left(\frac{E}{\hbar\omega}\right)^2\hbar d\omega. \tag{7}$$

The total electromagnetic radiation associated with the fragment bremsstrahlung $\mathcal{E}$ is given by the following expression:

$$\mathcal{E} = \frac{16}{45}\left(\frac{Z_1}{A_1}-\frac{Z_2}{A_2}\right)^2\left(\frac{2A_1A_2}{A_1+A_2}\right)^{1/2}\left(\frac{E}{mc^2}\right)^{5/2}\frac{mc^2}{Z_1Z_2}. \tag{8}$$

In writing Eq. (8) we have discarded terms of order $(R/a)^3$ and higher.

An estimate shows that the electromagnetic energy which arises from this source $\mathcal{E}$ may be as high as tens of thousands of electron volts. All the energy $\mathcal{E}$ is radiated by the fragments in moving through a region of order a; outside this region the bremsstrahlung is smaller than $\mathcal{E}(R/a)^3$.

If the charge-to-mass ratios of the fragments are approximately the same, the factor $(Z_1/A_1 - Z_2/A_2)^2$ tends to suppress the dipole radiation. In these cases, it is necessary to take account of the quadrupole radiation (the magnetic dipole radiation vanishes in any system which consists of only two particles). The energy associated with the quadrupole radiation $\mathcal{E}_q$ is given by the following expression:

$$\mathcal{E}_q = \frac{16}{1575}\left(\frac{Z_1}{A_1^2}+\frac{Z_2}{A_2^2}\right)^2\left(\frac{2A_1A_2}{A_1+A_2}\right)^{3/2}\times \times\left(\frac{E}{mc^2}\right)^{7/2}\frac{mc^2}{Z_1Z_2}. \tag{9}$$

It is apparent from Eq. (9) that the energy associated with the quadrupole radiation becomes important when the factor $(Z_1/A_1 - Z_2/A_2)^2$ is approximately equal to

$$\left(\frac{Z_1}{A_1}-\frac{Z_2}{A_2}\right)^2=\frac{2}{35}\left(\frac{Z_1}{A_1^2}+\frac{Z_2}{A_2^2}\right)^2\times \times\frac{A_1A_2}{A_1+A_2}\frac{E}{mc^2}. \tag{10}$$

LITERATURE CITED

[1] A. B. Migdal, J. Exptl.-Theoret. Phys. (USSR) 9, 1163 (1939).

[2] N. Bohr and J. Wheeler, Phys. Rev. 56, 426 (1939).

[3] Landau and Lifshits, Quantum Mechanics (State Tech. Press), p. 158.*

Received December 18, 1957

* In Russian.

NEW PHOTOMULTIPLIER FOR SCINTILLATION COUNTERS

A. G. Berkovskii

The multiplying system in the FEU-33 photomultiplier contains auxiliary accelerating grids (Fig. 1) which reduce the spread in the time of flight of secondary electrons in the gaps between dynodes; this spread arises as a result of the difference in initial electron velocities. These auxiliary electrodes also make it possible to operate the multiplier at higher current loads. The grids in front of the ith dynodes are connected to the $(i + 2)$-dynodes.

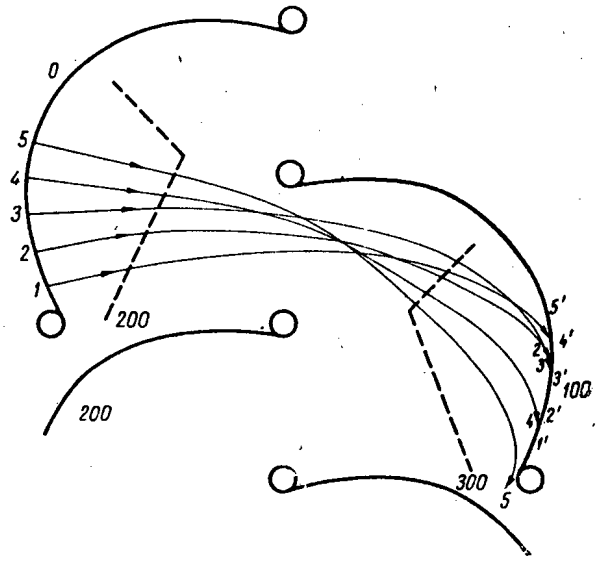

Fig. 1. Diagram of the multiplication system in the FEU-33.

The dynode profile comprises a circular section and two straight sections; the grid profile is comprised of two straight sections. Calculations show that the time of flight of an electron through the stage along the shortest trajectory is $2.4 \cdot 10^{-9}$ sec while the maximum time spread (Fig. 1, trajectories 1 and 4) is $4.5 \cdot 10^{-10}$ sec (with 100 v applied to the stage).

The area of the semi-transparent cesium-sulfide cathode of the FEU-33 is 9 cm^2. The mean integrated intensity for a light temperature of 2850°K is 40 μa/lumen while the minimum is 30 μa/lumen. The quantum yield of the cathode is controlled by the "blue" sensitivity (a FS-6 filter 1 mm thick).

The multiplying system, consisting of 13 cesium-sulfide dynodes, provides gain of 10^8 at voltages of 2500-3000 v with a uniform voltage distribution along the divider. The dependence of gain and thermal noise on the supply voltage for three FEU tubes is shown in Fig. 2.

In order to study the current characteristics of the FEU-33 in pulsed operation a special system was used in which a pulsed light source was employed. The flash repetition frequency was several hundred cycles per second and the duration of each flash was several millimicroseconds. The signal from the FEU was applied directly to the plates of a 13LO37 tube on the screen of which the spot deflection was calibrated with a 26-I oscillator.

Measurements of the pulsed current in a large number of FEU tubes show that at voltages of 3-4.5 kv the peak currents differ; the average current is 0.5 amp. In individual tubes the pulsed currents were as high as 1 amp; this current corresponds to a loading of approximately 0.5 amp/cm^2 at the least dynode. This value is somewhat higher than that reported in [1].

The voltage divider which provided the maximum output current was chosen individually for each multiplier. As a rule, the difference in the values of the resistance legs was small: R_1 = 200-220 kohm; R_2 = 20-70 kohm; R_{3-12} = 180-200 kohm; R_{13} = 300-500 kohm; R_{14} = 800-1000 kohm; R_{15} = 1.5-2.0 meg.

Measurements of the amplitude discrimination of the FEU-33 with a NaI(Tl) crystal and a Cs^{137} sample were carried out with a single-channel amplitude analyzer [2] at a supply voltage of 1400-1800 v; this quantity was found to vary from 8% to 11%. In most of the tubes the operating conditions for best amplitude discri-

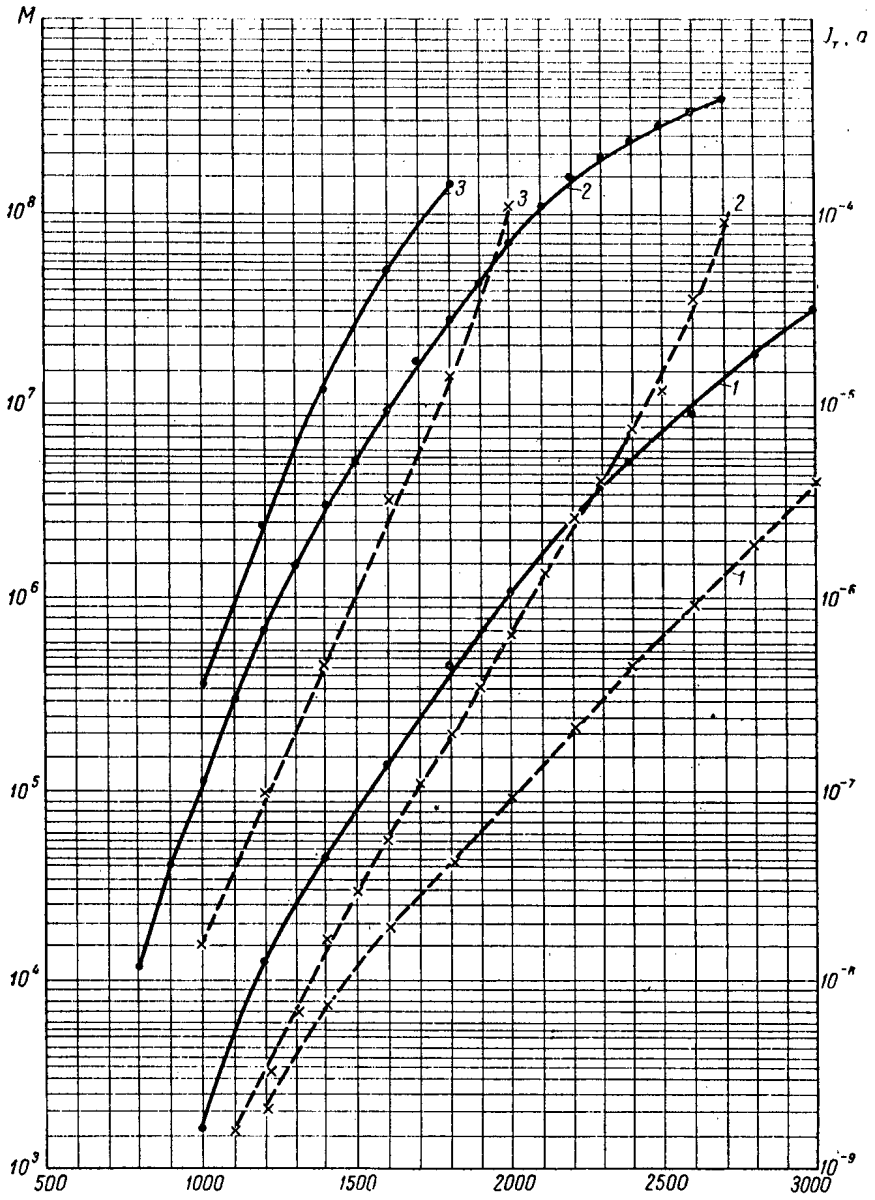

Fig. 2. The gain (solid lines) and noise currents (dashed lines) as a function of supply voltage for three FEU-33 tubes.

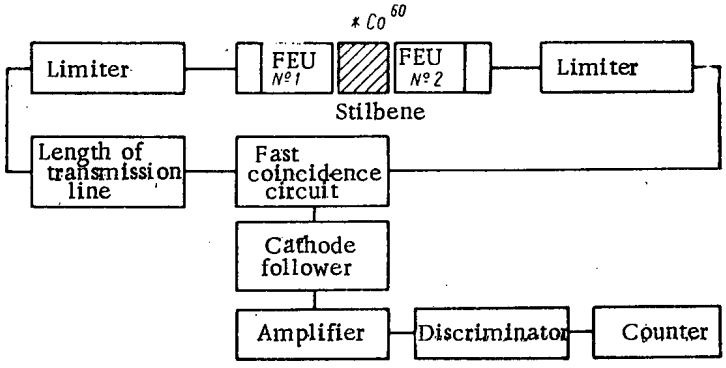

Fig. 3. Block diagram of the system for determining the time resolution of the FEU-33.

mination were similar to the conditions for maximum pulsed current. The mean noise on the NaI(Tl)–Cs^{137} scale was 3-4 kev. (The comparison was carried out at a background of 50 noise pulses per second.)

The time resolutation of the FEU-33 was studied with the system shown schematically in Fig. 3 (page 605). The limiter was a 6Zh1P tube with a 75-ohm load. The coincidence circuit made use of a DG-Ts8 diode. The length of the RK-50 shaping cable was 10 cm. The amplifier gain was approximately 7500 at a band width of 4 Mc/sec. The measurement showed that at a counting efficiency of approximately 50% the width of the coincidence curve at half height was less than $4 \cdot 10^{-9}$ sec. In individual tubes it was possible to achieve $2\tau = 2.2 \cdot 10^{-9}$ sec. Measurements of the time resolution of the FEU-33 carried out in a number of physics laboratories indicate similar results. The measurements with the coincidence circuit were carried out with the following divider: R_1 = 500 kohm; R_2 = 270 kohm; R_3 = 75 kohm; R_{4-12} = 160 kohm; R_{13} = 220 kohm; R_{14} = 400 kohm; R_{15} = 600 kohm.

Comparative measurements of the time resolution of the FEU-33 and other FEU tubes which make use of circular multiplying systems ([13],p. 135) carried out by us and in the laboratories of V. I. Veksler and G. D. Latyshev show that the FEU-33 has a somewhat better resolution.

At high values of the gain one usually observes damped oscillations at the end of the anode pulse (after-pulses); these have periods of 4-6 mμsec and the amplitude of the first after-pulse is approximately 0.1 of the amplitude of the main pulse. A similar effect has been observed in multipliers such as the N4646 ([3], p. 472), RCA-6810 [4] and in high gain tubes with circular dynode configurations.

In conclusion the author wishes to express his gratitude to A. E. Chudakov and P. V. Vakulov for placing the spark light source at the author's disposal and to Iu. I. Tuzhilkin for constructing the apparatus with which the current and time characteristics of the FEU were studied.

LITERATURE CITED

[1] J. S. Allen and L. R. Megill, IRE Trans. Nucl. Sci., NS-3, 4, 112 (1956).

[2] Leitenzen, Glukhovskii and Breido, Crystallography 2, 290 (1957).*

[3] Chechik, Fainshtein and Lifshits, Electron Multipliers (State Tech. Press, 1957), 2nd ed.**

[4] W. Widmaier and R. W. Engstrom, IRE Trans. Nucl. Sci., NS-3, 4, 137 (1956).

Received August 27, 1957

* See English translation.

** In Russian.

METHODS OF FABRICATING STABLE α-, β-, and γ-SOURCES USING INORGANIC ENAMELS

D. M. Ziv, G. S. Siuitsyna, I. A. Efros, and E. A. Volkova

The method of fabricating α-, β- and γ-sources known at the present time [1-3] frequently does not satisfy requirements which arise in science and technology. Sources fabricated without any protective covering are not safe when handled [4, 5]. Furthermore, as a rule these sources are unstable against changes in humidity, temperature fluctuations, vibration, etc. The use of organic films as protective covering for intense sources is very unreliable since these films tend to disintegrate under the effect of the radiation.

Below is described a method of fabricating α-, β- and γ-sources based on the suggestion of one of the authors of the present paper that inorganic enamels be used as a coupling and shielding material [6]. The choice of the enamel by means of which the radioactive material is held firmly to the substrate is determined by two conditions: 1) the enamel must exhibit good adhesive properties when in contact with the substrate material, 2) the radioactive material must be able to enter the enamel layer, forming a completely uniform mass.

Of the enamels which are commercially available it is easy to pick a material which is suitable for the present purpose. In order that the introduction of the radioactive material into the enamel layer be complete and uniform, the enamel should contain inactive isotopes, isomorphic elements or a simple analog of the radioactive element being introduced.

In the work carried out by the authors, the fabrication of stable α-, β- and γ-sources was carried out using radium salt. The substrate was gold. In order to make the radium adhere to the gold substrate an enamel of the following composition was used: SiO_2, 34%; PbO, 30%; Na_2O, 3%; BaO, 30%; B_2O_3, 3%. The radium was introduced into the enamel in the form of the oxide.

Characteristics of the Sources

Radium content on the substrate as determined from γ-radiation,* mC	Amount of radium deposited on substrate as determined	Yield from α-radiation, %	Radioactive evaluation, %
0,089	0,053	60	~1
0,099	0,077	78	~1
0,067	0,055	82	~1
0,099	0,071	72	~1
0,084	0,054	64	~1
0,081	0,043	53	~1
0,138	0,106	77	~1
0,130	0,103	79	~1
0,500	0,270	54	~1
1,100	0,430	39	~1

* The measurements of the radium by means of γ-radiation and α-activity of the samples were carried out after the radium and radon were in equilibrium.

The fabrication of radioactive sources involves the following operation: 1) preparation of a titrated enamel suspension; 2) preliminary enameling of the substrate; 3) deposition of the radioactive material on the enameled substrate; 4) deposition of a powdered enamel film. A short description of these operations is given below.

1. A carefully ground and sifted powder of the enamel with grains size of the order of 10 μ is mixed with water (4 g in 100 ml of water). The pulp is allowed to remain for fifteen minutes after which the enamel content in 1 ml of the suspension is determined by weight. The titration standard used by us for a purified suspension was approximately 20 mg/ml. The suspension can be used for 1-2 hrs after preparation. The suspension starts to coagulate after this period of time.

2. A preliminary enameling of the substrate surface is necessary, especially in those cases in which the substrate material is susceptible to corrosion (for example,

iron, aluminum, copper, etc.). On a degreased substrate approximately 0.1 ml of the titrated suspension is deposited (by calculation there are 2 mg of enamel in 1 cm^2). The solution is evaporated in air; the substrate is then dried and heated to a temperature of 850°C for 30 min and then allowed to cool slowly. As a result the enamel is spread over the substrate in a uniformly thin dense layer. The thickness of the priming layer is approximately 5 μ.

3. The radioactive material can be deposited on the substrate by various methods: evaporation, sublimation or together with the enamel. In the present case the radium was deposited on the enameled substrate as a solution of the hydroxide. The solution was evaporated in air and the residue was heated to 800-850°C and then allowed to cool slowly. As a result the RaO was firmly attached to the enameled surface of the substrate.

4. To prevent clumping the preparation was covered with an additional thin protective layer of enamel. The uniformity of the radium distribution on the substrate was checked by radiography.

After preparation of the sources measurements were made of the absolute amount of radium deposited on the substrate by measuring the γ-radiation of the decay products as well as the efficiency of the α-radiation and other radiation from the sources.

The results of the measurements are shown in the table.

The use, in the present work, of radium in conjunction with its decay products all of which provide α-, β- and γ-activity show that the present method can find practical application when any type of radiation is desired.

LITERATURE CITED

[1] M. Haisinssky, J. Chim. phys. et physchim. biol. 30, 1, 27 (1933); 43, 1, 21 (1946).

[2] A. Quinton, Brit. J. Appl. Phys. No. 2, 593 (1953).

[3] T. L. Martin, Electrif. Eng. 73, 1, 28 (1954).

[4] R. Lawson, Wienmitteilung der Inst. Erforsch 128, II-a, 708 (1919).

[5] W. Makower and S. Ross, Philos. Mag. 161, 19, 100 (1910).

[6] M. S. Petrova, D. M. Zeav, K. J. Schwebelbleet, J. J. Balaklajets, W. P. Sjtin and W. N. Jshessalin, New Preparation Methods of α-, β- and γ-Sources, UNESCO, International Conference on Radioisotopes in Scientific Research, Paris , 1957 (London).

Received January 15, 1958

RADIATION FIELD OF A RECTANGULAR PARALLELEPIPED WITH SELF-ABSORPTION TAKEN INTO ACCOUNT

L. N. Posik

In [1-7] different methods have been described for computing the radiation field of cylindrical and spherical sources when self-absorption of the active material is taken into account.

In a recently published paper [8] a solution has been given to the problem of determining the field of a rectangular plane source in which self-absorption and multiple scattering in the source were not taken into account.

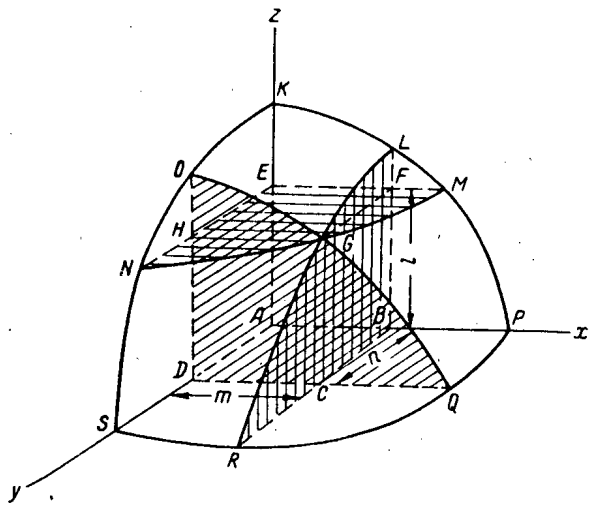

Figure for calculating the γ-radiation field of a rectangular parallelepiped.

In the development of instruments and methods for rapid analysis of loaded ore [9] it has become necessary to determine the field of a rectangular parallelepiped, taking self-absorption into account. In most cases of practical interest, the active material is placed in a metal cart of the indicated shape with walls thick enough to filter out soft scattered γ-radiation. Hence, in making these calculations it is not necessary to take account of the spectral composition of the radiation [10]; it is assumed that the absorption of the γ-radiation in the active material is described by an exponential function. For simplification it is also assumed that the active material is uniformly distributed over the volume of the source.

Under these conditions the γ-radiation dose at a point A (cf. figure) which coincides with the origin of coordinates is given by the expression

$$P = Kq_v \int_0^m dx \int_0^n dy \int_0^l \frac{e^{-\mu\sqrt{x^2+y^2+z^2}}}{x^2+y^2+z^2} dz, \qquad (1)$$

where K is the ionization constant of the active material, q_v is the volume concentration of the material, m, n, and l are the sides of the parallelepiped, μ is the γ-radiation absorption factor.

The triple integral in Eq. (1) can be converted into a single integral. It is apparent that J, the integral over the volume ABCDEFGH, is given by the following combination of integrals over portions of a sphere (cf. figure):

$$J = J_{quart.} - J_1 - J_2 - J_3 + J_4 + J_5 + J_6, \qquad (2)$$

where $J_{quart.}$ is the integral over a quarter of the sphere; J_1, J_2, J_3 are the integrals over the portions of the sphere NMEK, RLBP and OQDS; J_4, J_5, J_6 are the integrals over the portions of the sphere GRCQ, GQHN and GLFM.

Because of the symmetry of the integrands the integrals J_1, J_2, J_3 and J_4, J_5, J_6 differ only in the limits of integration (m, n, l).

We convert to spherical coordinates in order to compute $J_{quart.}$, J_1 and J_4. After some elementary transformations the integral J can be given in terms of a linear combination of exponential functions of the form $\alpha \exp(-\mu\beta a)$ (where α and β are coefficients and a is a parameter) and three single integrals with limits 0 and 1 which are amenable to numerical solution by the Gaussian method.

The integral J was computed on a BESM computer for six values of the absorption coefficients (cf. table). The values m = 2a and n = l = a were taken for the sides of the parallelepiped. These values of the dimension of the active parallelepiped and the factor μ correspond to an important case for rapid analysis in small loads which is frequently encountered in practice. The calculated results for J are given in the table.

Values of the Integral J

μ, cm^{-1} / a, cm^{-1}	0,05	0,08	0,11	0,14	0,17	0,20
15	20,41	15,89	12,73	10,50	8,88	7,65
30	27,30	18,72	13,96	11,07	9,12	7,72

If it is necessary to determine the radiation dose for a parallelepiped with sides twice as long as those taken, the value of J is determined by simple addition of the values of J for each component part. Thus, for example, using four volumes we can form an active body which, at large values of μ, may be considered a radiating semi-space [6].

Actually:

$$P_\infty = \frac{2\pi K q_v}{\mu} \quad \text{or} \quad J_\infty = \frac{P_\infty}{K q_v} = \frac{2\pi}{\mu}.$$

With μ = 0.20 cm^{-1},

$$J_\infty = \frac{P_\infty}{K q_v} = 31{,}4.$$

It follows from the table that with a = 30 cm and μ = 0.20 cm^{-1}, 4J = 30.88 and $\frac{4J}{J_\infty}$ = 0.98.

Consequently, the parallelepiped which has been taken is accurate enough to be used for an infinite semi-space.

A similar result can be obtained by adding eight volumes with radiation inside the active space.

In conclusion the author wishes to thank A. I. Kuleshev, N. A. Ronzin and E. D. Sushunov for carrying out the calculations on the BESM computer and Iu. P. Bulashevich and V. L. Shashkin for their interest in this work and a numberof valuable comments.

LITERATURE CITED

[1] S. Meyer and E. Schweidler, Radioaktivität 2 Aufl. (Leipzig-Berlin, 1927).

[2] W. R. Dixon, Nucleonics 8, 4, 68 (1951).

[3] E. Field, Nucleonics 11, 9, 66 (1953).

[4] G. V. Gorshkov, Gamma Radiation from Radioactive Bodies (LGY Press, 1956).*

[5] Bak, Patrzhak, and Romanov, J. Tech. Phys. (USSR) 26, 379 (1956).**

[6] Iu. P. Bulashevich, J. Tech. Phys. (USSR) 26, 2599 (1956).**

[7] Bibergal', Margulis, and Pertsovskii, J. Atomic Energy 2, 376 (1957).***

* In Russian.

** See English translation.

*** Original Russian pagination. See C. B. translation.

[8] Kovalev, Papov and Smirennyi, J. Atomic Energy 2, 181 (1957).*

[9] L. N. Posik and I. M. Tenenbaum, J. Atomic Energy 3, 28 (1957).*

[10] Galishev, Ogievetskii and Orlov, Usp. Fiz. Nauk 61, 161 (1957).

Received January 15, 1958

* Original Russian pagination. See C. B. translation.

ACTIVATION OF AIR BY RADIATION FROM THE SYNCHROCYCLOTRON

M. M. Komochkov and V. N. Mekhedov

Ever since the 680 Mev synchrocyclotron was put into operation at the Laboratory for Nuclear Problems of the Joint Institute for Nuclear Research a systematic program has been under way to study the various problems associated with dosimetry and radiation safety which arise in connection with work on high-energy particles.

The present paper is a short resume of research on one of these problems.

Measurements of the radioactivity of the air are useful for estimating the general level of activity in the air, for a study of the basic components of the isotopic composition, for establishing safe working conditions for personnel at the synchrocyclotron in determining the limits of the safe zone around the installation.

EXPERIMENTAL METHOD

The concentration of radioactive gases was determined by counting the β-particles in a sample of air which filled a counter chamber 7.5 liters in volume. The radiation detector was a cylindrical Geiger counter with aluminum walls 150 μ thick which was placed at the axis of the chamber.

The absolute loads were based on calibration measurements made with A^{41} samples. Depending on the problem, different methods were used in selecting the samples. To determine the concentration in the operating installation and to ascertain the effects of gas diffusion and convection mixing on activity, the counting chamber was filled with samples taken at various points in the vicinity of the accelerator by means of a rubber tube 40 m long and 8.5 mm in diameter. A comparison was made of the change of activity with continuous gas inflow and when the chamber was filled once. The measurements were carried out with the accelerator in operation and immediately after shut-down. The background was measured by filling the chamber with inactive air; in all cases measures were taken to reduce the background. In order to determine the maximum concentrations and the isotopic composition of the radioactive air the irradiation of the sample was carried out in a sealed container from which the air samples were taken to fill the counting chamber. The particle beam was monitored by two carbon slabs placed in front and in back of the container. Using the monitor readings it was possible to determine the arithmetic mean of the activity in both slabs. It was assumed that the cross section for the (p, pn) reaction with 660 Mev protons and the cross section for the (n, 2n) reaction with 580 Mev neutrons were the same. The difference in absorption of neutrons and protons in the walls of the container was neglected.

Results of the Measurements

In Fig. 1 are shown the results of the measurements of the activity of air samples taken by means of the rubber hose at various points around the accelerator. This is a polar plot of the distribution of neutron insensitivity in relative units and also shows the trajectory of the extracted proton beam. The experimental data have been corrected for dilution of the sample as a result of partial decay of the elements in the air in the rubber tube (25%) and as for the incomplete evacuation of the volume of the counter chamber in rapid alternate-filling operations (20%). As is apparent, the maximum activity is about $3 \cdot 10^{-8}$ curies/liter; this is observed at the output port of the accelerator chamber. After the machine is shut down the activity of the air falls off rapidly (by a factor of 4 or 5 in the first 30 sec) and after three minutes, at the most dangerous point, the activity has already fallen below the sensitivity of the apparatus, which is $0.05 \cdot 10^{-8}$ curies/liter. The rapid reduction in the activity results not only from the decay of the radioactive nuclides but also, and primarily, as a result of mixing of the irradiated

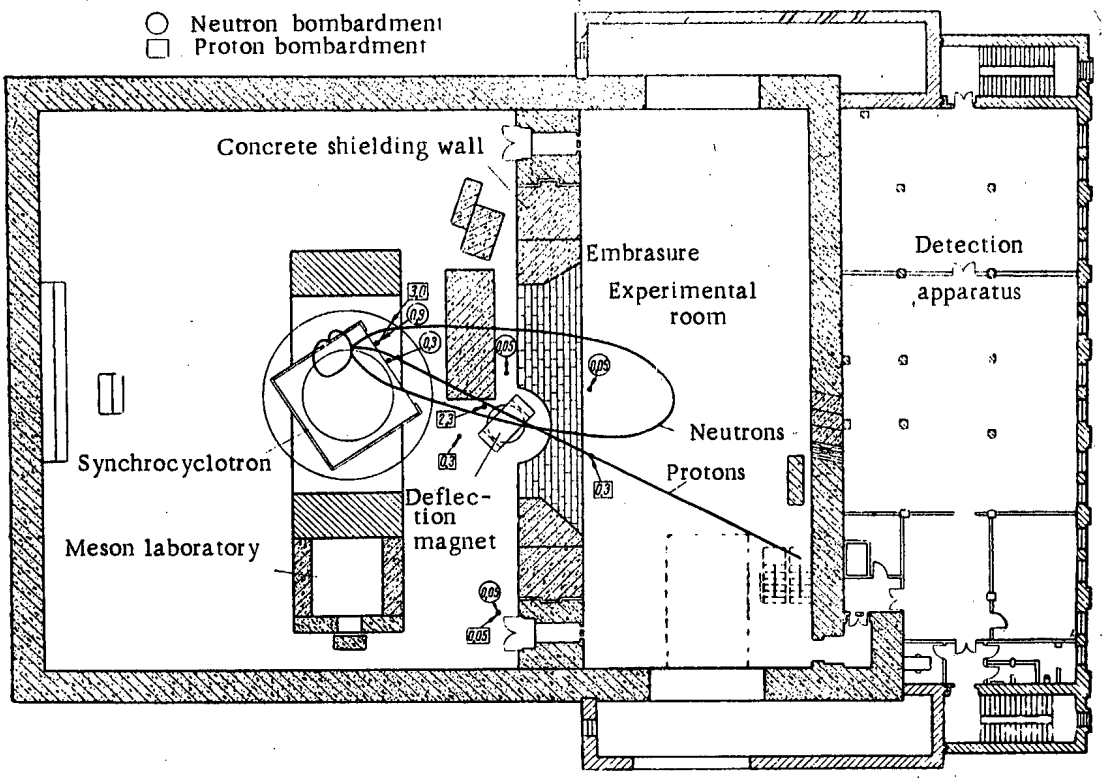

Fig. 1. Distribution of radioactivity in the air in the accelerator building.

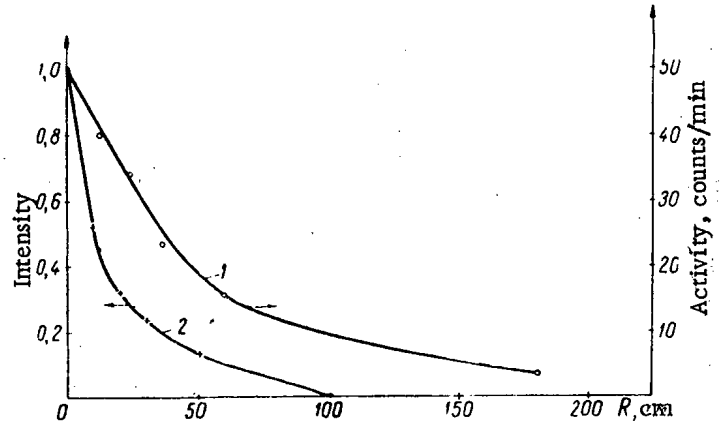

Fig. 2. Decay curves for the activity of the air (1) and the intensity of ionizing radiation (2) at various distances from the axis of the proton beam.

Nuclide	Half-life, minutes	Relative yield	
		protons	neutrons
O^{15}	2,1—3,0	0,12	2,7
N^{13}	9,3—13	0,06	0,31
C^{11}	19—22	0,06	0,46
A^{41}	120	—	0,04
F^{18}	~120 or greater	$3 \cdot 10^{-4}$	—

air with air which has not been irradiated. Experiments indicate that the points of maximum radiation intensity (activity ~ 10^{-8} curies/liter) are localized in the plane of the beam and in a small section of the room. For example, in neutron irradiation the ratio of activity for a sample taken in the orbital plane to that of a sample 20 cm above this plane is 2.0. Approximately the same result is for a comparable sample taken at the same distance from the axis of the proton beam (Fig. 2).

For purposes of comparison, a curve indicating the change of intensity of the ionizing radiation due to fast particles at various distances from the axis of the proton beam is shown. This measurement was made with an air ionization chamber 10 cm in diameter. It is apparent that the drop in air activity does not follow the drop in intensity of ionizing radiation and extends to larger distances because of diffusion and convection motion of the gas.

The composition of the products and the isotopic yield with respect to the C^{14} yield in the monitor in irradiation by protons and neutrons are shown in the table.* It is apparent from this table that the maximum yield is that of the short-lived isotope O^{15} and that the yield of radioactive products due to neutron activation is higher than that produced by proton activation.

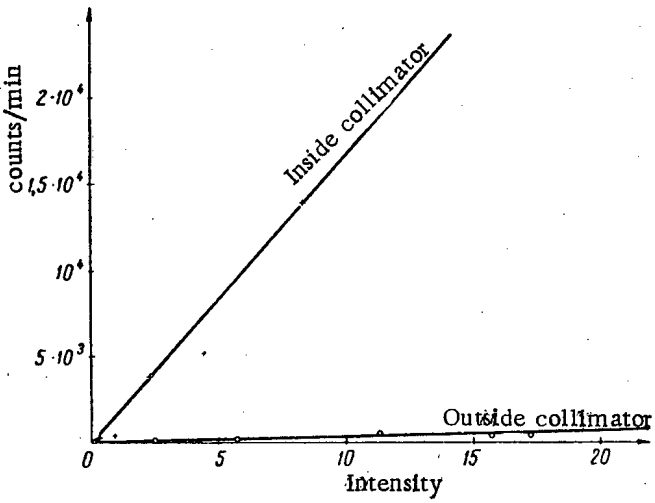

Fig. 3. Change in air activity in the collimator and outside the collimator as a function of the intensity of the proton beam.

The specific activity of samples irradiated in the container was found to be an order of magnitude higher than that of samples taken close to the accelerator. This difference arises from the fact that there is no constant dissipation of the radioactive products in the container. A calculation of the effects of diffusion and convection yields the following ratio for the activity of a sample irradiated in the container (A_{cont}) to that of a sample in the region of the particle beam (A_{open}):

$$\frac{A_{cont}}{A_{open}} = \frac{\lambda + \frac{1}{3}\bar{e}\bar{v}\frac{dN}{dx}}{\lambda} \approx 5-6.$$

In this expression λ is the decay constant for the nuclide, $\bar{e}$ is the mean free path, $\bar{v}$ is the mean velocity of the air molecules (at t = 20°C, $\bar{e} = 7 \cdot 10^{-6}$ cm, $\bar{v} = 400$ m/sec); $\frac{dN}{dx}$ is the activity gradient (it was found that $\frac{dN}{dx} = \frac{N - N/2}{20} = \frac{1}{40}$). A comparison of the decay curves for samples from the container and from the accelerator room shows, for example, that in the case of C^{11} the ratio is 11. The same activity ratios are obtained from a comparison of the air activity for samples taken directly from the channel of the proton collimator** and in the room along the axis of the beam at a distance of approximately 20 cm from the end of the collimator (at various beam intensities).

It is apparent from Fig. 3 that the activity of the air in the collimator is 20-40 times greater than the activity of air in the region of the beam outside the collimator (at almost all intensities).

In view of the qualitative nature of the estimates of diffusion and convection we may assume that the calculated activity ratio is in good agreement with the experimental value.

DISCUSSION OF RESULTS

Under the present conditions the maximum air activity was that close to the output port at a proton energy of 660 Mev and an intensity of $\sim 10^{10}$ protons/sec; this maximum intensity was $3 \cdot 10^{-8}$ curies/liter or lower. When neutrons are produced by charge exchange of protons on beryllium the maximum activity (close to the output port of the chamber) is $\sim 1 \cdot 10^{-8}$ curies/liter, which is the limiting permissible dose.

Control measurements of the radioactivity of the air in the ventilating shaft of the building which houses the synchrocyclotron indicate that with the accelerator in operation the activity of the exhausted air does not exceed the errors in the statistical spread of the background (the background is 220 counts/min). The radioactivity

* According to the data obtained with the monitor the intensity of the proton beam at the location of the steel container was $3.2 \cdot 10^3$ times greater than the intensity of the neutron beam.

** The collimator is in a four-meter concrete shield. A channel volume of 8 liters is used for transmission of the particles. The apertures in the collimator are covered with aluminum foil.

immediately after the accelerator is shut down is 35 ± 25 counts/min (background of 95 counts/min). This value is not very different from the mean value of the activity of the exhausted air (2-5 counts/min). The last quantity is found from the ratio of the volume of the building (35,000 m^3) to the volume of maximum activity for a beam activity of the gas in this volume, approximately 2000 counts/min. Since the air which is exhausted from the building is practically nonradioactive, it represents no danger to the personnel of neighboring laboratories.

For practical purposes it is obviously most important to know the accumulation of long-lived products H^3, Be^7, Be^{10} and C^{14}; however, these were not found in the present work because of the absorption of soft β-particles by the walls of the counter and the small equilibrium activity of these products. According to the most conservative estimates the formation of long-lived nuclides cannot increase the total activity of a sample by more than a factor of two beyond that which was observed. In view of the inexact knowledge of the level of the radioactive air exhausted from the accelerator building it may be said that no health hazard is presented.

The authors wish to thank V. P. Dzhelepov for proposing the problem and many discussions, and Iu. M. Kazarin for a number of valuable remarks.

Received June 21, 1957

DETERMINATION OF DENSITY OF ICE AND SNOW IN ANTARTICA BY MEANS OF GAMMA RAYS

O. K. Vladimirov and V. A. Chernigov

In 1957, in Antartica (in the region of the Soviet observatory, Mirny), the authors determined the density of ice and snow by measuring the decrease in intensity of the gamma rays passing through them. Determinations were made in the laboratory and in the field.

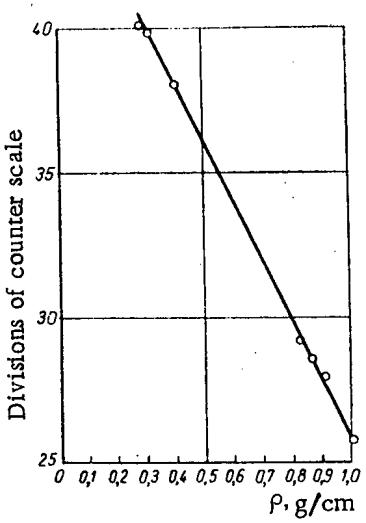

Fig. 1. Decrease in the intensity of γ-rays in samples of snow and ice as the function of density.

The possibility of using γ-rays for density determinations had already been shown theoretically and confirmed experimentally [1, 2].

In our experiments we used the field counter SG-42 made by the "Geolograzvedka" shops as the detector. A radium standard (0.1 mg of radium) served as the source of γ-rays.

In the laboratory experiments an undisturbed sample of ice or snow 25 x 25 x 25 cm was put in a plywood box of the same dimensions and placed between the source and the tube of the counter at a definite distance from the instruments. The distance between the centers of the source and the scintillator in the tube of the counter was constant and equaled 30 cm. The source of the γ-rays, the center of the scintillator and the center of the sample were on the same straight line.

To adjust the readings on the most sensitive scale of the counter, within the range of measurements from 0 to 50 mC/hr, to the intensity of the γ-rays from the standard after they had passed through the sample, the walls of the box were screened with 3 mm sheets of lead and the standard itself was not removed from its lead container.

In our experiments we used samples of ice with densities of 0.90, 0.86 and 0.83 and samples of snow with densities of 0.28, 0.31 and 0.40 as determined in the constant temperature laboratory of the glaciological section of the CAE* to within 0.01 g/cm^3.

The results of measurements are given in the graph of Fig. 1.

In determining the density of snow and ice in place, the container with the source of γ-rays was placed near the bottom of one of two holes bored in the snow or ice. The scintillator tube was inserted into the other hole 90 cm away from the first and the counter was placed near the top of the hole. The depth of the holes was 90 cm and the diameter 6.5 cm, a little larger than that of the scintillator tube.

* CAE – Complex Antarctic Expedition, Academy of Sciences, USSR.

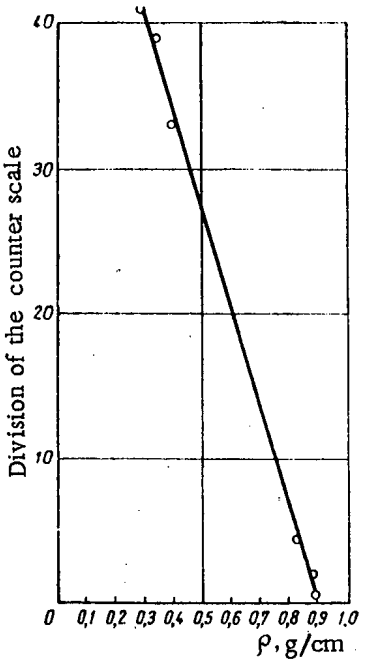

Fig. 2. Decrease in the intensity of γ-rays as a function of density, drawn on the basis of measurements in the field.

Altogether three pairs of holes were bored in snow and ice, which gave the following densities at different localities: for snow, 0.29, 0.32, 0.41; for ice, 0.83, 0.87 and 0.91.

The graph plotted on the basis of field measurements is shown in Fig. 2.

The experimental data obtained may be used for determination of density of ice and snow in the laboratory and, what is especially important, in the field as well. The latter presents a number of advantages over the usual method of determination of gravity by hydrostatic weighing, since measurements in the field are made on material with undisturbed structure under natural conditions of temperature and pressure and on large masses, thus providing representative data.

The precision of density determinations is ± 0.05 g/cm^3 and satisfies practical requirements.

The method is quite efficient. A single determination takes no more than one minute. Holes can be bored in less than one minute in snow and in up to five minutes in ice, while preparation (sawing) of samples of ice for laboratory determination of density requires hours.

It should be noted that, instead of being obtained from experimental curves, the density of ice and snow as the function of the decrease in the intensity of γ-rays may be computed [2]. In deep holes bored in ice for glaciological investigations, the density of ice may be successfully determined by γ-logging [3].

In conclusion, the authors extend their thanks to S. S. Vialov for his interest in their work and for making available the glaciological laboratory for the experiments.

LITERATURE CITED

[1] G. V. Gorshkov, Gamma Radiation from Radioactive Substances [in Russian] (Ed. LGU, 1956).

[2] A. A. Tatarnikov, Exploration and Conservation of Mineral Resources No. 4, 17 (1957).

[3] A. P. Ochkur, Density Logging [in Russian] (Moscow, 1957), p. 62.

Received December 23, 1957

A RADIOMETRIC METHOD OF CONTROL OF CONSECUTIVE TRANSMISSION OF DIFFERENT PETROLEUM PRODUCTS THROUGH THE SAME PIPE LINE

B. Z. Votlokhin, A. Z. Dorogochinskii, and N. P. Mel'nikova

The most convenient and economical method of transporting petroleum products is the pipe line method. To improve the efficiency of operation of pipe lines, in recent years it has become widely accepted practice to pump different petroleum products consecutively through the same pipe line, for example, following benzine kerosine is pumped, following kerosine diesel fuel, etc.

To decrease the volume of nonmarketable mixtures formed at the junction of two petroleum products, to control the consecutive flow, to receive the products at the pipe terminus, etc., it is essential to have precise means of control of the mixing boundaries.

Tests have been conducted at the Grozny scientific research institute, dealing with radiometric control of consecutive flow of petroleum products through large pipe lines, using radioactive isotopes. The method consists of introducing a radioactive substance at the junction of two petroleum products, and through measurements of radiation intensity at the proper points along the pipe line, the degree of mixing and the boundaries of the mixture are established.

The tracer substance used was an activated special compound – triphenylstybine, which dissolves well in petroleum products with the radioactive isotope of antimony, Sb^{124}, whose half-life is 60 days. A special radiometric installation was developed which gave remote readings of the radioactivity emanating from the liquid flowing through the pipe. The installation consists of: 1) the housing assembly which holds gas filled counters of the VS-9 type and electronic equipment, and 2) secondary electronic equipment.

The housing assembly was placed on the pipe line, enclosed in a special cover, and was connected by cable to secondary counting equipment and the electronic recording potentiometer type EPD-17. Figure 1 shows a general view of the housing assembly installed on a ten-inch pipe line.

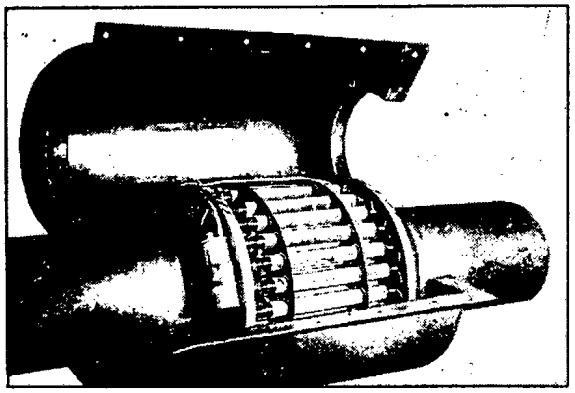

Fig. 1. General view of the housing assembly installed on a ten-inch pipe line.

The electronic equipment of the housing assembly, based on two dual triodes, type 6N15P, is essentially a conicidence cascade and a cathode repeater. Coincidence pulses are fed through a cable to a counter type PS-64, which feeds to a four-channel integrator type RS having semiconductor diodes marked D6Ts-7.

Voltage from the integrator goes to an electronic potentiometer type EPD-17, which records the average rate of the incoming pulses. A switching device in the potentiometer automatically transmits signals when the mixture first enters the field and when the mixture leaves the field. By choosing one of the counting scales (XI, X4, X16, X64) in the PS-64 counter and one of the ranges of sensitivity of the integrator (I, II, III and IV) it is possible to record a curve on an EPD-17 chart, showing the radioactivity at the average counting rate, from 300 to 200,000 counts/min.

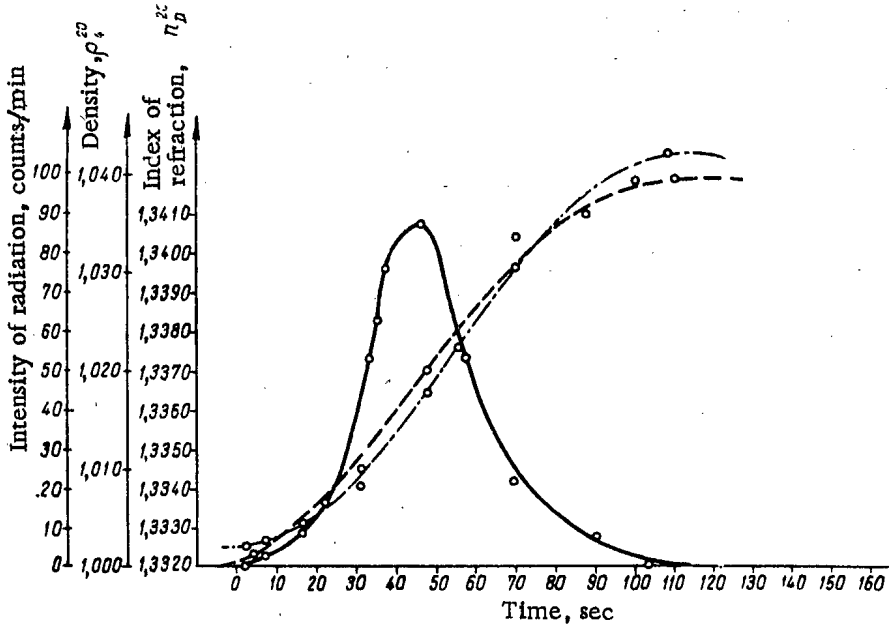

Fig. 2. Curves showing radiation intensity variation with time, density variation with time, and refraction index variation with time when a radioactive mixture flows through a pipe line. ——) Radiation intensity; ---) density; —·—·—) index of refraction.

In December 1956, the Petroleum Research Institute of Grozny, in cooperation with the Grozny petroleum transport administration, ran an operating test of control of consecutive flow of petroleum products through the pipe line running between Grozny and Trudovaia, 886.6 km long; the petroleum products were flowing at a velocity of 2.3-3.5 km/hr.

At the transmitting station of Grozny the radioactive substance of about 12 mC (dissolved in diesel fuel triphenylstybine) in an amount of 4 cm^3 was introduced into the pipe line at the junction of the two fluids being pumped – diesel fuel and kerosene.

Readings were taken at seven pumping stations, where samples were taken and curves of radioactivity were recorded. At all observation points the equipment clearly recorded the passage of the radioactive mixture, thus making possible the exact definition of the mixture's boundaries and of the concentration of one petroleum product in the other, which is particularly important for the receiving stations where the petroleum products are stored in various reservoirs.

The remote reading apparatus and the method of controlling consecutive pumping of petroleum products with radioactive tracer control, proved to be entirely adequate in operation, and the dose of radioactive substance used proved to be entirely adequate in quantity.

Figure 2 shows the experimentally obtained curves of density and refraction index, as well as the recorded radiation intensity.

The beginning of the rise in the radioactivity curve coincides with the approach of the mixture (the presence of small quantities of the second product in the first). The maximum point of the radioactivity curve coincides with a 50% concentration of the second product in the first. The absence of radioactivity indicates that "clean" second product is flowing through the pipe.

Simultaneously there occurs a change in the value of density and in the index of refraction from low values for the first product to higher values in the second product. Experiments and industrial experience with control of consecutive transmission by means of radioactive triphenylstybine showed that the radioactive substance dissolves rapidly in the petroleum products after its introduction into the pipe, the volume of mixture increasing from a value of 44 m^3 at the second observation point to a value of 204 m^3 at the sixth observation point in our experiment. Regardless of this, the radioactivity reading at the terminal station leads to the conclusion that a mixture

of still less activity could be used. The radiometric method can be applied to control of consecutive flow in main pipe lines of any length and any diameter.

The radioactivity emanating from the tracer does not constitute any hazard for the operating personnel of the pumping stations.

The curves of recorded radiation show that the background radiation is the same before and after passage of the tracer mixture. No contamination of the pipes with radioactive substance occurs.

At the present time the Grozny Scientific Research Institute in cooperation with the Grozny petroleum transport administration is adapting the method described here, and used on the line from Grozny to Trudovaia, for use in conjunction with the Kuibishev petroleum line administration on the Bavli-Kuibishev oil pipe line, where consecutive flow of various petroleum products will be controlled.

Received August 1, 1957

SCIENTIFIC AND TECHNICAL NEWS

THE 600-Mev SYNCHROTRON AT CERN

The CERN (Geneva) synchrotron (phasotron) went into operation in August 1957 [1, 2]. The energy of accelerated protons reached 600 Mev. During design of this accelerator, it was assumed that it would be the largest in the world. However, before it was completed, the proton energy in the Joint Institute for Nuclear Research (Dubno) was raised to 680 Mev in 1956, while the energy of protons was raised to 730 Mev [3] in the 184-inch synchrotron of the University of California (USA) in 1957, and thus the CERN synchrotron became the third in order of maximum energy.

The accelerator [4, 5] is installed in the center of a building built in the shape of a T (Fig. 2). The shielding walls surrounding the accelerator are made of high density barites concrete, and are 4-5.8 m thick. Beams of accelerated particles reach instrument chambers through beam holes in the shielding walls. Two breaches in walls are closed up by barites concrete blocks, that are installed on platforms and moved by a hydraulic actuator. Between the blocks, gaps may be left to allow passage of particle beams. A corridor 50 m in length joins the accelerator with the control room and the instrumentation room.

The electromagnet (minus the magnet spool weighs 2500 tons. Diameter of the pole pieces equals 5 m. The gap between the poles varies from 45 cm at the center of the magnet to 36 cm at the edges. Two aluminum magnet spools are joined in series and have 333 turns of winding each. Current through the spools is equal to approximately 1800 amps, and dissipated power is 800-900 kw.

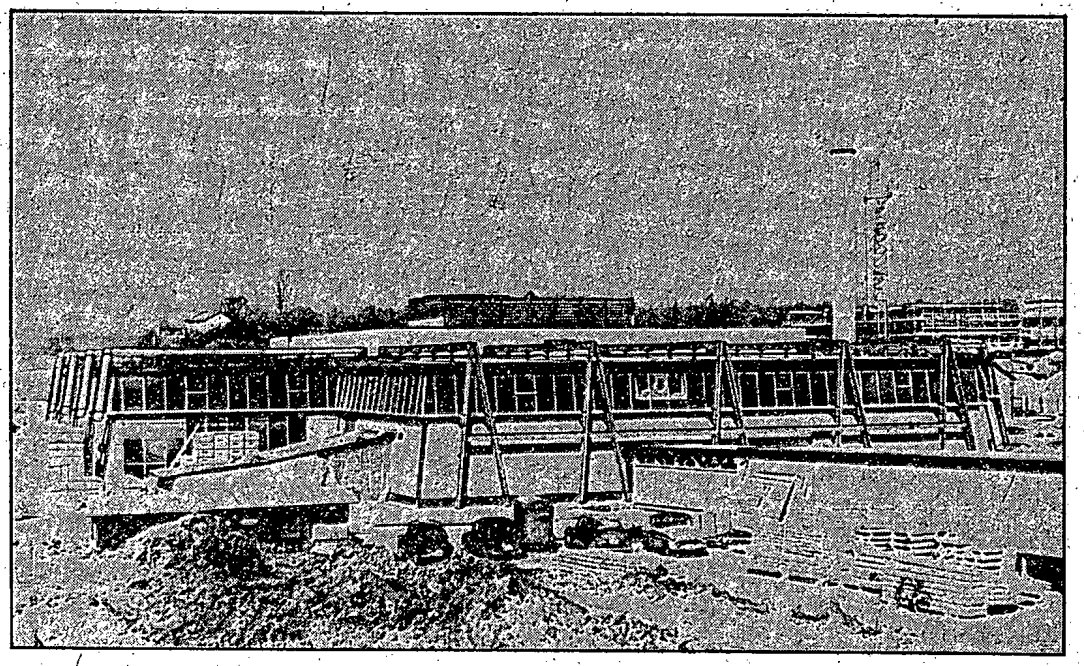

Fig. 1. External view of the CERN 600-Mev synchrotron.

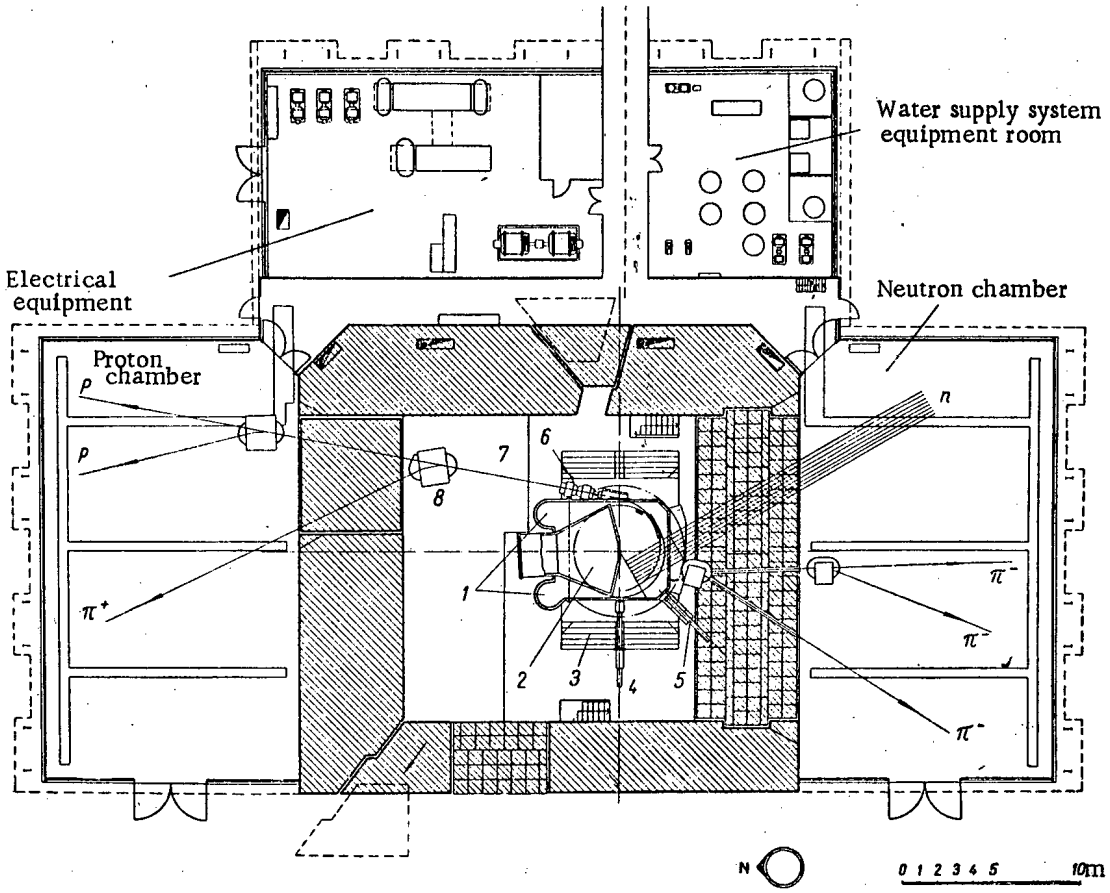

Fig. 2. Plan view of the synchrotron and arrangement of beams of various particles. 1) Diffusion pumps; 2) dee; 3) magnet yoke; 4) ion source; 5) movable target, may be placed in accelerator chamber; 6) magnetic lenses with strong focusing; 7) target; 8) magnet for focusing of π^+-meson beam.

A vacuum chamber made of stainless steel is connected to two diffusion pumps (evacuating rate of each is 12 m^3/sec at 10^{-4} mm Hg) and with three mechanical pumps (evacuating rate 170 m^3/hr each). Pressure in the chamber is $3 \cdot 10^{-6}$ mm Hg when ion source is not connected, and is $6 \cdot 10^{-6}$ mm Hg with the source in operation.

The dee is connected to a variable condenser through a transmission line. Two types of condensers are available: tunable vibrator and rotary condenser. Number of cycles of capacitance changes is about 55 changes per second. The range of frequency essential for acceleration of protons is 27 to 17 megahertz (10^6 cps). A high frequency generator (power required about 50 kw) is provided through a triode whose grid is water cooled. The potential amplitude at the dee changes during one cycle of acceleration from 12 to 4 kw. At the present time a high frequency system using a vibrator condenser is installed and undergoing tests.

The average proton current strength in the chamber is on the order of 0.1 μa. After some testing the current will be raised to 1-2 μa. The current of the external beam is about 3% of the current within the chamber (10^9 protons per impulse at a frequency of 55 impulses per second). For deflection of the beam a magnetic channel is used. After emerging from the chamber the beam is focused by magnetic lenses.

Cost of the synchrotron including the cost of the building and the salaries of the personnel, amounts to about 2 million pounds sterling. Erection of the building for the synchrotron (Fig. 1) was begun in the second half of 1954. Various parts of the accelerator were built in different countries: the magnet in France, the supply generator for the magnet spools in Switzerland, the spools proper in Belgium, the vacuum chamber in Sweden, pumps in Germany, the high frequency system in the Netherlands. Design of the synchrotron was done under the direction of St. John Becker (Netherlands) who is at present the general director of CERN.

N. F.

LITERATURE CITED

[1] Nucl. Eng. 2, 18, 403 (1957).

[2] Nucl. Power 2, 17, 353 (1957).

[3] Atomic Industry 6, 1, 9 (1958).

[4] Engineer 204, 5307, 538 (1957).

[5] A. Lunby, Discovery 19, 2, 56-59 (1958).

STORAGE OF RADIATION ENERGY IN GRAPHITE

The energy of neutrons slowed down in the core of a nuclear reactor as a result of elastic collisions is dissipated in the moderator. Part of this energy is given off as heat in the graphite and part of it is stored in the crystal structure. Even a small amount of this energy represents a danger if released suddenly. This energy storage (the so-called Wigner effect) is a particular case of radiation damage of materials and must be taken into account in constructing reactors with graphite moderators to avoid dangerous operating conditions [1].

Neutron irradiation of graphite affects the mechanical and electrical properties, the thermal conductivity and the dimensions [2, 3].

Stored energy. If the temperature of graphite is increased after irradiation the defects are partially annealed and the stored energy is released. Data on the amount of stored energy in graphite for various total neutron fluxes (at a temperature of 30°C) are shown in the table.

Amount of Stored Energy in Graphite (at Various Integrated Fluxes)

Total flux, neut./cm^2	$0.5 \cdot 10^{21}$	$1.0 \cdot 10^{21}$	$1.5 \cdot 10^{21}$
Energy, cal/g	250	400	500

Assuming that the specific heat of graphite changes with temperature from 0.2 to 0.4 cal/g·°C, in irradiation in a total flux of 10^{21} neut./cm^2 the release of stored energy may raise the graphite temperature to 1000°C.

If the energy is stored at a temperature T_0 and the temperature of the graphite is uniformly increased to a temperature T_1 which is higher than T_0 by approximately 100°C, almost no heat is released in the graphite. Above the temperature T_1 the rate of heat generation is approximately constant up to 1500°C. This effect is observed in samples which have been subject to long irradiation. In short term irradiation at low temperatures the energy-release characteristics are entirely different: starting with a temperature T_1 which, as before, is higher than the irradiation temperature by 100°C, the maximum amount of energy is released in the range 200-300°C. In Fig. 1 are shown curves for the rate of energy release as a function of annealing temperature for irradiation at temperatures of 30 and 150°C.

Annealing. As has already been noted the accumulated energy is released from the irradiated graphite by annealing at high temperatures. Similarly, the other changes in the physical property of graphite are reduced.

In actual fact the accumulation of energy in the graphite of a reactor is large. Hence, in constructing a reactor one must know: 1) the amount of accumulated energy in the graphite at any part of the reactor and at any moment of time during irradiation; 2) the corresponding amount of release energy if it is assumed that the graphite temperature is increased.

In order to calculate the amount of accumulated energy it is necessary to know the neutron flux and graphite temperature at the point under consideration. It is also necessary to know the rate of accumulation of energy under irradiation at a given temperature. In order to predict accurately the magnitude of this energy one requires experimental data for these characteristics.

An approximate calculation of the rate of energy release can be carried out under the assumption that this rate remains constant in the region from T_1 to 1500°C where T_1 is the temperature at which release is initiated. (This is a very rough approximation since close to the temperature 1500°C there is a maximum. Furthermore, this assumption does not apply for irradiation for short periods of time at low temperatures.)

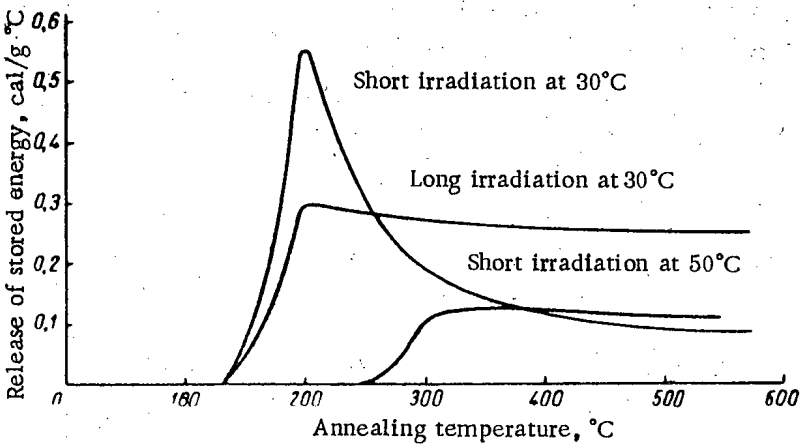

Fig. 1. Release of stored energy in graphite.

If the total accumulated energy for the irradiation of graphite at a temperature T_0 is equal to S, the energy released per unit increment of temperature is given by the expression:

$$\frac{dS}{dT} = \frac{S}{1500 - T_1} = \frac{S}{1500 - (T_0 - 100)} = \frac{S}{1400 - T_0}.$$

The danger due to the release of stored energy can arise only when the quantity dS/dT is greater than the specific heat of the graphite.

If there is no removal or loss of heat, all the accumulated energy is given off when the temperature T_1 is exceeded. The latter is taken as a criterion for estimating the danger due to the stored energy. In practice this limit may be exceeded without danger since there is always some heat removal through the coolant.

The problem is essentially that of computing the accumulated energy at various parts of the reactor and determining the most dangerous point. A calculation can be carried out by placing graphite samples in the reactor and measuring the released energy in the samples.

In the annealing process the temperature of the graphite is increased slowly by an external heat source and the accumulated energy is released. However, not all the energy is released because it would be necessary to increase the temperature of all the graphite in the reactor to 1500°C. If the annealing temperature is T_2, only part of the energy is released and this part is determined by the ratio $\frac{T_2 - T_1}{1500 - T_1}$ (Fig. 2). Thus, by applying a sufficiently high annealing temperature T_2, one can be sure that spontaneous release of energy will not take place

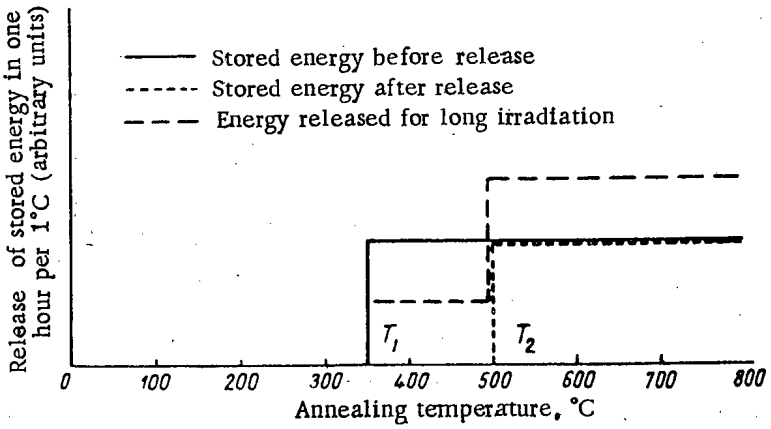

Fig. 2. Release of energy stored in graphite as a result of the Wigner effect.

even if there are points of local heating which exceed the danger temperature. Because of the high thermal inertia of the moderator, large temperature excursions in the blanket are not observed. Nonetheless, any measures which make it possible to extend the safety limits are desirable.

Iu. K.

LITERATURE CITED

[1] P. Grant, Eng. 185, 4794, 120 (1958).

[2] Wood, Bupp, and Fletcher, Metallurgy in Nuclear Power and Effective Radiation on Materials (Reports of the Foreign Delegation to the International Conference on the Peaceful Use of Atomic Energy) (State Tech. Press, 1956).*

[3] V. V. Goncharov, J. Atomic Energy 3 (1957).**

* Russian translation.

** See C. B. translation.

ON THE BEHAVIOR OF PLUTONIUM ALLOYS

According to observations on alloys of the heavy elements (uranium, neptunium, plutonium, etc.) with complex electron structures, having practical importance and representing great theoretical interest, as far as is presently known, there is no adequate explanation of the behavior of such alloys within the limits of existing theory.

A recent publication [1] has given data based on an investigation of the system Pu–Th (Fig. 1a). Following well-known considerations of valency, electronegativity and atomic size of components, it might be expected that, in these systems, no compounds should exist (especially, for example, in the system U–Th with its one eutectic [2]). However, this work led to the discovery of the compound ζ (having, according to preliminary data, a rhombic structure with parameters a = 9.820 A, b = 8.164 A and c = 6.681 A) for which, based on the experimental density equal to 14.0 g/cm^3, there corresponds the assigned formula $Th_{13}Pu_6$ (31.6 % thorium, d = 13.96 g/cm^3).

According to the elementary theory of alloys, the solubility of thorium in ϵ-plutonium is rather small (~ 5%), but with δ-plutonium it is larger (at the peritectoid temperature 496°C) than in ϵ-plutonium. The solubility of plutonium in thorium is considerable (48.5% at 615°C) and is accompanied by an anomalous expansion of the atom of plutonium from the maximum radius of pure plutonium (δ-phase), equal to 1.645 A, to an effective radius in solid solution with α-thorium, equal, according to x-ray data, to 1.697 ± 0.005 A or to 1.707 A from the extrapolation of experimental data on the density of alloys (d = 14.2 g/cm^3; see Fig. 1b). Thus the difference between the sizes of the atoms of plutonium and thorium diminishes to 5%. According to Zachariasen [3], the valence of an atom of plutonium having a radius of 1.70, according to theory, equals 4. The reason why the expansion of atoms of plutonium ceases at a point corresponding to a valence of 4 and does not continue further is unknown. It might be possible that this phenomenon proceeds as a result of rapid growth of the free energy of the plutonium atom with the reduction of its valence below 4.

An interesting comparison may be made between the above-mentioned data and the behavior of cerium alloyed with thorium [4], insofar as cerium is similar to plutonium to a great degree since it possesses several modifications and large changes in density (~ 16%), with a transition of the room temperature stable face centered form (a = 5.1502 kX) at low temperature (cooling in liquid air) to a high density form of the same structure (a = 4.84 ± ± 0.03 A) [5]. This conversion proceeds at room temperature only at a pressure of 12.43 metric tons/cm^2 and is correlated with the transition of a $4f$ electron to the 5d state, with a change in valence from 3.2 to 4. From the diagram (Fig. 2a) it is apparent that, in agreement with theory, cerium and α-thorium form a continuous series of solid solutions at room temperature, having an anomalous change in the lattice spacing (Fig. 2b). This anomaly is not connected with the scavenging action of cerium on the impurities in thorium (99.5% thorium; 0.02% calcium, part of which vaporizes in the preparation of the alloys; 0.015% nitrogen; the remainder is for the most part oxygen, a = 5.082kX), since it persists to ~ 30% cerium. It is also not explained by impurities in cerium, since there was used metal of high purity (99.95% cerium; 0.002 iron; < 0.05% lithium and traces of silicon, magnesium, sodium, molybdenum, copper and aluminum). The anomaly might be explained on the basis of interatomic actions. With the introduction of large atoms of cerium in the lattice of thorium, the cerium undergoes compression, which at insignificant cerium content is sufficient to transfer a $4f$ electron to the 5d shell. The previously mentioned high density modification of cerium remains in solution, but since its atomic diameter is small, similar to thorium, the lattice parameter of the alloys is diminished. With increasing content of cerium, the pressure is gradually decreased and a large fraction of the atoms is restored to the normal electron state. This data is substantiated by measurements of magnetic susceptibility of alloys.

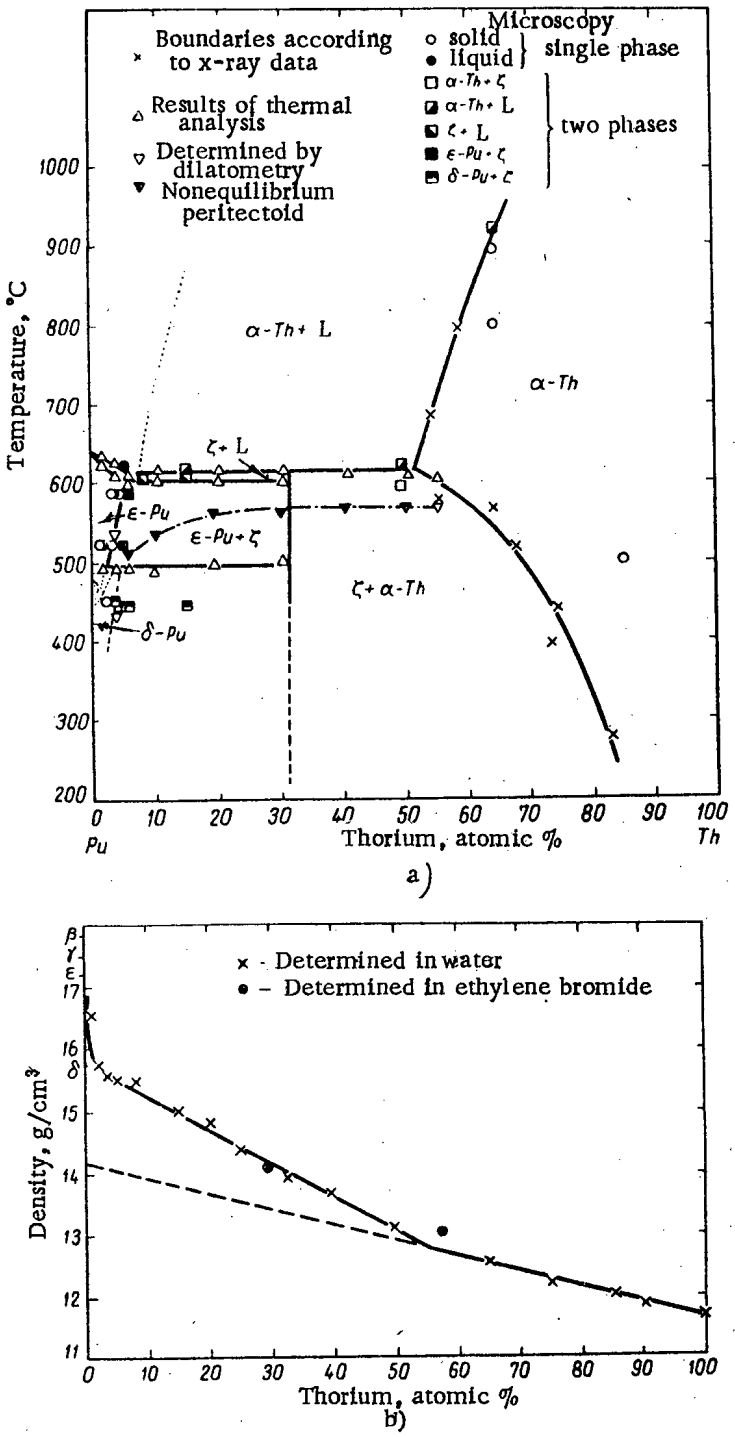

Fig. 1. System Pu–Th. a) Tentative equilibrium diagram; b) density of cast alloys. Density of α-plutonium is 19.7.

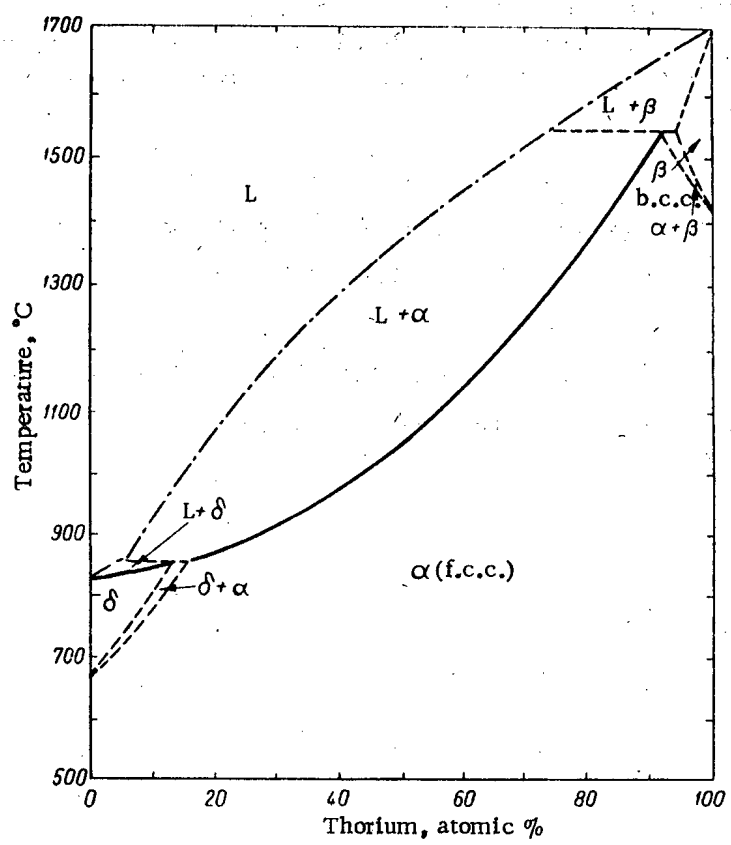

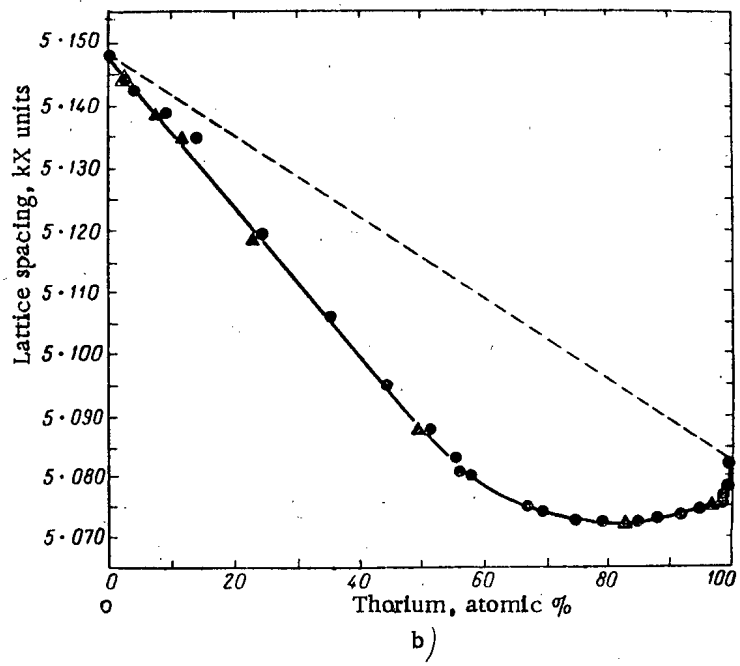

Fig. 2. System Ce–Th. a) Simplified equilibrium diagram, δ -probable high temperature phase of cerium with unknown structure; b) lattice spacing; ●) specified alloy content; ▲) contents by analysis.

In order to gain information about the change of free energy of the plutonium atom together with the change of its size and valence, an interesting experiment would be the measurement of the lattice parameter of solid solutions in the system Pu–Ce. The formation of such solid solutions between cerium and plutonium is possible if, in the valence state 4, they have the atomic radii 1.71 and 1.70 A, respectively, and with the lattice structure of the high density cerium and δ-plutonium identical.

LITERATURE CITED

[1] D. M. Poole, G. K. Williamson, and J. A. C. Marples, J. Inst. Metals 86, 172 (1957).

[2] H. A. Saller and F. A. Rongh, U. S. AEC publ. (BMI-1000), 1955.

[3] W. Zachariasen, J. Chem. Phys. 25 (1957).

[4] R. T. Weiner, W. E. Freeth and G. V. Raynor, J. Inst. Metals 86, 185 (1957).

[5] A. F. Schuch and I. H. Sturdivant, J. Chem. Phys. 18, 145 (1950).

SOME PROBLEMS OF THE EXTRACTION OF URANIUM FROM ORES

(from Data of the International Mineral Dressing Congress)

S. V. Shumilkin

The International Mineral Dressing Congress was held in Stockholm in September 1957; the Congress discussed the contemporary state of the theory and practice of crushing ores, their grading and gravity separation, flotation, magnetic separation, roasting and hydrometallurgical processing. Of the 33 reports examined at the Congress, two which deal with certain problems of the dressing and hydrometallurgical processing of uranium ores may be of interest to readers of the Journal of Atomic Energy.

The first part of E. Svenke's* report "Some Aspects of the Uranium Milling Industry" [1] contains data on the production level of uranium concentrates, their cost, regulations governing the uranium content of industrial ores and some data on the current state of the uranium milling industry, previously published in the foreign press.

The second part of the report describes the technological system used in the plant for processing uranium-bearing shales at Kvarntorp in Sweden.

The members of the Congress were also given papers containing some of the technical and economic results obtained at this plant [2]. Figure 1 shows the current flowsheet for processing shales.

The plant's annual capacity is 150 thousand tons of shale with a uranium content of 235 g per ton (0.023%). The continuous extraction of uranium from the ore in the final 70% concentrate was of the order of 42.5%.

The materials and power used per kg of uranium in the final concentrate were:

Crude shale	10.0 tons
Shale after preparation in dense media	7.0 tons
Sulfuric acid	0.4 tons
Calcium oxide	0.4 tons
Electricity	275 kw-hr
Steam	0.7 tons

I. B. Klemmer's** report "Applications of Solvent Extraction in Processing Uranium Ores" [3] gives a brief review of the results of laboratory and pilot-plant investigations carried out on behalf of the U.S. Atomic Energy Commission.

In the first stage, solvent extraction was used on a limited scale for freeing the U_3O_8 from admixtures of rare-earth elements; ethyl ether was used as the extraction agent.

In the second stage the use of solvent extraction was extended by using kerosene solutions: tributyl phosphate for the extraction of uranium from nitric acid solutions and dialkyl pyrophosphoric acid for the conjunct extraction of uranium from phosphate solutions.

* Director of the Department of Chemical Research and Production of the Swedish Atomic Energy Commission.

** Director of the Department of Mineral Technology, Department of the Interior, USA.

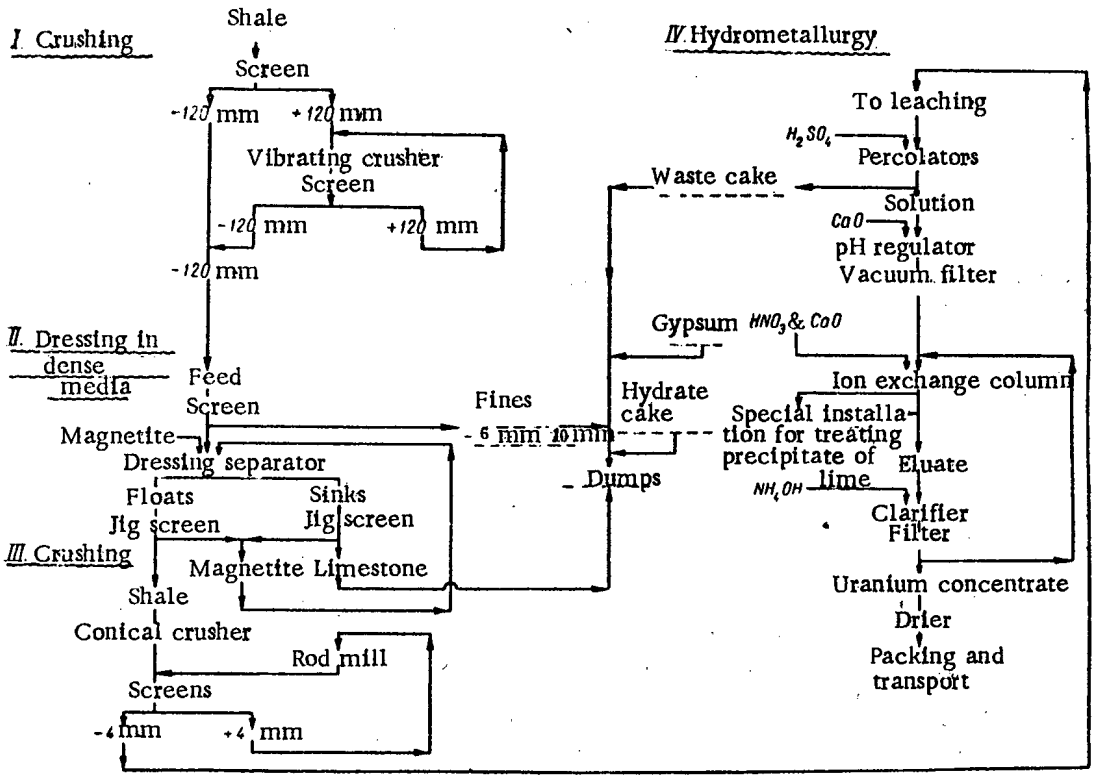

Fig. 1. Current flowsheet of the plant for processing uranium-bearing shales at Kvarntorp.

In recent years solvents have been found and processes developed which make it possible to use extraction not only for the separation of plutonium and the fission products from nuclear fuel and also for isolating uranium from sulfuric acid solutions and pulps obtained by leaching ores.

The extraction method is based on chemical reactions typical of anion and cation exchange. Extraction processes which are examples of liquid ion exchange proceed more rapidly, however, than processes of adsorption on resins because of the high contact surface area obtained by mixing two liquids. This is also true of re-extraction processes when they are compared with the desorption of uranium.

Klemmer gives the following comparative data: 1 ft^3 of resin (sorbent) gives from 2-3 pounds of U_3O_8 per day (or 1 m^3 of resin gives from 70-106 kg of U_3O_8); 1 ft^3 of a 0.1 M solution of extraction agent in kerosene gives from 4-8 pounds of U_3O_8 daily (or 1 m^3 of a 0.1 M solution of extraction agent gives from 141-285 kg of U_3O_8); 1 ft^3 of resin costs about 45 dollars; 1 ft^3 of a 0.1 M solution of extraction agent costs about 4 dollars.

These data indicate that the solvent method for extracting uranium from solutions is more economical and simple than the method of sorption of uranium on ion-exchange resins.

Solutions of organic amines, di-2-ethylhexyl phosphoric acid (EHPA) and dodecyl phosphoric acid (DDPA) in light fractions of kerosene are used as industrial extraction agents.

Amines (of the type R_2NH_2Cl) are the most selective and rapid-acting extraction agents with respect to uranium. Trivalent iron, which is extracted together with uranium, is a disturbing admixutre in the solutions. Where considerable amounts of trivalent iron are present in sulfate solutions from leaching, it is advantageous to reduce this iron to the bivalent form because the latter is not extracted by amines.

The re-extraction of the uranium and the simultaneous regeneration of the kerosene solution of amines are effected by a 1 M solution of sodium chloride acidified to a pH of 1. The final concentrate of U_3O_8 can be precipitated from this solution by ammonia or magnesium oxide.

The field of application of amines is limited to the extraction of uranium from clarified solutions only. Extraction from unclarified solutions or pulps is complicated by the formation of a tertiary emulsion phase.

Extraction by amines from solutions containing 1 g/liter of uranium is generally effected in 2-4 stages with an aqueous: organic ratio of 4 : 1. Re-extraction is carried out in 3-4 stages with an organic : aqueous phase ratio of 6 : 1.

Dodecyl phosphoric acid $C_{12}H_{25}OPO_3H_2$ (DDPA) is the cheapest of the organic compounds used for extraction and gives the highest coefficient of concentration of uranium after re-extraction. In contrast to amines, the presence of a considerable number of solid particles in the solution does not complicate re-extraction when this reagent is used and does not lead to an excessive consumption of reagents.

DDPA is less selective than amines and extracts a considerable amount of trivalent iron and a certain amount of titanium. Titanium reduces the extraction capacity of DDPA; if large amounts of titanium are present in the organic phase the latter is periodically removed by a 10% solution of hydrofluoric acid.

In view of the stable bond between uranium and DDPA, as strong a reagent as a 10 M solution of hydrochloric acid is used for re-extraction. About 80% of the hydrochloric acid is recovered in the re-extraction process by regeneration by evaporation.

The extraction of uranium by a 2.7% solution of DDPA in kerosene is carried out in 4-5 stages with an aqueous: organic phase ratio of 7: 1; re-extraction is carried out in 4-6 stages with organic: acid phase ratio of 10: 1.

Di-2-ethylhexyl phosphoric acid. As regards its selective capacity for the extraction of uranium $(C_8H_{17}O)_2 \cdot PO_2H$ (EHPA) occupies an intermediate position between amines and DDPA, and requires a longer period of contact and more intense mixing with the uranium-containing sulfate solutions.

The re-extraction of the uranium-containing organic phase of EHPA can be effected either by strong acids (similar to DDPA) or by a 10% soda solution.

In the latter case, to avoid the formation of a tertiary phase, which is the product of the reaction between the EHPA and the alkali, 3-5% tributyl phosphate (TBP) or alcohols (capryl, undecanol) are added to the kerosene solution of EHPA.

Iron and titanium are removed from the soda solutions in the form of hydrates and the uranium can then be precipitated by caustic soda; after carbonization the solution is conducted to the next re-extraction. In practice, however, difficulties arise with regard to the filtration of the uranate; after the removal of the iron and titanium, the carbonate solution is, therefore, usually neutralized to a pH of 4, the CO_2 is removed by boiling and the uranium concentrate is precipitated by ammonia or magnesium oxide. After re-extraction the kerosene solution is regenerated by contact with a saturated solution of sulfuric acid.

The extraction of uranium by a 3% solution of EHPA in kerosene is usually carried out in 4-5 stages with an aqueous: organic phase ratio of 6: 1; re-extraction by a 10% solution of soda is carried out in 2-3 stages with an organic: soda phase ratio of 10: 1.

In addition to extracting uranium, the above-mentioned extraction agents also satisfactorily extract molybdenum from sulfate solutions, thus making it possible to carry out the composite dressing of ores from several deposits. The separate extraction of uranium and molybdenum is obtained by using different systems of re-extraction.

Various kinds of apparatus are used for the contact and separation of the aqueous and organic phases, including: thickener-clarifiers, pump precipitators, pulsating columns, contactors with rotating plates, hydrocyclones, and centrifugal contactors. High-capacity centrifugal contactors with small surface requirements are principally used for multi-stage extraction.

In conclusion, Klemmer indicates that the low capitol costs, the flexibility of control of the process and the low working costs, together with the high degree of extraction and purity of the final product lead one to believe that solvent extraction will occupy an important place in the hydrometallurgy of uranium and other ores.

LITERATURE CITED

[1] E. Svenke, "Some Aspects of the uranium milling industry," International Mineral Dressing Congress (IMDC), Stockholm, 1957.

[2] Swedish Mineral Dressing Mills, IMDC, Stockholm, 1957.

[3] I. B. Klemmer, "Applications of solvent extraction in processing uranium ores," IMDC, Stockholm, 1957.

THE LARGEST OPERATION FOR MINING AND PROCESSING URANIUM ORES IN NONCOMMUNIST COUNTRIES

The Consolidated Denison Mill with a capacity of 6 thousand tons of ore per day (Fig. 1) located in the Blind River region of Canada, started operating in 1957. The mill near Lake Nordic in the same region has a capacity almost as great (4 thousand tons per day) [1]. At present the largest uranium mills in the USA do not produce more than 3 thousand tons of ore per day. Some mills at Witwatersrand in the Union of South Africa process up to 7 thousand tons per day [2].

If it is taken into consideration, however, that the ores at Witwatersrand have a composite character and that the uranium is obtained as a component which forms an impurity of gold, the Consolidated Denison Mill in Canada may be considered as the largest uranium plant in the noncommunist world operating specifically on uranium ores.

The construction of this plant was carried out in a relatively short period.

The presence of uranium mineralization was established in 1954 and in 1955 the ore body was revealed by drilling. Two winning shafts were sunk in the first half of 1956: No. 1, 557 m deep and No. 2, 710 m. The construction of the surface installations and the mill were begun in January 1956. In September 1957 the mill was put into operation at the full planned capacity.

The mining level of the Consolidated Denison unit consists of two or more seams of pebble conglomerates containing uranium. The individual ore seams are divided by thin quartzitic bands. The average thickness of the ore body is 4.5 m, the dip is 19°. The proved length of the ore level is about 4.5 km along the strike and 3 km to the dip. The uranium is found in the form of brannerite, less frequently as uraninite and pitchblende. Monazite and sulfides (principally pyrite) are found.

The average content of U_3O_8 is 0.14%. The reserves of ore, calculated from drilling data, are 136,750 thousand tons [3], corresponding to 190 thousand tons of U_3O_8. The uranium reserves of this district are, therefore, considerably larger than the total reserves of all uranium deposits in the USA and constitute more than 60% of the uranium reserves of Canada.

The technique employed for processing uranium ore at this mill differs little from that used in other plants in the Blind River region. Sulfuric acid leaching is used at this mill, followed by ion-exchange extraction of the uranium. Figure 2 shows the flowsheet of the Consolidated Denison Mill. Dissolution by sulfuric acid is carried out by treating the crushed ore for 48 hrs at a temperature of 110°F. Ion-exchange extraction is carried out in filtration columns. In the first months of the mill's operation the extraction of uranium was 90% [1]. The U_3O_8 content in the concentrate was 75% [3].

The plant differs from others in the Blind River region by the fact that the crushing and fine grinding of the ore is carried out directly at the hoist of the shaft and it is then pumped in the form of a pulp through pipes to the mill.

About 125 men are employed at this plant. The cost of treating 1 ton of ore is 8-8.5 dollars. It is intended to increase the capacity of the plant to 10 thousand tons of ore per day.

Fig. 1. The Consolidated Denison uranium ore processing mill in Canada.

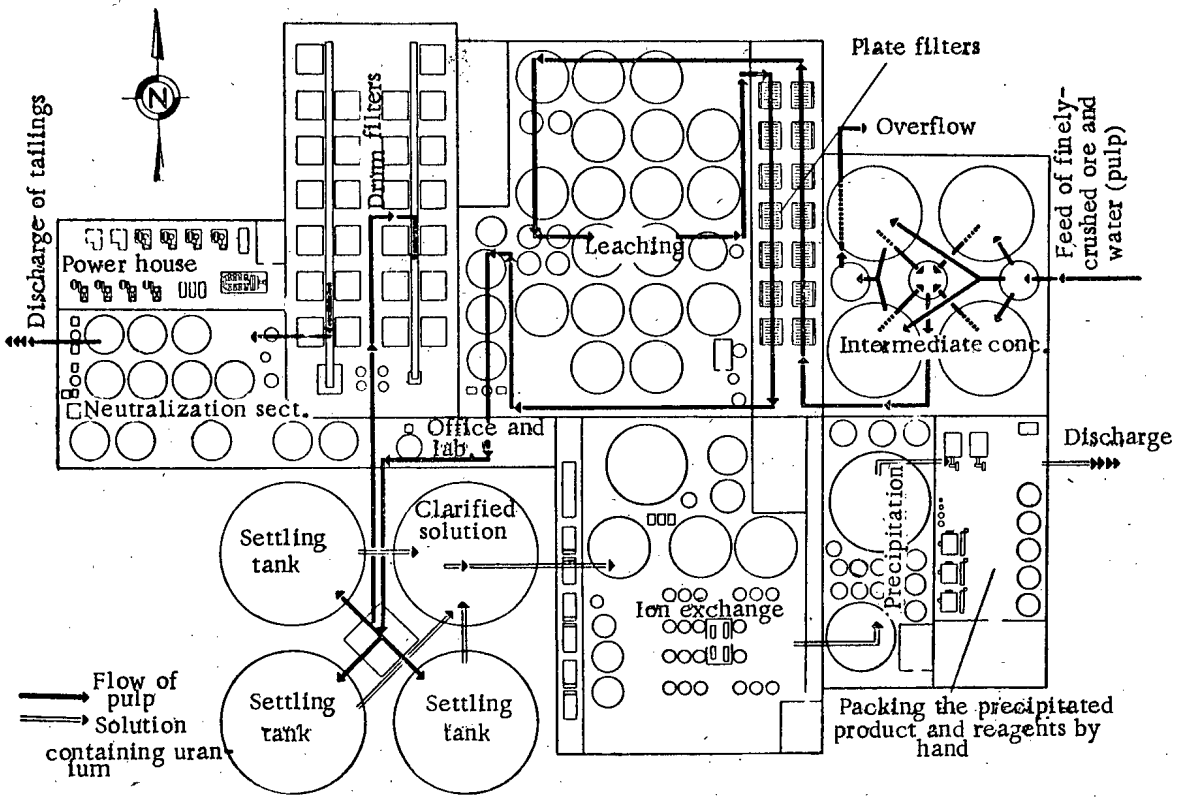

Fig. 2. Flowsheet of the Consolidated Denison Mill.

LITERATURE CITED

[1] Canadian Mining Journal No. 10, 113 (1957).

[2] The Mines Magazine No. 11, 24 (1957).

[3] Canadian Mining Journal No. 6, 125 (1957).

M. K.

THE "PRONTO REACTION" OF P. RAMDOHR

During the investigation of uranium deposits in recent years there has been increasing attention given to the determination of the absolute age of the minerals. On the basis of these determinations, conclusions are drawn regarding the time of formation of the deposits, their correlationship with a specific stage in the development of the particular section of the earth's crust, the connection of the mineralization with a particular intrusion, etc.

In many instances, however, the absolute age is determined dogmatically without taking into consideration the concrete geological conditions and the frequently very complex history of development of the particular region. The geological data show an increasing disagreement with the absolute ages calculated on the basis of the isotope composition. The determination of the ages of the minerals of the same deposit frequently gives results which are so contradictory that no acceptable geological explanation can be found.

In the light of this, the results of the recent investigations by P. Ramdohr, the well-known investigator of ore material, on the Blind River uranium-bearing conglomerates [1] acquire considerable importance.

When studying the ore of the Pronto district, P. Ramdohr established that the principal uranium mineral of the Blind River deposit, brannerite, is a secondary mineral, formed as pseudomorphs after uraninite or rutile. Careful microscopic investigations made it possible to establish the following process of formation of brannerite.

The grains or fine pebbles of ilmenite are converted to rutile. As a result of the chemical reaction between the grains of uraninite and rutile, brannerite is formed, pseudomorphs after either uraninite or rutile being developed according to the ratio of the masses of these two minerals.

According to P. Ramdohr the process takes place according to the following reaction which he has called the "Pronto reaction":

$$UO_2 + 2\text{-}3\,TiO_2 = UTi_{2-3}O_{6-8}$$
(uraninite) (rutile) (brannerite)

In some regions of the deposit this reaction takes place completely, in others only partially, while in some cases it does not occur at all. In particular, when uraninite occurs in carbonaceous material, initially represented by mobile hydrocarbons, the "Pronto reaction" does not occur.

The variation of the temperature, the composition of the surrounding strata and other factors connected with orogenic phenomena, intrusive activity, etc. can evidently serve as causes for the appearance of this reaction.

The determination of the absolute age of uraninite and brannerite cannot be used for solving the problem of the primary age of a uranium mineralization in conglomerates when the "Pronto reaction" is present. It was as a result of the presence of this particular process that the determination of the absolute age of the Blind River deposit gave very contradictory results, with a variation in the age found from 2000 million years and more to 350 million [2].

P. Ramdohr notes that the "Pronto reaction" also took place in the ores of the Witwatersrand deposits, where he also observed the formation of brannerite after uraninite.

It is very probable that under different conditions other reactions of a similar type to the "Pronto reaction" take place between the minerals of uranium and the material of the surrounding strata, leading to the formation of different secondary minerals.

These data indicate the necessity for careful study of the ore material and all the geological conditions of formation of the deposit in order to give a correct assessment of the significance of the absolute ages found for the minerals. They also indicate the inadmissibility of the mechanical use of figures of absolute ages for determining the time of formation of deposits and the surrounding strata.

LITERATURE CITED

[1] P. Ramdohr, Pronto-Reaktion, Neues Jahrbuch für Mineralogie, 1958, pp. 217-222.

[2] L. R. Stief, T. W. Stern, C. M. Cialla, and I. I. Warr, Bull. Geol. Soc. Amer. 67, 12, 1736 (1956).

M. K.

URANIUM RESOURCES IN CAPITALIST COUNTRIES

N. Zontov

Systematic prospecting for uranium in capitalist countries began after the second world war. Several uranium deposits were known at that time, including the Great Bear Lake deposit in Canada and those of the Colorado Plateau in the USA and Shinkolobwe in the Belgian Congo. A great deal of prospecting work has been carried out in all capitalist countries during the past 10-12 years, as a result of which numerous new deposits of uranium of various geological types, occurring under different geological conditions, were found. The greatest success in finding sources of raw material was achieved by Canada, the United States of America and the Union of South Africa who occupy the leading positions in the capitalist world at present with regard to the mining and processing of uranium ores. Considerable deposits of uranium were found in Australia and France. As a result of the exhaustion of its reserves, the Belgian Congo, which at one time was the largest supplier of rich uranium ores, is now only a secondary supplier of uranium. Uranium ores are also found to a greater or lesser extent in other countries.

The uranium ore mining and processing industry has undergone considerable development on the basis of the uranium deposits found.

During 1957 a considerable amount of statistical material was published in foreign technical journals; this gives an idea of the scale of the resources and the extent of the mining and processing of uranium ores in capitalist countries. The present review is based on these data.*

Canada. The main uranium ore regions of Canada are the Great Bear Lake (Northwest Territories), Beaverlodge Lake (Saskatchewan), Blind River and Bancroft (Ontario) and Reckspar (British Columbia).

The uranium deposits of the Great Bear Lake which were discovered in 1930 were the first major source of rich uranium ores to be found in Canada. The uranium ores belong to "five-metal" formation; apart from uranium they contain nickel, cobalt, bismuth and native silver. In places the uranium pitch forms rich vein ores. The deposit is worked to a depth of about 600 m. The ore is processed at the site in the Eldorado Mill which has a capacity of 200 tons per day; the old tailings from the gravity separation plant, extracted by means of a dredge from the creek where they were dumped, are also dressed [1].

A small deposit of uranium pitch ores in quartzitic veins is worked in the Marion Lake region, 420 km south-east of the Great Bear Lake. A 150 tons-per-day mill has been built to dress these ores; the uranium content in the ore is 0.30-0.34% [2].

The uranium ores in the Beaverlodge Lake region which were discovered in 1935 were first worked in 1953. As a result of intensive prospecting work in 1944 a large number of industrial deposits of uranium were discovered and, in consequence, the Beaverlodge Lake region has become one of the most important in Canada. The uranium mineralization is of the hydrothermal type and is represented principally by ores of simple composition, uranium pitch with hematite; the ores of the individual deposits, like, say the Nicholson deposit, contain nickel and cobalt in addition to uranium. The uranium content in the ores mined varies from 0.12 to 0.17% and is sometimes as much as 0.25%; rich uranium ores are not found.

Fifteen mines and three refining mills were constructed within a brief period on the deposits of the Beaverlodge Lake region. The Eldorado Mill, built in 1933, has now been extended and the capacity has been increased

* Foreign sources generally give data on the uranium content in the ore and on the reserves and production of uranium with reference to the oxide U_3O_8; in this review these data are converted to metallic uranium.

to 2000 tons per day; ores from the Fay, Ace and Verna deposits, in addition to ores brought in from outside the region, are dressed at the mill. The Gunnar Mill, with a capacity of 1650 tons per day, was put into operation in 1955 to treat the ores from the Gunnar deposit. The Eldorado Mill with a capacity of 500 tons per day commenced operation in 1957, the ores from the Eldorado deposit being refined at this plant. The total capacity of the three mills is 4150 tons per day [1].

The Blind River Region is the largest uranium region of Canada, the uranium deposits there being discovered in 1953. It is in a favorable economic location, being located near a railway; it contains large reserves of uranium. The uranium ores are quartzitic-pebble conglomerates, the cement of which contains dispersed uranium minerals, brannerite (the most widely distributed), and also uranium pitch and uraninite; large amounts of monazite, the mineral of thorium and the rare-earth elements, are found. The ore mined at the present time in the Blind River region contains one part of thorium to two parts of uranium; the problem of extracting and utilizing the thorium is, therefore, encountered [3].

Four processing mills with a total capacity of 10,500 tons per day are in operation at present in the Blind River region. The Pronto Mill with a capacity of 1500 tons per day started operating as early as August 1956. The Denison Mill is the largest and has a total capacity of 6000 tons per day; the first processing line with a capacity of 3000 tons per day went into operation in 1957. In addition, eight other mills (including the second line of the Denison Mill) with a total capacity of 23,800 tons per day are under construction. Upon completion of construction, expected by the end of 1958, 12 mills with a total capacity of 34,300 tons per day will be operating in the Blind River region; the uranium content in the ore processed varies from 0.068 to 0.085% [1, 4].

In the Bancroft region the uranium mineralization, discovered in 1952, is correlated with dikes of pegmatites, occurring among gneisses. In contrast to usual pegmatities, these contain considerable amounts of fluorite and calcite; the uranium content in the form of uraninite and uranothorite varies from 0.07 to 0.11%. There are no data on the reserves of these ores but judging from the large scale of construction operations they are evidently considerable. Two uranium ore processing mills with a capacity of 2350 tons per day are under construction [1, 4].

One small deposit of uranium ores, the Reckspar, has been discovered so far in British Columbia; in this deposit uranium pitch and uranium-bearing thorite form lenses in micaceous shales. A 750-tons-per-day mill is under construction in this deposit; the uranium content in the ore is 0.07% [1, 4].

By the end of 1957, 11 uranium ore processing mills with a total capacity of 16,750 tons per day were in operation in Canada, 12 mills with a total capacity of 26,900 tons per day are under construction. In 1956, 2800 tons of uranium concentrate was produced in Canada [5]; the expected uranium production in 1957 is 4200 tons and with the completion of the construction of new mills, 12-13 thousand tons of uranium concentrate will be produced by the end of 1959 [6]. The known reserves are sufficient to ensure this production level for approximately 20 years. The total reserves are estimated at 320 million tons of ore with a content of 0.09% (or 200 thousand tons of uranium) in the uranium-bearing Blind River conglomerates [8] and 95 million tons of ore with a content of 0.12% (or 120 thousand tons of uranium) in the hydrothermal and pegmatitic deposits.

United States of America. The principal sources of uranium ore in the USA are the numerous deposits in the Mesozoic sandstones distributed over the Colorado Plateau and in the western states of Colorado, Utah, Arizona, New Mexico, etc. The uranium-bearing lignites in South Dakota, the black marine shales found in many states, the phosphorites of the Florida peninsula, etc. are potential sources of uranium; the uranium content in these strata is, however, very low (up to 0.01-0.03%) and at the present they are not used, therefore, for the extraction of uranium. Information is available [9] that uranium is extracted as a conjunct component from phosphorites with a uranium content of 0.01-0.02 at the chemical works at Bonny in Florida. Investigations are being carried out on the extraction of uranium from lignites.

Hydrothermal deposits of uranium ores exist in many parts of the western states. The most important of these are the Marysvale deposit in Utah, the group of deposits in the Front Range of Colorado and in the Boulder region in Montana. In these regions there is a small amount of hydrothermal ore mining.

The Colorado Plateau, where the presence of uranium ores has been known since 1898, is the oldest center of the uranium industry in the USA. Intense geological investigations and the rapid development of the mining and processing of uranium ore have taken place on the Colorado Plateau since the U.S. Atomic Energy Commission announced its ore-buying program. Numerous deposits of uranium ore on the Colorado Plateau are now known; these include a number of large deposits which have served as the basis for the construction and operation of hundreds of mines.

The majority of the uranium deposits of the Colorado Plateau are closely associated with the sandstones of the Shinarump and Chinle formations of Triassic age and the Morrison formation of Jurassic age. Vanadium-uranium, copper-uranium and uranium ores proper may be distinguished according to their content of these metals. They are usually oxidized from the surface and are represented by secondary minerals, carnotite and partly tyuyamunite; with increasing depth the secondary ores are replaced by primary ones, in which uranium occurs in the form of uranium pitch and coffinite; in addition, sulfides of copper and other metals are contained in copper-uranium ores. The uranium content in the ores mined in the Colorado Plateau varies from 0.085 to 0.42%.

The uranium deposits of the Colorado Plateau are grouped in four major regions; Uravan in Colorado, Big Indian and White Canyon-Monument Valley in Utah and Ambrosia Lake in New Mexico.

A large number of deposits with small reserves are known in the Uravan region. The numerous mines of this region have a daily output of 1700 tons of ore but the largest of these do not produce more than 70 tons of ore per day.

The largest uranium-vanadium deposit, Mi Vida, was discovered in the Big Indian region in 1952. At present this region has an output of about 2000 tons of ore per day; the largest mines have a daily output of 300-600 tons of ore. The White Canyon-Monument Valley region is characterized by numerous small deposits. The Ambrosia Lake region, in which uranium ores were discovered in 1955, is the largest in the USA as regards its reserves of uranium, which are estimated at 47 million tons of ore with a content of 0.25%, or 120,000 tons of uranium [10]. The uranium ores are closely associated with the level of asphalt-bearing sandstones of the Morrison formation (Jurassic); the depth at which the ore lies varies from 100 to 400 m, the thickness of the ore bodies is 0.3-30 m. The Ambrosia Lake region is planned to have a daily output of about 8000 tons of ore; the individual mines will have a daily output of 500-1000 tons of ore. These mines are in the preparatory stage [11].

The total reserves of the USA are 67 million tons with a mean content of 0.23% or 150,000 tons of uranium [4], the ores of Ambrosia Lake region forming 80% of this total.

Considerable progress has been achieved in mining and processing uranium ores in the USA. Whereas 70,000 tons of ore were mined and processed in 1948 the figure for 1956 was 3 million tons. In the latter year 5100 tons of uranium concentrate was produced while according to Johnson, the director of the Department of Raw Material of the AEC, it was 8500 tons in 1957 [11].

By 1957, 14 processing mills with a total capacity of 10,000 tons per day, including the large 3000 tons-per-day Anaconda Mill in New Mexico, were in operation in the USA. Nine new mills with a total capacity of 8825 tons per day, including the large Kermac mill, with a capacity of 3300 tons per day, in New Mexico, are under construction. According to Johnson's statement [4], when these mills have been completed by the end of 1959 the USA will produce about 13,000 tons of uranium concentrate. The available reserves of uranium ore will ensure this production level for a period of approximately 10 years.

The Union of South Africa has recently become one of the major producers of uranium in the capitalist world as a result of the discovery of this metal in the well-known gold-bearing conglomerates of Southern Transvaal and the Orange Free State. The uranium mineralization is closely associated with the seams of gold-bearing conglomerates and occurs in the form of uraninite and thucholite. The gold-bearing conglomerates consist of pebbles of quartz, quartzite and siliceous shale, bound together by a siliceous-arenaceous cement. The uranium minerals are distributed in the cement. They are present in all the conglomerates but the uranium content is not always proportional to that of the gold. Some seams rich in gold are relatively poor in uranium while other seams, unworkable as regards gold content, are suitable for the extraction of uranium and gold. The uranium content in the ores mined varies from 0.008 to 0.10%.

From published information, the total reserves of uranium ores are estimated at 1.1 milliard tons with an average content of uranium of about 0.03%, or 300,000 tons [12]. The uranium is extracted from the tailings after the ore has been processed to obtain the gold. Since the costs for mining and crushing the ore are included in the cost of the gold, the extraction of uranium from the tailings is profitable in spite of the very low content of it in the latter. The first uranium mill was put into operation in 1952 and 17 mills with a total capacity of 62,000 tons per day, which process the tailings from 29 mines, are now working. In 1956, 3740 tons of uranium concentrate were produced in the Union of South Africa [11], and in 1957 the figure was 4200 tons [13]. By the end of 1959 the production of uranium concentrate will have increased to 5100 tons [11]; the known reserves are sufficient to ensure this level of production for ~ 50 years.

The uranium concentrates from the Union of South Africa are sent to Britain and the USA, Britain receiving $^1/_3$ and the USA $^2/_3$ of the production in accordance with the respective proportion of their investments [14].

Belgian Congo. The well-known Shinkolobwe uranium deposit, where working commenced in 1923, lies in the famous Katanga-Northern Rhodesia copper belt which is the largest source of cobalt in the noncommunist world and one of the chief sources of copper. The uranium deposit is of the hydrothermal type; the uranium minerals form irregular veins of rich ore and a dispersed impregnation in the wall rock. The uranium occurs in the form of crystalline uraninite, sulfides of nickel and cobalt and a slight admixture of copper sulfides being found together with it.

For a considerable time the Shinkolobwe deposit was the largest source of rich uranium ores. The intensive working of the deposit led, however, to a considerable exhaustion of the reserves. According to the data of Derricks and Vaes [15], given at the Geneva Conference on the Peaceful Uses of Atomic Energy in 1955, the deposit has been prospected in great detail by underground mine workings to a depth of 255 m. Boreholes were drilled for prospecting great depths. As was shown by these operations, the rich vein ores terminated with increasing depth and at the 255 m level only poor disseminated mineralization was encountered by the workings. At the present time the Belgian Congo has an annual output of about 850 tons [16]. New districts are being prospected toward the east and it is expected that a displaced part of the deposit will be found in this area.

Industrial uranium ores have recently been found in the copper belt in Northern Rhodesia where uranium is contained in shales with copper mineralization. A mine has been constructed on the basis of this deposit; the uranium mill at Mindol near Kitva was put into operation in March 1957. 370 tons of uranium were obtained in Northern Rhodesia in 1957 [17]; the planned annual output for 1958-1959 is 420 tons of uranium [18].

Australia. The known industrial deposits of Australia are of the hydrothermal type and are located along the outer part of the pre-Cambrian shield in three states: the Radium Hill deposit in South Australia, the Mount Isa deposit in Queensland and the Rum Djungle deposit in Northern Territory. Mining and processing of uranium ore commenced at Radium Hill in 1952; the mines and the mill at Rum Djungle were put into operation in 1954; an operation for the mining and processing of uranium ores is now under construction at Mount Isa.

The uranium ores in the Radium Hill deposit form a series of steep veins in crystalline shales and gneisses. In contrast to other uranium deposits, the principal uranium mineral at Radium Hill is davidite, a complex iron titanate containing 6.8-7.8% uranium and about 8.3% rare-earth elements.

The Rum Djungle uranium deposits are located on the flank of a domal structure in pre-Cambrian sedimentary strata; the uranium mineralization is closely associated with layers of carbonaceous shales in the direct vicinity of a large fault. Two groups of deposits of uranium-copper and uranium ores are found. In the first group the uranium pitch, together with chalcopyrite, forms a fine dissemination and veins in the shales; small amounts of copper are contained in the second group.

Several uranium deposits were found in the Mount Isa region, the largest of these being the Mary Catlin. The uranium ores form a number of steep zones of considerable extent in which the principal ore mineral is uranium pitch in association with carbonate.

There is very little published information on the extent of the reserves, the mined output and the processing of uranium ores in Australia. It is stated that the known deposits are of large dimensions but characterized by a low uranium content in the ore. The uranium ores of Radium Hill are prepared in dense media and by flotation in a dressing plant located at the deposit; the chemical treatment of the concentrate is carried out in a mill at Port Pirie, 320 km from the deposit. The mill produces 170 tons of uranium concentrate [27]. After the Mary Catlin Mill with a capacity of 1000 tons per day has been put into operation in 1958 [28], Australia will have an annual uranium production of 850 tons [16]. The entire production of the uranium industry is sent to the USA and Britain.

France. The uranium deposits in metropolitan France are located in the Massif Central: in the departments of Haute-Vienne (Crouzille), Saône-et-Loire (Grury), Puy-de-Dôme (Lachaux) and Vendee. The uranium ores are of the hydrothermal type and are represented by veins of uranium pitch occurring in granites or crystalline shales. The known reserves of uranium in the French deposits are 10,000 tons; the estimated reserves are 50-100 thousand tons.

The uranium ores are processed in a mill with an annual capacity of 50,000 tons; the uranium content in the ore processed varies from 0.10 to 0.8%. Two new mills with a total annual capacity of 500,000 tons of ore are under construction in the departments of Haute-Vienne and Vendee. It is planned to produce 500 tons of uranium concentrate in 1957; a further increase in production is planned as follows: 1000 tons of uranium concentrate in 1961, 2500 tons in 1970 and 3000 tons in 1975. The entire production of uranium in France is used for the country's own requirements [20].

Other countries. Insignificant amounts of uranium ore are mined in some other countries.

The uranium mill at Kvantorp (Sweden), constructed in 1953, has an annual production of 5 tons of uranium from bituminous shales; the reserves of uranium in shales containing 0.02-0.03% are estimated at more than 1 million tons. It is planned to build a second mill in 1962 with an annual capacity of 100 tons and this will make it possible to satisfy Sweden's uranium requirements by 1965.

In Western Germany there are several small uranium deposits in Bavaria, Hesse and other regions; it is planed to produce to tons of uranium in the second half of 1958; by 1960 Western Germany will be able to produce 50 tons of uranium.

The construction of an industrial plant for the annual production of 15 tons of uranium metal is planned in Portugal.

There are estimated to be 6000 tons of uranium in ore with a content of 0.20% in the deposits of the Maritime Alps in Italy; an experimental plant with an annual production of about 5 tons of uranium metal has been constructed on the basis of these ores [21].

In India the monazite sands of Travancore with estimated uranium reserves of 6-7 thousand tons are major sources of uranium; similar ores have recently been discovered in Bihar in northeastern India, the reserves of uranium being ascertained as 10,000 tons [22]. The copper shales of Bihar (Singhbhum), containing 0.03-0.10% uranium, are also a considerable source of uranium; the estimated reserves in these are 3-4 thousand tons [23]. 100 tons of uranium metal are produced annually from monazite sands in a mill in Bombay and 25 tons are extracted annually from the tailings of copper ores [24].

Eight uranium deposits are worked in the Argentine; the ore mined is processed in a mill in Cordoba [25].

The total production of uranium in capitalist countries may be represented in the form of the following table based on the above-mentioned data:

Name of country	Production level, tons		
	1956	1957	end of 1959
U.S.A.	5 100	8 500	13 000
Canada	2 800	4 200	13 000
Union of South Africa	3 740	4 200	5 100
Belgian Congo	850	850	850
Southern Rhodesia	—	370	420
Australia	400	400	850
France	300	380	1 000
Other countries	210	200	280
Total	13 400	19 100	34 500

According to the statement of W. Libby [26], the representative of the U.S. AEC, uranium is principally used for military purposes in capitalist countries; the uranium requirements for this purpose are not known. W. Libby estimates that the USA's requirements of uranium for peaceful purposes (power) in the next 10-20 years are 17,000-25,000 tons per year.

To complete its program for the construction of 19 atomic power stations Britain requires 7-10 thousand tons of uranium [14]. W. Libby estimates that the total annual requirements of capitalist countries for peaceful purposes are 34-85 thousand tons. The prospect of such a high increase in the use of uranium will undoubtedly stimulate further prospecting work and the mining and processing of uranium ores.

LITERATURE CITED

[1] F. R. Joubin, S. A. Min. Eng. J. 68, part 1, 3346, 561 (1957).

[2] F. R. Joubin, Can. Min. J. 78, 4, 88 (1957).

[3] Appl. Atomics No. 89, 13 (1957).

[4] A. H. Lang, Mines Mag. 47, 10, 52 (1957).

[5] Min. J. Ann. Rev. 51 (1957).

[6] Min. J. 248, Suppl. 1 (1957).

[7] P. Kihss, New York Times, October 29, 1957.

[8] B. F. Rummerfield, Mines Mag. 47, 10, 73 (1957).

[9] Rock Production 59, 6 (1956).

[10] R. T. Zitting, Mines Mag. 47, 3, 53 (1957).

[11] J. C. Johnson, Mines Mag. 47, 11, 23 (1957).

[12] Atom Industry 4, 5, 2 (1957).

[13] Rhodesian Min. J. 29, 361, 167 (1957).

[14] Min. Ind. Rev. 101, 3, 15 (1957).

[15] J. J. Derricks and J. F. Vaes, "The geology of atomic raw material," Reports of Foreign Scientists at the International Conference on the Peaceful Uses of Atomic Energy [Russian translation] (State Geolog. Tech. Press, 1956), p. 323.

[16] Min. J. 248, 487 (1957).

[17] Rhodesian Min. J. 29, 360, 143 (1957).

[18] Min. Ind. Rev. 101, 4, 19 (1957).

[19] Min. J. 249, 44 (1957).

[20] M. G. Guille, Atomics Nucl. Energy 8, 2, 51 (1957).

[21] L'industrie devant l'energie nuclear (Paris, 1957), pp. 237-247.

[22] P. R. Rajagopalan, Indian Min. J. 1, 4, 11 (1957).

[23] Indian Min. J. 3, 3, 24 (1957).

[24] New Scientist 2, 43, 32 (1957).

[25] Appl. Atomics No. 105, 7 (1957).

[26] W. F. Libby, Min. Ind. Rev. 101, 5, 18 (1957).

[27] S. A. Min. Eng. J. 69, part 1, No. 3388, 99 (1958).

[28] Atom. Industry 6, 2, 15 (1958).

N. Zontov

A CONFERENCE ON THE APPLICATION OF RADIOACTIVE ISOTOPES IN ANALYTICAL CHEMISTRY

A conference on the application of radioactive isotopes in analytical chemistry was held in Moscow on December 2-4, 1957; this conference was convened by the Chemical Sciences Section of the USSR Academy of Sciences, and the Commission on Analytical Chemistry of the V. I. Vernadskii Institute of Geochemistry and Analytical Chemistry. About 450 people attended the Conference; they represented scientific research institutes, universities, and industrial enterprises, and included over 30 scientists from England, Bulgaria, China, Poland, Rumania, the United States, and Czechoslovakia.

The aim of the Conference was to reflect the latest work in the USSR on the use of radioactive isotopes for developing new analytical methods based on radioactivity, the development of the theoretical foundations of analytical chemistry, on improvements and checking on methods of isolating and separating the elements, and on the determination of physicochemical constants of analytical importance. About 50 communications were presented at the Conference, of which 26 were read at the sessions, while the remainder were published as theses. All the papers presented at the Conference will be published as a collection entitled "The Application of Radioactive Isotopes in Analytical Chemistry."

Analytical methods based on radioactivity. A number of reports were devoted to the method of isotopic dilution which has found wide application in modern analytical practice. The main advantage of this method is the possibility of carrying out quantitative determinations of elements without isolating them completely. A new variant of the method whereby it is possible to determine very small amounts of impurities – the so-called multi-radioactive dilution – was proposed by I. E. Zimakov and G. S. Rozhavskii (State Institute of Nonferrous Metals). The new technique obviates the necessity of measuring the specific activity of the preparations, a factor which simplifies the analysis considerably. In their report, I. P. Alimarin and G. N. Bilmovich (GEOKhI) dwelt on methods they had developed for separating tantalum from titanium, zirconium, and niobium, and for the determination of tantalum by the isotope dilution method. Tantalum is precipitated by a new organic reagent – ammonium benzeneselenate. Other examples of the isotope dilution method were also given.

Two reports dealt with radiometric titration – a new volumetric method in which the equivalence point is established by measuring the activity of the solution. K. B. Iatsimirskii and E. N. Rosliakova (Ivanov Chemicotechnological Institute) reported on the use of solutions of complex compounds (luteo-salts) of Co^{60} for determination of large anions such as phosphates, sulfates, and molybdate by radiometric titration. I. M. Korenman and F. P. Sheianova (Gorky State University) pointed out the possibility of the wide use of nonisotopic indicators in radiometric titration, and in other branches of analytical chemistry. For example, mercury can be determined in its mixtures with zinc by titration with dithizone using Zn^{65} which is a nonisotopic indicator for mercury.

A. I. Kulak (D. I. Mendeleev Moscow Chemicotechnical Institute) reported on the determination of microamounts (10^{-6} to 10^{-5}%) of cobalt, copper, tellurium, arsenic, and antimony in ferric oxide by radioactivation analysis.

A new, express method of analysis has been developed in the USSR which is based on the reflection (backscattering) of β-rays (the work of A. A. Zhukhovitskii). V. B. Gaidadymov (GEOKhI) and L. I. Il'ina (Moscow Electric Lamp Factory) reported on the determination of the composition of binary tantalum-niobium alloys by this method.

Methods of isolating and separating the elements. A considerable number of reports dealt with this question, which was also amplified in the discussions.

Radioactive isotopes are widely used during chromatographic separation of elements both as indicators for following the course of an experiment, and for studying the distribution of a material between solution and sorbent. Moreover, as M. M. Seniavin (GEOKhI) pointed out in his report, problems exist in chromatography which, in principle, could not be solved without employing radioactive isotopes, e. g., studies on the separation of limitingly small amounts of material, quantitative analysis by isotope dilution, etc. E. I. Il'enko, B. P. Nikol'skii, and A. M. Trofimov (RIAN) gave results on a study of the absorption of ruthenium on ion exchange resins, while L. V. Borisova (GEOKhI) gave results of a study of the distribution of rhenium and molybdenum between the anion exchange resin EDE-10 and hydrochloric acid solutions.

It is known that the choice of complexing agent whose solution is used for eluting the ions from the column, is of great importance for the chromatographic separation of the rare earths. The communication of A. K. Lavrukhina, K. Iun-Pina, and V. Knoblokh (GEOKhI) dealt with a new complexing agent – trihydroxyglutaric acid – which has been found to be no less effective than lactic acid used at present.

One of the sessions was wholely devoted to the use of radioactive isotopes for the study of the separation of elements by coprecipitation methods. A new line in this field is the use of organic coprecipitants for extracting very small amounts of material. V. I. Kuznetsov and T. G. Akimova (GEOKhI) showed in their paper that uranium can be completely extracted from sea-water by coprecipitation of the thiocyanate complex of uranium with the precipitate of the thiocyanate of a large organic cation – methyl violet.

Five communications, some of which were read at the Conference, were devoted to coprecipitation of inorganic collectors. Mention should be made of the following reports: Iu. V. Morachevskii and A.I. Novikov (Leningrad State University) "Coprecipitation of Certain Elements at Low Concentrations with Metal Hydroxides,"* I. E. Starik and A. N. Apollonova (RIAN) "The Carbonate Method of Isolating Microamounts of Uranium from Weighable Amounts of Iron."

A. K. Lavrukhina (GEOKhI) dealt with the characteristic behavior of small concentrations of radioactive isotopes in solution, and the experimental difficulties connected with loss of the elements as the result of adsorption on filters and glass, formation of radiocolloids, etc. V. P. Shvedov and L. M.Ivanova (RIAN) described methods of separating the isotopes Mo^{96}, Ag^{111}, Cd^{115} and Ba^{140} from complex mixtures.

General questions in analytical chemistry. Of undoubted interest is the use of radioactive isotopes for determining a number of physicochemical constants, which are of analytical importance – solubility, instability constants of complex compounds, etc.

The effect of the nature of the solvent on the solubility of silver and cesium chlorides was the subject of the report given by N. I. Izmailov and V. S. Chernyi (Kharkov State University). The authors related the value of the solubility to the dielectric constant of the solvent. D. M. Ziv and I. A. Efros (RIAN) reported on a topic which is interesting from a methodological point of view; they suggested a technique for the determination of solubility by an ultramicromethod.

The same is true of the communication of N. P. Komar (Kharkov State University) on the use of radiochemical measurements in conjunction with determination of molar extinction coefficients for studying complex ions in two-phase systems.

I. M. Kolthoff (USA) participated in the Conference. Using radioactive isotopes, the author has obtained new data characterizing ageing processes and the formation of crystalline precipitates.

The use of radioactive isotopes as indicators, permits complicated studies to be carried out on the analytical properties of the elements. In the report given by A. K. Lavrukhina and S. S. Rodin (GEOKhI) results were given of some experiments on the behavior of element 87 (Francium) during coprecipitation with various carriers, during extraction with solvents, etc. I. M. Irving (Oxford University, England) dealt with the study of the analytical properties of indium by means of radioactive isotopes.

A considerable number of the reports given at the Conference were concerned with the use of a radioactive isotopes for production control, e. g., for the production of rare metals (A. A. Griznik and N. I. Marunina, Giredmet).

* Strontium, lanthanum, cerium, yttrium, rhenium, gallium, indium, zirconium (Author's note).

As the chairman of the organizing committee of the Conference, Academician A. P. Vinogradov remarked in his concluding remarks the Conference convincingly demonstrated that radioactive isotopes are widely used in many fields by Soviet analytical chemists.

Iu. A. Zolotov

NEWS ROUNDUP

USSR. At Dubno (Moscow oblast), the Conference on nuclear reactions under the influence of multiply charged ions completed its labors. Upwards of 100 scientists from 10 member-nations of the Joint Institute for Nuclear Research took part in the Conference. The Conference drew up a balance sheet of work in the area of investigation concerned, performed in the USSR and outside, and discussed the work plans of the recently set up Laboratory of Nuclear Reactions attached to the Joint Institute for Nuclear Research. Ways of coordinating the work of this laboratory with research being carried out in scientific institutions of member-nations of the Joint Institute were mapped out.

USSR. At the Scientific Research Institute of the Rubber Tire Industry, work has been carried out with the cooperation of the Karpov Scientific Research Physicochemical Institute on radiation vulcanization of three models of tire treads for trucks. The material for the tire treads was composed of carbon black mixtures based on natural rubber and caprone cord. Vulcanization of the tire tread models was carried out on an installation for radiochemical research using a Co^{60} radiation source with an activity of 21,000 g-equivalents of radium and in the γ-field of an experimental nuclear chain reactor.

In comparison with improved sulfur rubbers containing the same quantity of filler material, the radiation vulcanizates exhibited a resistance to ageing 4-5 times stronger (at a temperature of 130°C), small residual strains, low hysteresis, high durability in the course of repeated strains and high temperature stability.

Australia. At Sydney, a conference of the peaceful uses of atomic energy applied to Australian conditions is scheduled for June 2-6, 1958. Panels of the Conference will take up the following questions: reactor materials, power engineering, accessory power equipment, chemical treatment and economics of nuclear power development, theoretical research, radioisotope production, safety instrumentation and techniques.

Australia. Large accumulations of pitchblende have been discovered in an abandoned copper mine in Yudnamutan, 16 km from the Mt. Painter uranium site.

England. In March 1958, the third reactor of the atomic electric power station at Calder Hall went critical.

Greece. Important deposits of uraniferous and thorium-bearing ores have been uncovered in western Thrace. Sites containing pitchblende were discovered in the vicinity of villages Kotili and Dimarion, south of the Bulgarian frontier; other sites have been discovered at Kyrki village, in the neighborhood of the Evros river.

Italy. The International Exposition and Congress on Electronics and Atomic Energy will convene at Rome, June 16-30, 1958.

Canada. In a new uranium ore area on the Labrador peninsula, in the Maccovine region, drilling explorations have laid bare an ore body tracked down to a length of 210 m, with a width of 1.5 m and an average U_3O_8 content of 0.9%.

USA. From the f-m cyclotron (450 Mev) at the Enrico Fermi Nuclear Research Institute of the University of Chicago, a proton beam has been produced into the newly installed measurements hall. The accelerator will be used for physical and biological research.

USA. The 86-inch proton cyclotron (26 Mev energy) at Oak Ridge, with vertically mounted dees, is being modified to produce an inclined beam.

USA. Nuclear-grade niobium is being produced in the USA at the following prices per pound: disks $55-70, segments $60-75, and untreated ingots (of 100 mm diameter and weighing 27 kg) $65-80.

USA. In due time, AEC has set prices for the extraction of uranium and plutonium nitrates from spent fuel brought back from privately owned reactors. The cost of reprocessing these salts to uranium hexafluoride and metallic plutonium has been announced recently, in addition. Buyback prices are: 1) for converting pure uranyl nitrate (containing up to 5% U^{235}) to the hexafluoride: $5.60 for 1 kg of uranium; with over 5% U^{235} content: $32 for 1 kg of uranium; 2) for reprocessing pure plutonium nitrate to metallic plutonium: $1.50 for 1 g of plutonium.

USA. Radium Corporation of Morristown, New Jersey has put out new signal lamps (priced at $35-75) in which light is excited by beta rays from Kr^{85} (0.74 Mev energy, half-life of 9.4 years) impinging on a special phosphor. Light from the lamp is visible at a distance of 450 m; reading may be done with ease at 3 m from the light source.

Finland. Uranium deposits have been uncovered in Northern Karelia. Prospecting and exploration work is going on.

West Germany. Near Jülich (in Westphalia) ground has been broken for an atomic research center, the biggest atomic center in West Germany. For this center, Britain is installing a Merlin type research reactor of 5000 kw power, and plans for a DIDO reactor of 10,000 kw power.

Institutes will be set up at the center for medicine, biology, agriculture, radiochemistry, reactor design, reactor materials, nuclear fusion, aircraft propulsion engines and a plutonium institute.

An isotope separation plant and a breeder reactor will be transferred to the center.

France. In France, construction of a uranium isotope separation plant has been decided upon, with an output of 1500 kg of U^{235} annually, using the gaseous diffusion technique of separation. The plant will cost 55 billion francs, and will cover a total area of 170 hectares. The plant will be built in the vicinity of an electric power source. It took 3 years to work out the mechanics of the process, and an experimental chain of 12 stages was set up at Saclay. The results of the investigations will be reported on at length at the Second International Conference on the Peaceful Uses of Atomic Energy.

France. Commissioning of the EL-3 reactor at Saclay made it possible for France not only to dispense with importing radioactive isotopes Co^{60} and C^{14}, but even to begin exporting radioactive isotopes to other countries, Britain in particular.

BIBLIOGRAPHY

USEFUL TRANSLATION COLLECTION

As research in the USSR on the utilization of atomic energy involves more and more people, it becomes desirable to acquaint them with the results of work in this field carried on in other countries. Thus, in September of 1957 publication was started in the Soviet Union of a monthly translation collection called "Foreign Nuclear Technology."

The collection consists of translation of papers, surveys, and other references to foreign scientific and technical journals which deal mainly with problems of reactor construction, radiation shielding, extraction and processing of nuclear fuel, behavior of materials, installation and outfitting of nuclear reactors and laboratories, production and utilization of radioactive isotopes and accelerator technology. The subject matter to be emphasized is readily apparent from the first issue: the material offered emphasizes the practical aspects of the field; the papers in the collection are all of technological nature.

Main emphasis is on reactor construction. The collection contains translations of survey papers and papers which describe individual nuclear reactors.

Examples are the papers "Design and Construction of an Engineering Test Reactor" (No. 2, 34, 1957); "English Research Reactor MERLIN" (No. 4, 27, 1957); "Research Reactor Argonaut" (No. 4, 3, 1958). Along with these there are papers which describe several projected or operating power reactors: "Experimental Boiling Water Reactor EBWR" (No. 1, 11, 1957); "U. S. Demonstration Nuclear Power Reactor" (No. 2, 13, 1957); "Hinckley Point Electric Power Station" (No. 4, 72, 1957).

Also of great use is the publication of sketches of various units and individual construction elements of foreign equipment as is the case, for example, in the paper "Nuclear Gas-Turbine High Power Systems Using Closed Cycles for Merchant Ships" (No. 1, 31, 1957) and several others.

A large number of translations are concerned with problems relating to reactor construction. The production and processing of nuclear fuel, technology of reactor materials, installation of nuclear reactors, etc. Some of these papers includes the following: "Processing of Metallic Uranium in France" (No. 1, 41, 1957); "Uranium Regeneration at the Oak Ridge Gaseous Diffusion Plant" (No. 2, 45, 1957); "Pumps for Use in Nuclear Power Systems" (No. 4, 72, 1957).

The collection contains material on the outfitting of hot laboratories, the application of radioactive isotopes, dosimetry apparatus, removal of radioactive waste, radiation damage in materials, separation of isotopes and a number of other questions. These papers include "Remote Control of Operations Carried Out in a Hot Chamber" (No. 1, 55, 1957); "Application of Radioactive Isotopes in Industrial Research and in Control of Industrial Processes" (No. 2, 57, 1957); "Alpha Scintillation Dosimeter for Measuring Contamination of Hands and Clothing" (No. 3, 54, 1957); "Removal of Radioactive Waste at Hanford" (No. 4, 61, 1957); "Metallurgical Research in Nonfissile Metals Subject to Neutron Irradiation" (No. 1, 40, 1958); "Magneto-Ionic Expander – A New Device for Isotope Separation" (No. 1, 54, 1957).

Material on accelerator technology is included. For example, the paper "Certain Engineering Problems in the Design of the Synchrotron at the European Nuclear Research Organization (CERN)" (No. 3, 45, 1957).

There are also translations of survey papers which review the state of the art in various countries. These include "The State of Nuclear Power in the USA" (No. 1, 5, 1957); "Work in Reactor Construction in England" (Nos. 2, 3, 1957); "State of Nuclear Power in France" (No. 3, 3, 1957). The editors of the collection have conducted a wide survey of the state of research in foreign countries on problems of nuclear power, including problems involved in the realization of a controlled thermonuclear reaction. An example of this work is the article

"Work in the Field of Controlled Thermonuclear Reactions in England and the USA" (No. 1, 74, 1957); "The Pinch Effect" (No. 1, 51, 1958); "A Plasma Fission Reactor for Continuous Production of Electrical Power" (No. 4, 3, 1957); "Catalysis of Nuclear Fusion by μ-Mesons" (No. 2, 67, 1957); "Problems in the Design of Nuclear Powered Airplaines" (No. 3, 58, 1957).

Finally, mention should be made of papers, references, and brief reports of the latest events in this field. Wide coverage is given to the international nuclear scene, including announcements and descriptions of exhibitions on the use of atomic energy in foreign countries, various new applications and events in this field, etc. Actually, the editors of the collection are open to some criticism because of the excessive space devoted to the military aspect of atomic energy. It is hardly necessary to publish in each number of the journal material on atomic-powered boats, battleships, guns, atomic bomb tests, etc. In journals published in capitalistic countries this subject is discussed widely but with a completely different point of view in mind so that the choice of material of this kind for publication in a Soviet journal must be carried out with great care. It would also be desirable in translating and editing articles for the journal to compress or even omit certain details and to avoid repetition of certain fundamental and well-known material. However, these shortcomings are unimportant compared with the value of this undertaking. The editors are to be congratulated on an important and useful journal.

Iu. K.

NEW LITERATURE

Books and Collections

Nuclear energy in England, 1957. The English Central Information Bureau in 1957 published a brochure called "Nuclear Energy in England." This publication contains information on the state of research in nuclear physics in England before the war, during the war, and immediately after the Second World War; the various establishments and organizations which are responsible for coordinating and carrying out research and work in nuclear energy in England are described and it is reported that in February of 1957 a national institute for nuclear research was formed whose main purpose will be to assist universities and other organizations in the utilization of equipment and expensive installations; a program for the construction of electrical power stations was also announced.

It is reported that in 1967 the power requirement of the country will be increased by 50% as compared with the present level. Inasmuch as ordinary power sources are limited a comprehensive program for the construction of nuclear power stations is being undertaken.

On March 5, 1957, the government published a tentative program, according to which the power developed by nuclear stations in 1965 will be 5-6 million kw (15% of the entire electrical power available) instead of the 1.5-2 million kw which had been originally planned. The total capitalization costs required to realize this program, including the auxiliary installations for transmission of the electrical power, are estimated as 3350 million pounds. The cost of obtaining thermal-fission elements from natural uranium for use in reactors will depend on certain conditions; however, for the first power stations, this figure will run to about twenty thousand pounds per ton. In a graphite-moderated reactor with a capacity of 150 thousand kw approximately 250 tons of nuclear fuel are required. This is approximately equivalent to the initial capitalization cost (30 pounds per kw of electrical power). If it is assumed that the loading factor is 75%, the cost of a kw-hr will be approximately 0.06 pence.

The raw material requirements will be met for many years at the beginning of the program. However, at the end of 60 years, because of the intense development of nuclear power stations the uranium requirements will increase. The development of improved reactors within the next 70 years should make it possible to increase the power of nuclear power stations without increasing the natural uranium requirements.

Up to this time a search for uranium in England has not uncovered any deposits, the development of which would be profitable from an economic point of view. The uranium used in England is obtained from the Belgian Congo, the Union of South Africa and Australia.

A great deal of attention is being given to the production and use of isotopes and radioactive materials, particularly in medicine. For example, at one hospital an installation has recently been completed for the treatment of cancer by radioactive cesium. This is the first case of the utilization for medical purposes of radioactive by-products at Windscale. Radioactive cesium is now being produced in England in large quantities.

At the present time England is also exporting a large number of radioactive isotopes. More than one thousand firms are now concerned with the manufacture of apparatus, instruments, and materials needed for the development of atomic energy in England.

Technical cooperation between England and other countries is carried out on the basis of bilateral agreements. For example, it is reported that a contract has been signed with Western Germany for the construction of a nuclear power station of the Calder-Hall type. The export of equipment for nuclear power stations to Japan, Italy and Holland has also been given consideration.

A. I. Danilin, Application of Nuclear Radiation in Hydro-Meteorology (Hydro-Meteorology Press, Leningrad, 1957), 69 pp., 1 r, 30 k.

This monograph is concerned with problems which arise in the application of radioactive isotopes in hydrometeorological measurements. It is intended for engineers and technicians who work in meteorology and hydrology and are interested in moisture conditions in soil and the ground.

Iu. D. Ianishevskii, Actinometric Instruments and Methods of Observation (Hydro-Meteorology Press, 1957), 413 pp., 16 r 80 k.

This is a handbook on measurements and detection of radiation in the atmosphere. Descriptions are given of instruments used in meteorological stations and by expeditions. The book is intended for geophysicists and meteorologists concerned with the calculation of radiation and teachers in courses on meteorology and agrometeorology.

Problems of Kinetics and Catalysis, IX. Isotopes in Catalysis. Edited by Corresponding Member of the Academy of Sciences A. Z. Roginskii and others (Acad. Sci. USSR Press, 1957), 443 pp., 23 r 74 k.

Collection IX presents lectures delivered at a scientific conference on isotopes and catalysis (Moscow, March 31 to April 5, 1956). The collection starts with the lecture by S. Z. Roginskii, "Isotopes in Catalysis." The collection is made up of the following sections: catalytic reaction, catalytic oxidation, catalytic cracking of hydrocarbons, other catalytic reactions, isotope exchange, investigation of catalytic agents by isotope methods, the isotope effect, physical and physicochemical methods of investigation, synthesis of tracer materials.

This collection is intended for specialists in physics, inorganic, organic, and analytic chemistry, scientists in general and university teachers.

A. I. Shatenshtein, E. A. Iakovlev, and E. N. Zviagintseva and others. Isotopic Analysis of Water. Second edition (Acad. Sci. USSR Press, 1957), 236 pp., 14 r.

This book offers a critical analysis of problems which arise in isotopic analysis of water. Data are given on the isotopic composition of natural water and methods are described by which water is purified. In the first part of the book the theoretical bases for the methods are described, the conditions upon which the accuracy of the measurement depend are considered and methods of carrying out the calculations are treated. The second part of the book is a practical handbook on the application of methods of isotopic analysis of water (in the form of detailed instruction).

Research in Measurement of Ionizing Radiation. Trudy VNIIM No. 30 (90) edited by K. K. Aglintsev. (Standards Press, Moscow-Leningrad, 1957), 148 pp., 4 r 65 k.

This collection presents the results of work carried out at the radiometry laboratory of VNIIM on the reproduction, maintenance and transfer of values of standards used in radioactivity, x-ray work and γ-radiation.

A. A. Kanaev, Water Mill to Atomic Engine (Mashgiz, 1957), 236 pp., 6 r 35 k.

This book describes the development of power machinery from primitive times to the present. About half of the book is devoted to the utilization of atomic power. A brief schematic presentation is given of the structure of the atom and the principles of nuclear fission. Particular attention is paid to a description of apparatus and principles of operation of nuclear power reactors. The feasibility of using atomic engines in ships, airplanes and locomotives is discussed.

This book is semi-popular and meant for a wide readership.

Izvestia Akademiia Nauk 22, 1 (1958).

This journal contains material presented at the First All-Union Conference on the synthesis and investigation of scintillators for detection of nuclear radiation, which was held in Moscow October 23-25, 1956.

The various talks are concerned with problems associated with the production of different scintillators, measurements of luminescence and scintillation properties, the development of new photomultiplier tubes, and the application of these devices in physics research and in industry. A number of articles describe methods of growing scintillation crystals. The amplitude resolution of NaI—Tl crystals under excitation by γ-radiation from Cs^{137} is 8-12% (when used with photomultipliers such as the FEU-C or FEU-24.

The properties of a number of scintillators in the detection of fast neutrons and slow neutrons are considered. BaF_2 crystals (without an activator); LiI activated with Tl or Sn; scintillators containing organic compounds, industrial types of detectors for thermal neutrons and fast neutrons, etc.

Several reports are concerned with plastic scintillators. These discuss methods of producing scintillators using a polystyrene base with good transparency for natural radiation and the best ratio of energy yield to flash duration B_e/τ. The results of studies of the mechanism for the transfer in energy in scintillators, the dependence of lumination yield on temperature and damage to plastic scintillators by ionizing radiation are considered.

The constructional and operational parameters for new domestic photomultipliers such as the 1S, 1B, 1V, 2M and 2B are described. Scintillation methods of detecting β - and γ -radiation in various instruments based on these methods were also described.

Short Glossary of Various Terms and Definitions Used in Nuclear Power, Nuclear Weapons and Protective Shielding, compiled by Ia. M. Gorelik, M. B. Dobrovol'skii, and S. B. Rubin (DOSAAF Press, 1958), 62 pp.,1 r.

This pamphlet is the first attempt in the USSR to systematize and explain new terms which are used in connection with the development of nuclear power. The glossary contains about 300 terms; the majority of these refer to military applications of nuclear power while the remainder are applicable in reactor design and nuclear physics.

Journal Articles

L. P. Adamovich and B. V. Iutsich, "Photometric determination of beryllium in compounds of black metals," Ukrainian Chemical Journal 23, 6 (1957).

Kh. I. Amirkhanov et al., "Determination of the absolute age of sedimentary minerals by radioactive methods," Doklady Akad. Nauk SSSR 117, 4 (1957).

M. S. Bykhovskaia, "Comparative evaluation of various methods of determining beryllium and its compounds as applied to the analysis of air," Industrial Hygiene and Occupational Disease No. 6 (1957).

Ia. M. Varshavskii and S. E. Vaisberg, "Thermodynamic and kinetic features of isotopic exchange reactions in hydrogen," Progress of Chemistry 26, 12 (1957).

Ia. M. Varshavskii et al., "Isotopic exchange between gaseous hydrogen and solid polymers under the influence of nuclear radiation," Doklady Akad. Nauk SSSR 118, 2 (1958).

V. M. Vdovenko, "Extraction as a method of separation and study of radioactive elements," J. Inorg. Chem. 3, 1 (1958).

V. M. Vdovenko and L. N. Lazarev, "Extraction of uranium in the form of anilinuranyltriacetate," J. Inorg. Chem. 3, 1 (1958).

S. A. Voznesenskii et al., "Absorption of radioactive isotopes by aluminum hydroxide," J. Inorg. Chem. 3, 1 (1958).

V. A. Vodianitskii, "Is it safe to deposit wastes from atomic industries in the Black Sea?" Nature 2 (1958).

A. M. Gabril'ian, "Some data on the total isotopic composition of water in petroleum deposits in Fergan," Izv. Akad. Nauk Uzb.SSR Geological Series 4 (1957).

M. L. Gol'din, "Calculation method for determining the density of mud by γ -ray absorption," Cement 6 (1957).

V. I. Grebenshchikova and V. N. Bobrova, "Deposits of lanthanum, cerium and americium in potassium sulfur dioxide," J. Inorg. Chem. 3, 1 (1958).

A. A. Grinberg, "Value of complex compounds in radiochemistry," J. Inorg. Chem. 3, 1 (1958).

G. Egizarov, "The effect of ionizing radiation on meat (Problems of cold sterilization)," Meat Industry 6 (1957).

Iu. L. Egorov, "Material on the gross features of flames of rare metals – tantalum and niobium," Industrial Hygiene and Occupational Disease No. 6 (1957).

G. Ershov, "Instrument with radioactive thulium for determining and rotting of live trees. (From the foreign literature)," Timber Economy 12 (1957).

A. K. Kir'ianov, "Prospective application of radioactive isotopes in the copper industry," Proc. Ural Scientific Research Inst. for Copper Industry No. 2 (1957).

N. I. Krylova and M. N. Nabiev, "Investigation of certain properties of ammonium nitrate by means of radioactive isotopes," Acad. Sci. Ukr.SSR Press, Chemical Science Series No. 4 (1957).

J. D. Lawson, "Certain criteria relating to the operation of thermonuclear power reactors. Problems of contemporary physics," Collection of Translations from the Foreign Literature No. 1 (1958).

S. V. Maleev, "Polarization of slow neutrons in scattering in crystals," J. Exptl.-Theoret. Phys. (USSR) 34, 1 (1958).

A. N. Proptopopov and V. P. Eismout, "Angular anisotropy for fragment emission in fission of Pu^{239} by 14 Mev neutrons (letter to the editor)," J. Exptl.-Theoret. Phys. (USSR) 34, 1 (1958).

O. V. Prudkovskaia, "Theory of diffusion oscillations in the plasma of a gas discharge," Doklady Akad. Nauk SSSR 117, 4 (1957).

J. Ridberg and B. Bernstrom, "Study of the extraction of complex metallic compounds. Distribution of certain fission products between methylisobutyl-ketone and water solution of HNO_3 and $Ca(NO_3)_2$," Chemistry and Chemical Technology, Collection of translations from the foreign literature No. 1 (1958).

M. Rozenblat and K. Lougmire, "Stability of a plasma confined by a magnetic field," Problems of Con-Contemporary Physics, Collection of translation from the foreign periodical literature, No. 1 (1958).

R. V. Teis, et al., "Determination of paleotemperature by the isotopic composition of oxygen in organic calcite," Bulletin of Moscow Naturalists' Society, Ser. Geol. Vol. 32, No. 6 (1957).

V. F. Turchin, "Excitation of optical oscillations of a crystal by slow neutrons" (letter to the editor), J. Exptl.-Theoret. Phys. 34, 1 (1958).

N. N. Shumilovskii and L. V. Mel'ttser, "Quality control by radioactive methods," Standardization No. 6 (1957).

V. Ia. Eidman, "Radiation of an electron moving in a magneto-active plasma," J. Exptl.-Theoret. Phys. USSR 34, 1 (1958).

J. G. Ball, "Metallurgical research in the nuclear power industry," J. Brit. Nucl. Energy Conf. 3, 1, 1 (1958).

C. Beets and H. Breny, "Use of nuclear emulsions for measuring the density of thermal neutrons in homogeneous media," J. Nucl. Energy 6, 3, 197 (1958).

I. B. Bernstein et al., " Energy principles in problems of hydrodynamic stability," Proc. Roy. Soc. A 244, 17 (1958).

L. Colli et al., "Further measurements of the (n, p) reaction for 14 Mev neutrons," Nuovo cimento 7, 3 400 (1958).

A. H. Cottrell, "Effect of neutron irradiation on metals and alloys," J. Brit. Nucl. Energy Conf. 3, 1, 50 (1958).

P. C. Davidge and C. J. L. Lock, " Poisoning of reactors by gaseous fission products," J. Nucl. Energy 6, 3, 191 (1958).

"Progress of construction at Bradwell," Engineer 205, 5321, 85 (1958).

"Utilization of atomic energy in Sweden," Engineer 205, 5321, 111 (1958).

K. E. Larsson et al., "Measurement of the slow neutron spectrum at the Swedish Heavy Water Reactor R1," J. Nucl. Energy 6, 3, 222 (1958).

G. J. McCallum, "Total neutron cross section for U^{234} and U^{236}," J. Nucl. Energy 6, 3, 181 (1958).

A. B. McIntosh and K. Q. Bagley, "Choice of a material for the shell of the TVE reactor with cooling by sodium potassium and carbon dioxide," J. Brit. Nucl. Energy Conf. 3, 1, 15 (1958).

M. J. Makin and F. J. Minter, "Effect of neutron irradiation on the mechanical properties of titanium and zirconium," J. Brit. Nucl. Energy Conf. 3, 1, 68 (1958).

M. J. Makin and E. Gillies, "Effect of neutron irradiation on the mechanical properties of molybdenum and tungsten," J. Brit. Nucl. Energy Conf. 3, 1, 74 (1958).

H. M. Skarsgard and C. J. Kenward, "Measurements of the energy dependence for effective number of secondary neutrons in Pu^{239} and U^{235} over the energy range 0.006-0.36 ev," J. Nucl. Energy 6, 3, 212 (1958).

G. W. C. Tait, "Problems of population safety in reactor operation," Nucleonics 16, 1, 71 (1958).

K. M. Towers, "Possible energy-storage methods and their economy," Nucl. Eng. 3, 23, 47 (1958).

SIGNIFICANCE OF ABBREVIATIONS MOST FREQUENTLY ENCOUNTERED IN SOVIET PHYSICS PERIODICALS

AN SSSR	*Academy of Sciences, USSR*
FIAN	*Physics Institute, Academy of Sciences USSR*
GITI	*State Scientific and Technical Press*
GITTL	*State Press for Technical and Theoretical Literature*
GOI	*State Optical Institute*
GONTI	*State United Scientific and Technical Press*
Gosenergoizdat	*State Power Press*
Gosfizkhimizdat	*State Physical Chemistry Press*
Gozkhimizdat	*State Chemistry Press*
GOST	*All-Union State Standard*
Goztekhizdat	*State Technical Press*
GTTI	*State Technical and Theoretical Press*
GUPIAE	*State Office for Utilization of Atomic Energy*
IF KhI	*Institute of Physical Chemistry Research*
IFP	*Institute of Physical Problems*
IL	*Foreign Literature Press*
IPF	*Institute of Applied Physics*
IPM	*Institute of Applied Mathematics*
IREA	*Institute of Chemical Reagents*
ISN (Izd. Sov. Nauk)	*Soviet Science Press*
I YaP	*Institute of Nuclear Studies*
Izd	*Press (publishing house)*
KISO	*Solar Research Commission*
LETI	*Leningrad Electrotechnical Institute*
LFTI	*Leningrad Institute of Physics and Technology*
LIM	*Leningrad Institute of Metals*
LITMiO	*Leningrad Institute of Precision Instruments and Optics*
Mashgiz	*State Scientific-Technical Press for Machine Construction Literature*
MATI	*Moscow Aviation Technology Institute*
MGU	*Moscow State University*
Metallurgizdat	*Metallurgy Press*
MOPI	*Moscow Regional Institute of Physics*
NIAFIZ	*Scientific Research Association for Physics*
NIFI	*Scientific Research Institute of Physics*
NIIMM	*Scientific Research Institute of Mathematics and Mechanics*
NII ZVUKSZAPIOI	*Scientific Research Institute of Sound Recording*
NIKFI	*Scientific Institute of Motion Picture Photography*
OIYaI	*Joint Institute of Nuclear Studies*
ONTI	*United Scientific and Technical Press*
OTI	*Division of Technical Information*
OTN	*Division of Technical Science*
RIAN	*Radium Institute, Academy of Sciences of the USSR*
SPB	*All-Union Special Planning Office*
Stroiizdat	*Construction Press*
URALFTI	*Ural Institute of Physics and Technology*

NOTE: Abbreviations not on this list and not explained in the translation have been transliterated, no further information about their significance being available to us.—*Publisher.*

recent Russian research
—in complete English translation

A Supplement to "HELIUM"

BY *E. M. LIFSHITS*
AND *E. L. ANDRONIKASHVILI*

THIS NOTABLE volume consists of two supplementary chapters, by these outstanding Soviet physicists, which were added to the Russian translation of W. H. Keesom's classic book "HELIUM."

The first chapter, by Lifshits, is a concise resume of the Landau theory of superfluidity *(quantization of the motion of a liquid; superfluidity of Helium II; macroscopic hydrodynamics of Helium II)*. The second chapter reports in considerable detail the experimental work conducted by Peter Kapitza and E. L. Andronikashvili in this field *(motion of Helium II due to the influx of heat; the two forms of motion in Helium II; viscosity of the normal component; reversibility of hydro-thermal processes and the thermo-mechanical effect; critical velocities; heat transport in slits and capillaries; heat transport in free Helium II; second sound; films; impurities)*.

Recent experiments on the superfluidity of helium make A SUPPLEMENT TO "HELIUM" of major interest to all researchers in low temperature physics.

cloth bound • 175 pages • $7.50

CB translations are by bilingual scientists, and include all photographic, diagrammatic and tabular material integral with the text.

Complete Table of Contents

CONSULTANTS BUREAU, INC.
227 WEST 17TH STREET, NEW YORK 11, N. Y.